NUREG/CR-4324
SAND85-1481
R3
Printed December 1985

Testing of Nuclear Qualified Cables and Pressure Transmitters in Simulated Hydrogen Deflagrations to Determine Survival Margins and Sensitivities

Vincent J. Dandini

Prepared by
Sandia National Laboratories
Albuquerque, New Mexico 87185 and Livermore, California 94550
for the United States Department of Energy
under Contract DE-AC04-76DP00789

Prepared for
U. S. NUCLEAR REGULATORY COMMISSION
SF2900Q(8-81)

Available from

Superintendent of Documents
U.S. Government Printing Office
Post Office Box 37082
Washington, D.C. 20013-7982

and

National Technical Information Service
Springfield, VA 22161

NUREG/CR-4324
SAND85-1481
R3

TESTING OF NUCLEAR QUALIFIED CABLES AND PRESSURE TRANSMITTERS IN SIMULATED HYDROGEN DEFLAGRATIONS TO DETERMINE SURVIVAL MARGINS AND SENSITIVITIES

Vincent J. Dandini

December 1985

Sandia National Laboratories
Albuquerque, New Mexico 87185
Operated by
Sandia Corporation
for the
U.S. Department of Energy

Prepared for
Electrical Engineering
Instrumentation and Control Branch
Division of Engineering Technology
Office of Nuclear Regulatory Research
U.S. Nuclear Regulatory Commission
Under Memorandum of Understanding DOE 40-550-75
NRC FIN No. A-1270

ABSTRACT

Uncertainties exist in the assessment of the survival of safety-related equipment during hydrogen burns in reactor containment buildings. These uncertainties are associated with the simple equipment models currently incorporated in hydrogen burn computer codes and scaling related to volume and geometry differences between vessels used in hydrogen combustion experiments and reactor containments.

In order to evaluate the margins for equipment survival in a hydrogen burn, a series of equipment tests was conducted at Sandia National Laboratories Central Receiver Test Facility. These tests subjected artificially aged and unaged specimens of qualified Brand Rex electrical cable and Barton Model 763 pressure transmitters to heat flux pulses simulating increasingly severe hydrogen burns. The initial base heat flux pulse used in the tests was representative of a hydrogen deflagration in a large dry containment building resulting from a 75 percent metal-water reaction. Starting with the base pulse, the test specimens were exposed to increasingly severe heat flux pulses until a pulse whose heat flux levels were three times those of the base pulse was reached. Specimen performance was checked during and after exposure to each of the simulated hydrogen burns.

All specimens functioned properly during exposure to all of the hydrogen burn simulations. An applied potential was maintained throughout the cable tests. No short or open circuits were detected. The transmitters showed no signs of degraded performance.

High potential withstand (hi-pot) tests conducted in the posttest examination displayed slight differences between the thermally aged and unaged cable insulation behavior. The aged cables exhibited higher leakage currents than the unaged cables. In absolute terms, leakage current values remained near those of an unexposed, unaged sample (10^{-1} - 10^{-2} mA/ft). The insulation of one conductor in the unaged cable exposed to the most severe pulse broke down within seconds of the application of the 2400 Vac hi-pot test potential.

Transmitter output measurements performed between exposures to the heat flux pulses indicated slight changes in transmitter calibration from test to test for both specimens. These changes were generally larger in the unaged transmitter.

Calibration checks conducted in a pressure lab at the conclusion of the entire test series showed that the performance of both transmitter specimens (aged and unaged) fell

outside of manufacturers' technical specifications. For laboratory conditions, the accuracy should have been ±0.8 percent of full scale. The maximum deviation was -2.85 percent of full scale for the unaged transmitter at 1000 psig (the upper end of its operating span) and -2.15 percent for the aged transmitter (also at 1000 psig).

These tests demonstrate that the cables and transmitters, in both unaged and aged condition, can withstand exposure to very severe simulated hydrogen burn heat flux pulses and remain functional.

CONTENTS

LIST OF FIGURES

LIST OF TABLES

ACKNOWLEDGMENTS

The tests described in this report could not have been completed without the efforts of several individuals. The author gratefully acknowledges the contributions of Dave Johnson and Arlene Vance of Sandia Division 6222 who operated various CRTF systems used in these tests and Cheryl Maxwell of Division 6222 who supervised the operation of the CRTF during the tests. The contributions of Dave Furgal of Division 6433, whose detailed knowledge of the workings of the Barton pressure transmitter proved very valuable, are also gratefully acknowledged.

A special acknowledgment is due John Aragon, currently of Division 6433, whose efforts in preparation of the samples and setup of the test systems contributed greatly to the successful completion of the test series.

EXECUTIVE SUMMARY

The hydrogen burn event during to the Three Mile Island accident raised concern that a similar event at some future time could have a detrimental effect on equipment needed to monitor the reactor and maintain it in a safe condition. Since the accident, a large amount of analytical and experimental research addressing the question of equipment survivability in hydrogen burns has been conducted. Analytical efforts have included the development of computer codes which characterize the hydrogen burn pressure/temperature environment and which model equipment as a simple slab surface. Experimental work has included testing the thermal and operational responses of specimens of safety-related equipment to both actual and simulated hydrogen burns. The hydrogen burn tests have been conducted in vessels of various sizes, all of which are smaller than typical containment building volumes. Simulations of analytically characterized hydrogen burns in full-sized containments have also been performed using thermal radiation test facilities.

The analytical and experimental efforts to date have some limitations. The computer codes developed have been lumped parameter codes, which predict volume averaged and not local conditions. The thermal models of equipment are simple and, at best, only predict approximate thermal, and not operational, equipment responses. Uncertainties exist in extrapolated experimental results due to volume and geometry differences between the experimental vessels and actual containment buildings. Experimental results for a given set of preburn conditions (such as hydrogen and steam concentrations) cannot yet be extrapolated to a containment building with the same preburn conditions with the desired degree of confidence.

In order to address the uncertainties of equipment survival in hydrogen burns, a series of equipment tests was conducted at the Sandia National Laboratories Central Receiver Test Facility (CRTF). Specimens of nuclear qualified Brand Rex XLP/CU three-conductor cable and Barton Model 763 pressure transmitters were subjected to simulated hydrogen burns at increasing heat flux levels and their temperature response and performance were monitored. The cables and transmitters were tested in both an artificially (thermally) aged and unaged condition.

The test specimens were first exposed to a base heat flux pulse that conservatively simulated a deflagration resulting from a 75 percent core metal-water reaction in a reactor housed in a large dry containment building. After the base pulse, successive pulses were applied at heat flux levels which increased in increments of 50 percent of the base heat flux pulse. The heat flux levels throughout the final pulse were 300 percent of those of the base pulse. (This pulse is referred to as the factor 3.0 pulse. Similar designations apply to the other pulses used in the tests; i.e., factor 1.5 implies a pulse whose flux levels are 150 percent of those of the base pulse.) A separate cable sample was used for each cable test. The same transmitters were exposed to the succession of pulses. The objective of the test series was to study the response of the cables and transmitters to thermal pulses which enveloped, to the extent possible, margins in possible hydrogen burn thermal environments and to determine the effects of artificial aging on equipment exposed to those heat flux pulses.

Visually, the aged cables experienced less damage than the unaged cables when exposed to the same heat flux pulse. The differences were most pronounced for the initial base (factor 1.0) pulse and decreased as the severity of the pulses increased. All cables exhibited evidence of combustion. For the initial pulse and at flux levels 150 percent of the base pulse this evidence was confined to scorch marks on the sample mount. At flux levels greater than 150 percent of the base pulse, there were heavy soot deposits on the sample mounts.

Physical damage to the cables took the form of charring and mild blistering of the cable jacket at the lowest flux levels and severe blistering and cracking of the jacket at all higher levels. In some cases the jacket cracking was deep enough to expose the insulation of the cable conductors. However, the insulation remained intact and no insulation melting occurred. The white, fibrous, polymeric filler material packed between the cable conductors and the outer jacket did melt but had no apparent effect on cable performance.

The cables were electrically powered during exposure to the heat flux pulses and monitored for short circuits and open circuits. No shorts or open circuits were detected.

After exposure the cables were subjected to posttest high potential withstand (hi-pot) tests at 600, 1200, and 2400 Vac and insulation resistance (IR) was measured at 50 Vdc. Two samples, one unaged and one aged, which had not been exposed to the simulated hydrogen burns, were also included in the hi-pot and IR tests. These unexposed cables served as control samples for comparison with cables that were exposed to the heat flux pulses. Leakage currents during the hi-pot testing were on the order of 10^{-1} to 10^{-2} mA/ft for all samples, both unaged and aged, at all test voltages with one exception. The black wire insulation in the unaged cable exposed to the factor 3.0 pulse broke down within seconds after the application of the 2400 Vac potential.

Aging had a slight effect on the hi-pot leakage current results. The differences in leakage current between the aged cables and the unaged control were consistently greater than the differences between the unaged cables and the unaged control. Thus, aging plus exposure to the simulated hydrogen burns was found to increase leakage currents by a greater amount than exposure to the simulated burns alone. There was one exception to this trend. At the factor 3.0 exposure, the leakage current differences between the aged sample and unaged control were lower than the differences between the unaged exposed 3.0 sample and unaged control.

Aging did not have as great an effect on the insulation resistance measurements. All measured IR values were on the order of 10^{12} ohm-ft. The insulation resistance differences between the aged samples and unaged control were approximately the same as those between the unaged samples and unaged control.

The metal case of both the unaged and aged Barton transmitters reached high temperatures during testing. For the most severe pulses the highest measured casing temperature approached 500°F and the highest measured temperatures of the electronics inside the case were near 300°F. Despite these high temperatures, both transmitters performed properly during exposure to the simulated hydrogen burns and during posttest examinations.

Transmitter checks conducted immediately after each exposure to the heat flux pulses, while the specimens were still at elevated temperatures, indicated only slight changes in the calibration of both the aged and unaged transmitter from test to test. Generally, these changes were somewhat larger for the unaged transmitter.

Calibration checks conducted at ambient temperature in a pressure laboratory at the completion of the entire test series indicated a slight departure from the instrument's technical specifications at laboratory conditions. The specifications called for a maximum percent of full scale deviation (PFSD) of $\pm$0.8 percent. The maximum PFSD for the unaged transmitter at the completion of the test series (compared with its pretest calibration) was -2.85 percent at 1000 psig, the upper end of its operating range. The maximum PFSD for the aged transmitter was -2.15 percent, also at 1000 psig.

Several conclusions can be drawn from these tests. First, unaged and artificially (thermally) aged Brand Rex XLP/CU three-conductor cable was found to function during exposure to a heat flux pulse whose flux levels were 300 percent of those postulated to result from the combustion of hydrogen produced by a 75 percent core metal-water reaction in a reactor housed in a large dry containment building. With one exception, the cable samples displayed no significant insulation degradation in postexposure testing.

Second, thermal aging only slightly affects the degree to which Brand Rex insulation electrical properties change when exposed to a severe heat flux pulse. In quantitative terms, the leakage currents measured during high potential withstand tests following test exposure were low for both unaged and artificially aged samples (except for the unaged sample exposed to the factor 3.0 pulse whose black wire insulation broke down during the most severe hi-pot test). The changes in insulation resistance as measured at 50 Vdc were about the same for the unaged and thermally aged samples.

Third, both the unaged and thermally aged Barton Model 763 pressure transmitters withstood heat flux pulses considerably more severe than those anticipated for the 75 percent core metal-water event and continued to deliver a signal corresponding to the applied pressure.

Exposure to these severe heat flux pulses, individually and in toto, produced only small changes in transmitter calibration. (Results of these tests indicate that, while changes were quite small, the changes in the thermally aged transmitter were smaller than those of the unaged transmitter.)

1.0 INTRODUCTION

One of the many events that occurred during the Three Mile Island accident was a hydrogen burn which raised the pressure inside the containment building and, due to the heat of combustion, caused thermal damage to some materials inside the structure.[1] The damage to the materials inside the building raised a concern that a similar event in the future might degrade or incapacitate equipment necessary to monitor the reactor and maintain it in a safe condition.

Since the Three Mile Island accident a large amount of research has been done on equipment survival in hydrogen burns. This research has included both analytical computer code development and experimentation to verify the code models and study equipment behavior.

Two examples of the codes developed are HECTR (Hydrogen Event:Containment Transient Response)[2] and HYBER (Hydrogen Burn Equipment Response).[3] HECTR is a lumped parameter multi-volume code developed primarily to characterize the pressure/temperature response of the containment atmosphere to hydrogen burns. The code also contains simple models of metallic surfaces which serve as surrogates for actual pieces of equipment and which can be used to estimate equipment temperatures for predicted hydrogen burn environments resulting from different accident sequences. The surfaces are modeled as vertical one-dimensional slabs which are insulated on the back. HYBER is a single volume, lumped parameter code developed specifically for the analysis of equipment thermal response to hydrogen burns. The combustion and heat transfer models are similar to those in HECTR. The equipment models are also similar to the one-dimensional slab models in HECTR. HYBER was developed specifically for use with the IBM PC.

Experimental work has included tests of the thermal and operational responses of nuclear plant safety-related equipment to actual hydrogen burns in closed vessels. These tests have been conducted in vessels ranging in size from a few cubic meters to hundreds of cubic meters and have considered a wide range of steam and hydrogen concentrations.[1,5] Experimental simulations of analytically characterized hydrogen burns have also been performed.[6]

While all of these efforts have been helpful in assessing the survivability of safety-related equipment in hydrogen burns, some uncertainties have remained concerning equipment performance. Computer codes have been useful in describing global (i.e., volume-averaged) pressure-temperature environments resulting from hydrogen burns in closed vessels. Code results have compared very well with the large scale experimental results.[7] However, in terms of code predictions of equipment response, several uncertainties remain. First, all codes are global in nature. They predict global or average conditions for the volume under consideration. The extent to which global conditions are indicative of local conditions at a specific equipment location is not certain. Second, the models used to predict equipment thermal response are currently very simple. Equipment is generally modeled as a one-dimensional slab. There are no models of potentially flammable equipment such as cables. Third, codes can only be used to predict thermal response. There are no means by which actual equipment performance can be predicted.

The uncertainties in predicting equipment survival in containment buildings using experimental results are due to volume and geometry differences between actual containment structures and the test vessels. The severity and duration of hydrogen burn thermal environments for a given set of preburn conditions are very dependent upon the volume in which the burns occur.[8] The largest vessels currently used in hydrogen burn experiments are considerably smaller than typical reactor containment volumes.[4]

Geometry differences between experimental vessels and reactor containments also contribute to uncertainties in predicting equipment survival in containments from experimental results. Experimental vessels are, for the most part, cylindrical or spherical and have a single volume in which burns occur. Reactor containment buildings, while having a simple exterior geometry, are complex structures on the inside. The typical reactor containment consists of many interconnected compartments, passageways, and partitions. It will also contain large pieces of equipment such as coolant pumps and heat exchangers. These all affect, to varying degrees, parameters which ultimately determine the hydrogen burn environment. These parameters include hydrogen and steam transport, local hydrogen and steam concentrations, flame acceleration and local heat fluxes.

Uncertainties in analytical tools can be reduced at the expense of more complex computer codes and the use of more detailed equipment models. Such solutions would more accurately determine the thermal response of equipment when subjected to the hydrogen burn environment but would still not explicitly address the question of equipment performance.

Uncertainties in predictions of equipment survival based on experimental results can be lowered by conducting the experiments in vessels whose volume and geometry are similar to those of an actual containment. The definitive experiments would be ones which were conducted in an actual containment building. The cost and time associated with such endeavors is clearly prohibitive.

A series of tests was conducted at the Sandia National Laboratories Central Receiver Test Facility (CRTF) which used an alternative approach to reduce uncertainties in equipment performance in hydrogen burns. Specimens of nuclear-qualified cable and pressure transmitters were exposed to a simulation of a heat flux pulse from an experimental 13 volume-percent hydrogen deflagration in a large closed vessel.[5] This environment had been simulated previously at the CRTF[9] and, because of its high hydrogen concentration, had been determined to conservatively represent the analytically determined heat flux profile for a hydrogen burn in a large-dry reactor containment building.[10] After the initial exposure, which was a simulation of the actual burn, the specimens were exposed to heat flux pulses which simulated burns of increasing severity. The most severe heat flux pulse used had heat flux levels throughout the pulse that were three times as high as the initial pulse. Thus, the integrated incident flux was three times greater for the most severe exposure.

Specimens were tested in artificially aged and unaged condition.

The objectives of the test series were to study the response of typical pieces of safety-related equipment to severe thermal pulses that enveloped, to the extent possible, uncertainties in analytically and experimentally determined hydrogen burn thermal environments, and to determine the effects of aging on the response of the specimens to each pulse.

The temperature measurement results can also serve as a basis for the development of more accurate thermal models of equipment, which can be incorporated into existing hydrogen burn codes.

2.0 THE TEST ENVIRONMENT

The intent of this series of CRTF tests was to expose thermally aged and unaged pieces of safety-related equipment to heat flux pulses that enveloped, to the extent possible, uncertainties in the characterization of the thermal environment resulting from a credible hydrogen burn event in a large dry reactor containment. This was done by first exposing the specimens to a base heat flux pulse that simulated a postulated hydrogen burn event. Subsequent tests exposed the specimens to pulses whose heat fluxes at corresponding times in the pulse were raised in 50 percent increments above the base pulse flux levels. These exposures were conducted until a pulse was used whose flux levels were 300 percent of the base pulse flux levels.

The base pulse used for the CRTF tests was a simulation of a 13 volume-percent hydrogen premixed deflagration, which was one of several tests conducted by the Electric Power Research Institute (EPRI) at the Nevada Test Site (NTS).[9] The EPRI designation for this test was P20. To aid in the selection of the base case, a HECTR analysis of a hydrogen burn in a large, dry PWR containment was performed.[10] The HECTR analysis considered a hydrogen deflagration resulting from a 75 percent metal-water reaction. Comparison of the HECTR and P20 fluxes showed the flux profiles to be very similar and the peak heat flux from the P20 test to be slightly higher than the peak from the HECTR analysis. Because the P20 pulse had been previously simulated[9] and represented a slightly conservative pulse (due to the slightly higher peak) it was chosen as the base case for this series of CRTF tests.

The average total and average radiant heat fluxes produced by the EPRI-NTS 13 percent burn were determined using the SMOKE data reduction and analysis code.[11] These fluxes, the results of some of the earliest SMOKE analyses, are shown in Figures 2-1 and 2-2. The convective heat flux was taken to be the difference between the total and radiative fluxes.

Using the methods introduced in Reference 6, a separate set of solar heat flux profiles was determined for the transmitter and cable samples. The severity of the first profile corresponded to the EPRI-NTS P20 test and is equivalent to the sum of incident radiative and convective heat fluxes during that test. Subsequent profiles increased the heat flux at corresponding times in the pulse in 50 percent increments of the first pulse flux. Thus, at a given time in the second pulse the flux level was 1.5 times that of the first pulse. At the same time in the third pulse the flux level was 2.0 times the first pulse flux level and so on.

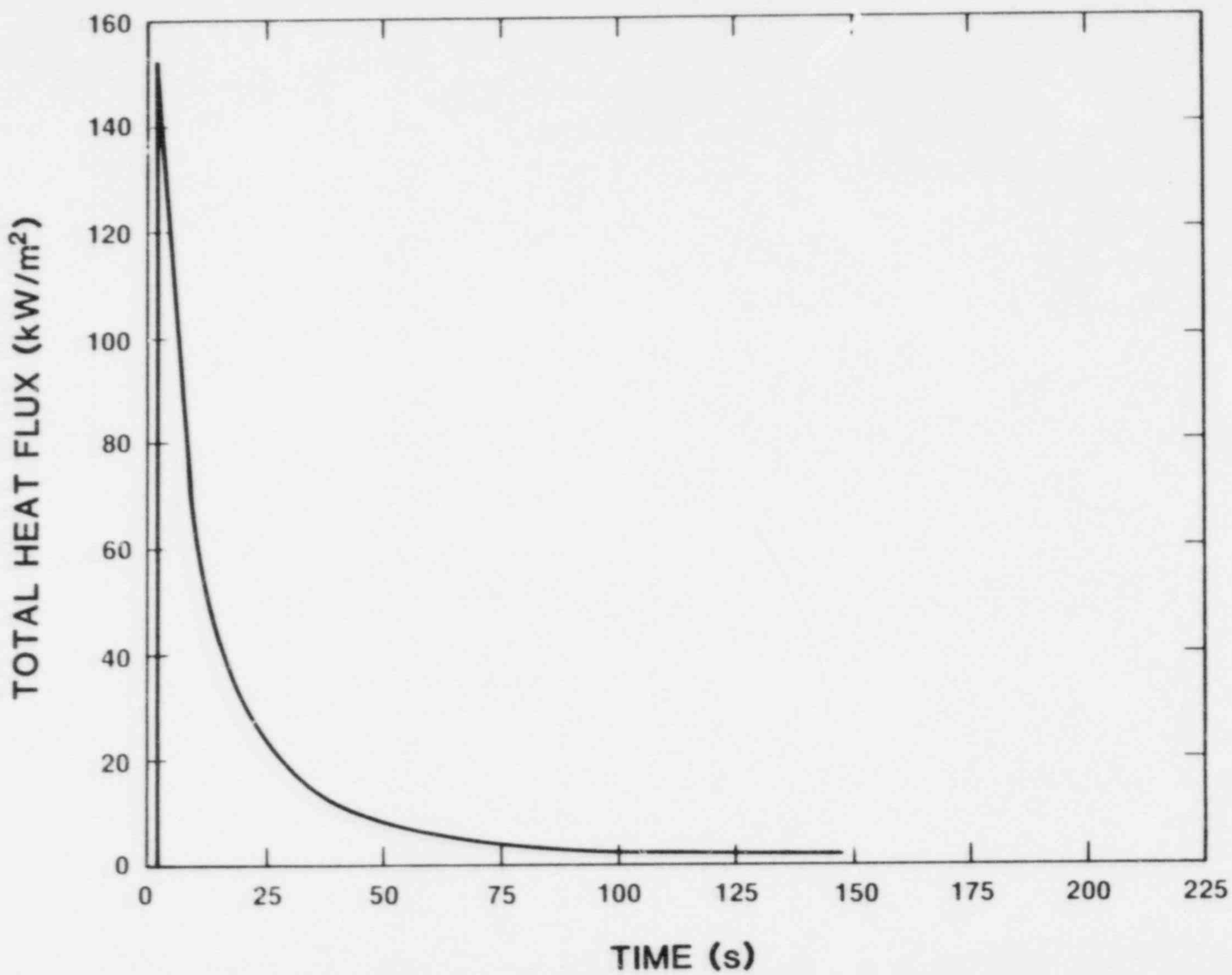

Figure 2-1. Average Total Heat Flux During the EPRI-NTS P20 Burn

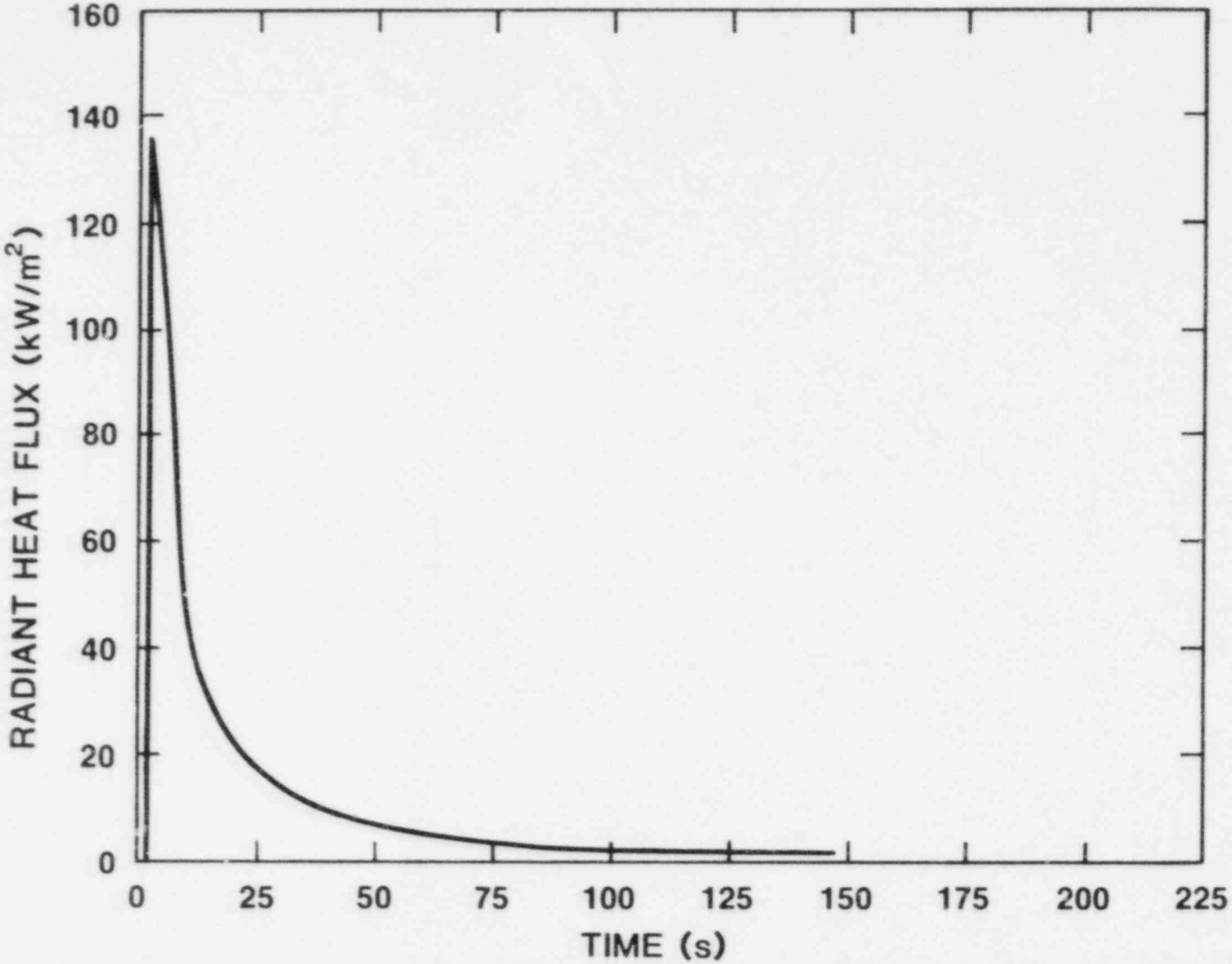

Figure 2-2. Average Radiant Heat Flux During the EPRI-NTS P20 Burn

Once the equivalent solar heat flux profiles were calculated, appropriate heliostats (solar reflecting mirrors) were selected from the CRTF heliostat array whose sum of flux-on-target capabilities was equal to the peak calculated flux. A removal scheme for these heliostats, corresponding to the flux decay of the calculated solar pulse, was then programmed into the CRTF heliostat control computer. The first flux profile in the cable profile sequence is shown in Figure 2-3. This profile corresponds in severity to the EPRI-NTC P20 test and in the sequence of cable profiles was designated the Cable Factor 1.0 Profile. The profile whose flux levels throughout the pulse were 1.5 times as great as the P20 base pulse fluxes was designated Factor 1.5, and so on. Thus, the integrated incident heat flux for each pulse, when compared to the base pulse, also corresponds to its factor designation.

Prior to exposure to the simulated hydrogen burn the transmitters were slowly preheated to approximately 250°F. The transmitter cover plate temperature was monitored during preheating. The rest of the transmitter was at a somewhat lower temperature than the cover plate. The 250°F preheat temperature was chosen in the interests of conservatism. It is approximately midway between the HECTR-determined initial cover plate temperature (138°F) of the aforementioned HECTR analysis[10] and a typical equipment qualification temperature (340°F).[15] It is also very near the predicted preburn temperature for the same surface in a previous analysis of a hydrogen burn in an ice condenser containment (242°F).[6]

The cable samples were not preheated. Because of their low heat capacity, cables would warm very rapidly even under the flux of a single heliostat and, due to the mechanics of bringing the remainder of the heliostats on target for the hydrogen burn simulation,[6] would also cool rapidly prior to exposure to the heat flux pulse. The absence of cable preheating had no effect on the results of these cable tests. Previous tests using the same type of cable[9] showed that the cables ignited immediately upon exposure to the heat flux pulse and it was the heat from the cable combustion that drove the initial temperature rise in the cable samples. The pulse used in this previous test series corresponded to the factor 1.0 pulse in the present tests. Thus, as the cable test series progressed to higher factors, preheating of the cable samples became even less important.

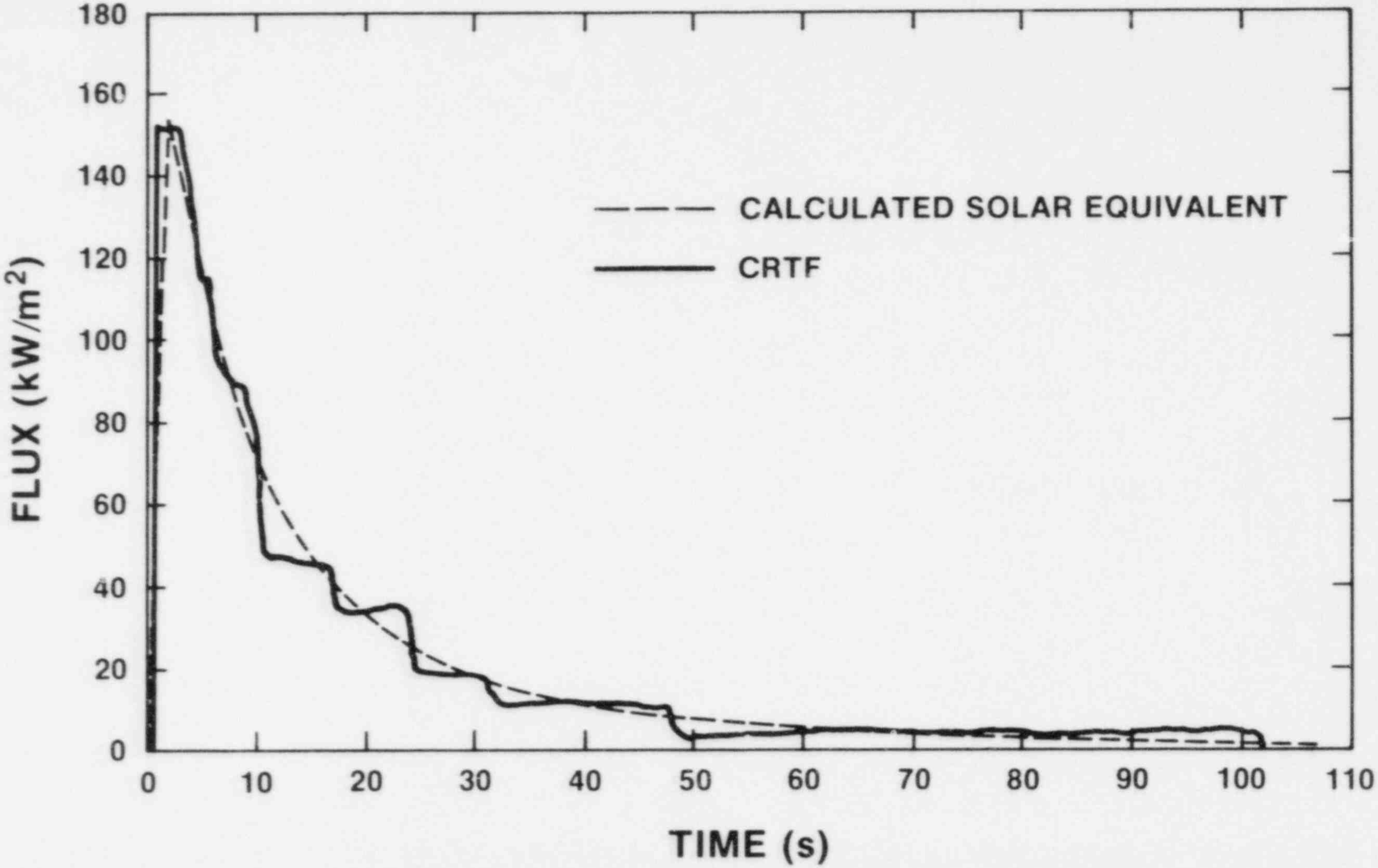

Figure 2-3. Cable Factor 1.0 CRTF Heat Flux Profile

3.0 TEST SPECIMENS AND TEST MEASUREMENTS

3.1 Cables

All cable samples used in the tests were sections of Brand Rex XLP/CU 12 AWG three conductor (3/C) cable. This cable was chosen because of its performance during a previous series of tests conducted at the CRTF.[10] Of several types of cable tested during the previous series, the Brand Rex 3/C sample exhibited the most vigorous combustion during testing and still functioned properly. (All other samples tested in the previous series also functioned properly but burned less vigorously during exposure to a simulated hydrogen burn.)

During exposure, the cables were connected in series with a resistance and a constant applied potential of 10 Vdc maintained across the cable-resistor circuit. Cable samples were monitored for open circuits and short circuits between conductors and to the test fixture upon which they were mounted. A separate cable sample was used for each test.

An unpowered length of cable was included in each test. This unpowered sample contained two thermocouples which provided sample temperature profiles during exposure to the heat flux pulses. Placement of the thermocouples is shown in Figure 3-1. The spacing in Figure 3-1 is exaggerated. The interior conductors and cable jacket are actually in close contact with each other. Thermocouple leads were routed to protect them from direct exposure to the heat flux pulses.

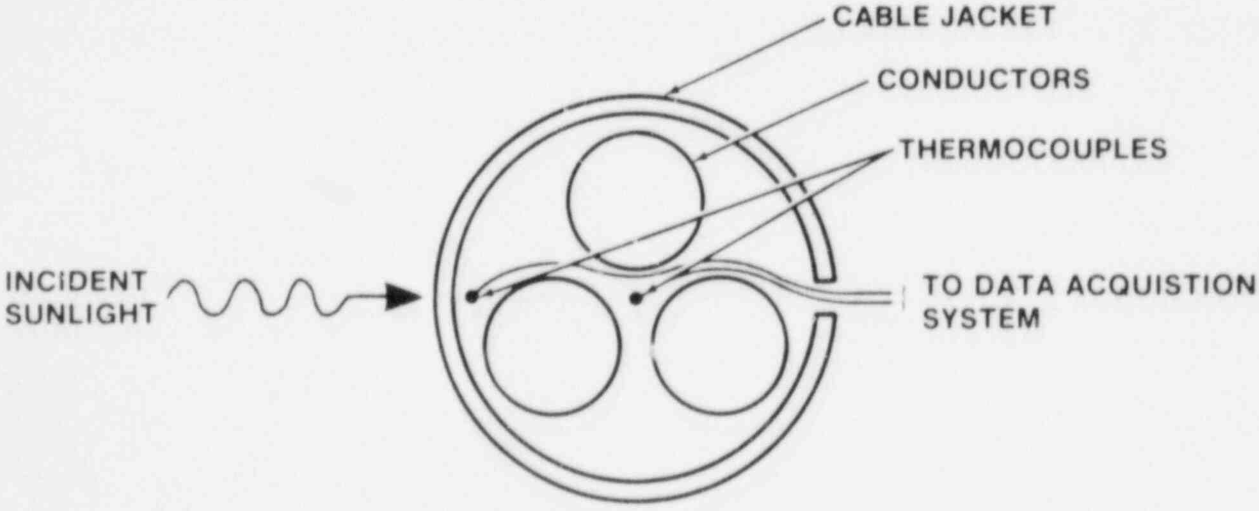

Figure 3-1. Unpowered Cable Thermocouple Placement

Aged cable samples were placed in that condition by thermal aging in an oven at 136°C (277°F) for 168 hours.[12] Unpowered samples used for temperature measurement during exposure of the powered aged samples were also aged.

3.2 Pressure Transmitters

The pressure transmitters used in these tests were both Barton Model 763 gauge pressure instruments. The operational pressure span of each was 0 to 1000 psig, with a signal output of 4 to 20 mA corresponding to the endpoints of the pressure range.

The pressure transmitter test setup is shown in Figure 3-2. The transmitter was the only portion of the setup which was exposed to the heat flux pulses. Each transmitter was tested separately.

After unpacking from their shipping cartons and initial examination, the calibration of each of the transmitters was checked and set per the manufacturers instructions[13] by the Test Measurements and Mechanical Design Division of Sandia National Laboratories, whose equipment calibration is traceable to the National Bureau of Standards. After calibration, one transmitter was aged at 125°C (257°F) for 1830 hours.[14]

After mounting the test specimen in the CRTF test bay, the calibration of each transmitter was checked over its operating span using the CRTF data acquisition system with the instrument at ambient temperature. The calibration of each transmitter was also rechecked after exposure to each heat flux pulse while the instruments were still at an elevated temperature. After completion of all exposures, each transmitter was returned to the Test Measurements and Mechanical Design Division for a final calibration check.

During testing the transmitters were held at a constant pressure of about 750 psig. Instrument output signal was monitored by passing the power supply current through two 1000-ohm resistors connected in parallel and measuring the voltage drop across this resistance. The voltage reference output voltage, the current amplifier output resistor voltage and the op-amp feedback loop output voltage were also measured.

Seven temperature measurements were also taken during each exposure. The temperatures of three electronic components were monitored: the Noise Suppression Capacitor, the Current Amplifier Output Transistor and the Voltage Reference Output Transistor. All of these electronic components are mounted on the printed circuit board inside the transmitter case. Temperatures of portions of the case were also monitored: the inside surface of the cover plate, the rear of the case, the potentiometer bracket, and the air inside the

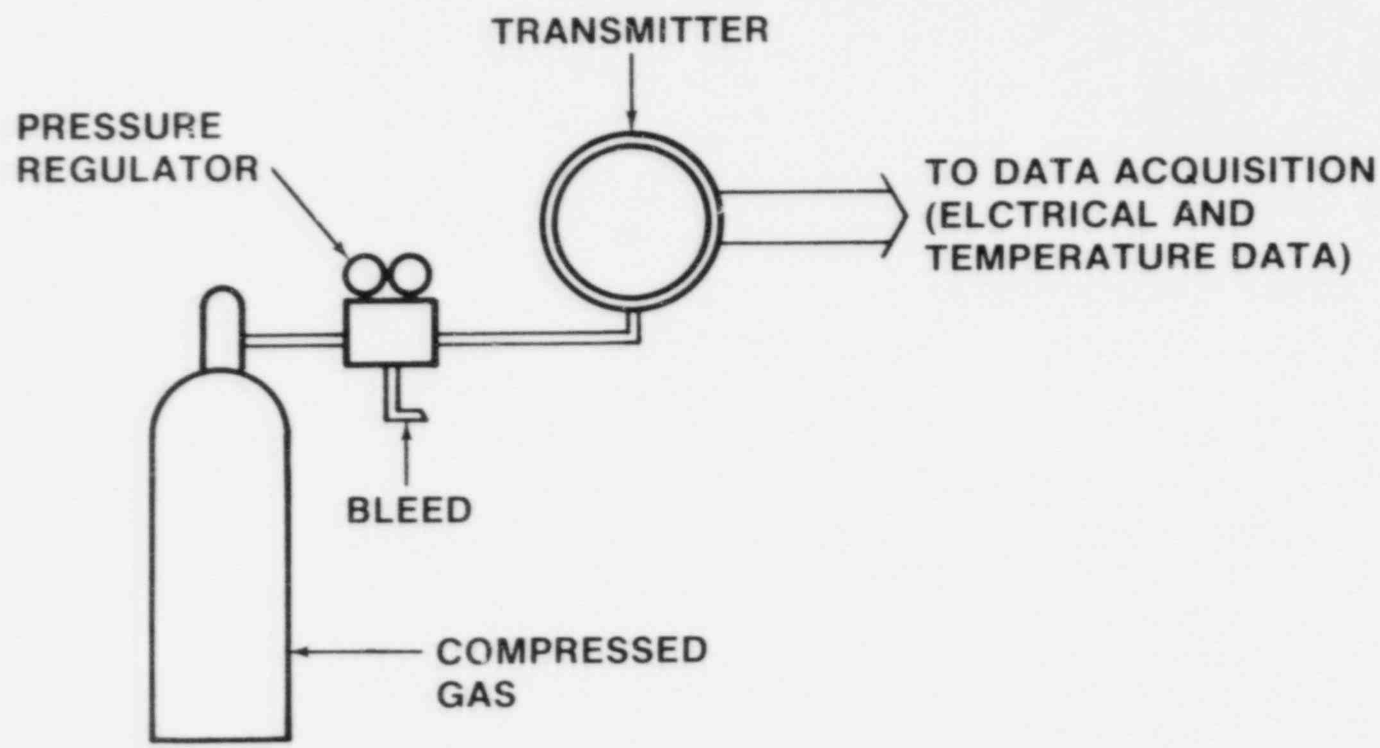

Figure 3-2. Pressure Transmitter Test Setup

transmitter case. Two thermocouples were mounted on the inside surface of the cover plate, one for monitoring by the data acquisition system and one connected to a hand-held digital thermometer for monitoring the temperature during preheating prior to the exposure to the simulated hydrogen burn.

4.0 RESULTS

4.1 Cables

The effects on cables, of exposure to the simulated hydrogen burns, fall into two categories: visible physical effects to the cable jackets and conductor insulation and changes in the electrical resistance properties of the cables.

4.1.1 Visible Effects

After exposure, all samples exhibited charring and blistering. The degree of visible damage varied with the severity of the pulse (i.e., factor 1.0 damage was less severe than factor 1.5 damage) and the preconditioning of the sample (aged or unaged). Observed damage is summarized in Table 4-1. Posttest photos of the cable specimens are shown in Figures 4-1 through 4-5. All samples and their sample mount fixtures showed evidence of combustion to varying degrees. The factor 1.0 and 1.5 sample mounts had some scorch marks and light soot deposits on them. Beyond factor 1.5 the soot deposits were heavier with increasing flux factors. For both of the factor 1.0 samples the small wires used to hold the cables on the sample mount provided some very localized protection from the test environment. A shadow effect from the test bay shutter cable which hung a few inches in front of the samples is also evident on these two cable specimens. At exposures above factor 1.5 the combustion of the cable jacket material negated the shielding provided by the moun wires and shutter cable shadow. Generally, for each pair of samples, the damage was somewhat more severe for the unaged samples than for the aged samples. This may be due to the effects of the artificial aging. The aged cables were brought to that condition by baking them in an oven at 277°F for 168 hours. This technique of achieving accelerated aging has been adopted as a standard for equipment qualification.[15] However, in terms of cable ignitability, this aging environment may have driven off many of the flammable jacket constituents which, in the unaged samples, were liberated and which ignited upon exposure to the heat flux pulse. The ignition of this additional fuel in the vicinity of the unaged cable samples would have resulted in a more severe local environment for those specimens. The flux levels of the higher factor pulses compensated for the missing cable jacket constituents and the damage to the aged and unaged cable specimens during the 2.5 and 3.0 exposures is more nearly the same.

The cracking and blisters on the unaged 2.5 and 3.0 samples showed a scalloped pattern. This pattern was most pronounced on the loops of cable closest to the center of the sample coil (see Figures 4-4 and 4-5). The sample bend

Table 4-1

Cable Physical Damage Summary

Pulse Factor	Sample Precondition	Observed Damage
1.0	Unaged	Continuous straight blisters and powdery char along entire jacket length. No interior insulation exposed. Mount wires provided localized protection. Shadow from shutter cable provided protection. Type and degree of damage comparable to NTS simulation test.[9] Scorch marks on mount.
1.0	Aged	Some char and minor blistering and flaking. Damage far less severe than 1.0 unaged sample. Mount wires provided protection and shutter cable shadow is evident. Light scorch marks on mount.
1.5	Unaged	Continuous straight blisters and powdery char along entire jacket length. Interior conductor insulation exposed in three locations. Slight insulation deformation at one of these locations. No protection from mount wires or shutter cable shadow.
1.5	Aged	Continuous straight blisters, flaking, and char along entire jacket length. Small hole in jacket with slight exposure of interior insulation. No degradation of the insulation was evident. No protection from mount wires or shutter cable shadow. Degree of damage is roughly the same as the 1.5 unaged sample.
2.0	Unaged	Continuous blisters and char along entire sample length. Edges of blisters were scalloped and blisters' height varies. Cracks in jacket followed contours of blisters exposing interior insulation. No protection from mount wires or shutter cable shadow.

Table 4-1 (continued)

Cable Physical Damage Summary

Pulse Factor	Sample Precondition	Observed Damage
2.0	Aged	Straight cracks along straight blisters of consistent height. Slight exposure of interior insulation. No protection from mount wires or shutter cable shadow. Severity of damage is somewhat less than that of unaged 2.0 sample.
2.5	Unaged	Scalloped blistering of jacket similar to unaged 2.0 sample but much more pronounced, especially at innermost loop of sample. This may be due to bending of sample (the bend radius was approximately 4" on inner loop). Insulation exposed in two areas. No insulation deformation was evident. No protection from mount wires or shutter cable shadow.
2.5	Aged	Straight, consistent height blistering along entire sample length. Cracking along length, interior insulation exposed, melted filler material in one location. Conductor was not exposed. No protection from mount wires or shutter cable shadow.
3.0	Unaged	Severe char and scalloped blistering and cracking, most pronounced on inside loop of sample. Insulation exposed in several places, melted filler material is evident. No conductors were exposed. Overall damage was most severe of all samples tested. Mount wires and shutter cable shadow gave no protection. Heavy soot on sample mount.
3.0	Aged	Continuous straight blistering, not as severe as the unaged 3.0 sample. Cracking, insulation exposed in several places, filler material melted. Mount wires and shutter cable shadow gave no protection. No conductors were exposed. Damage is severe but not as bad as the unaged 3.0 sample.

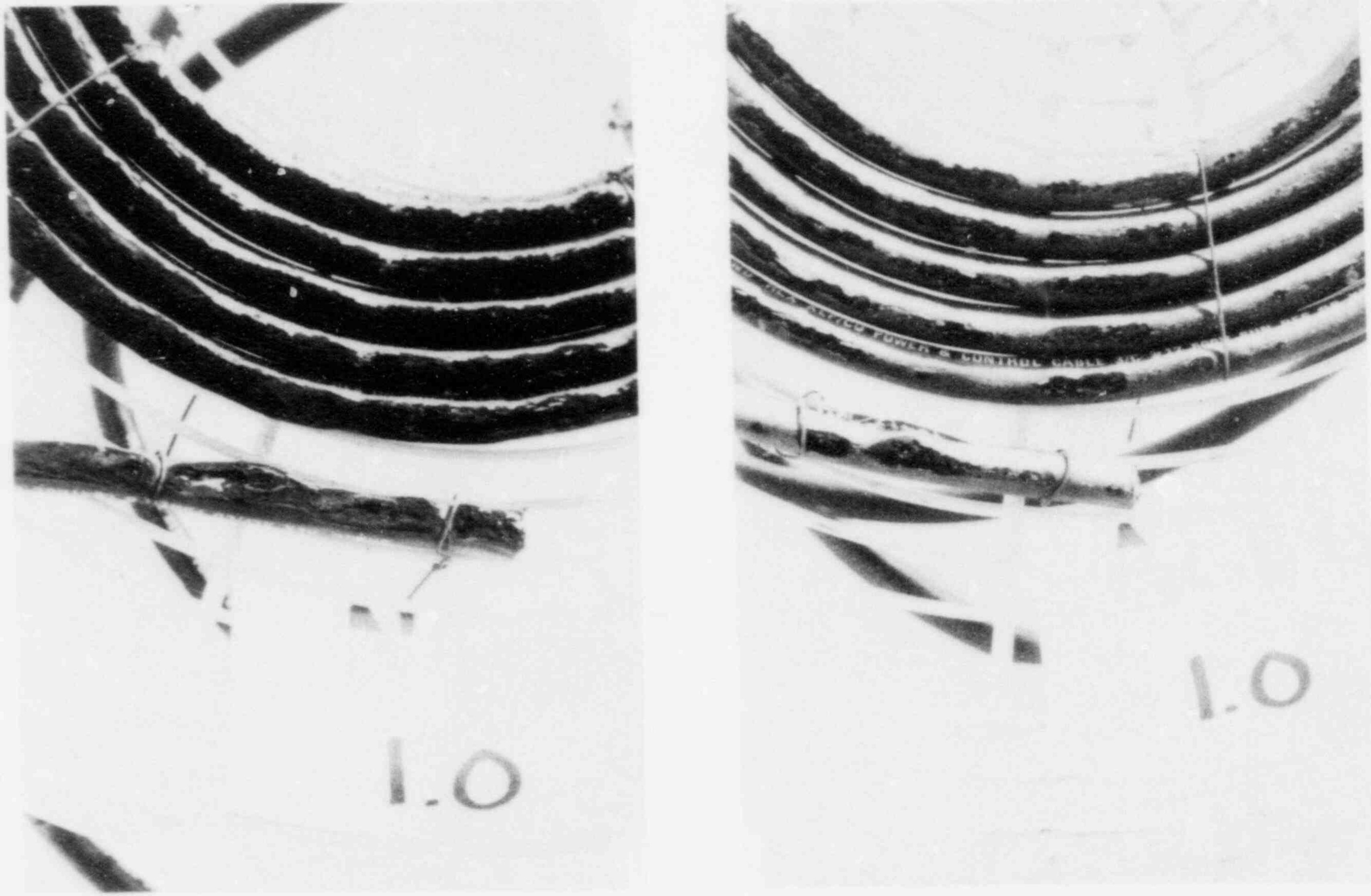

Unaged　　　　Aged

Figure 4-1. Factor 1.0 Cables After Exposure

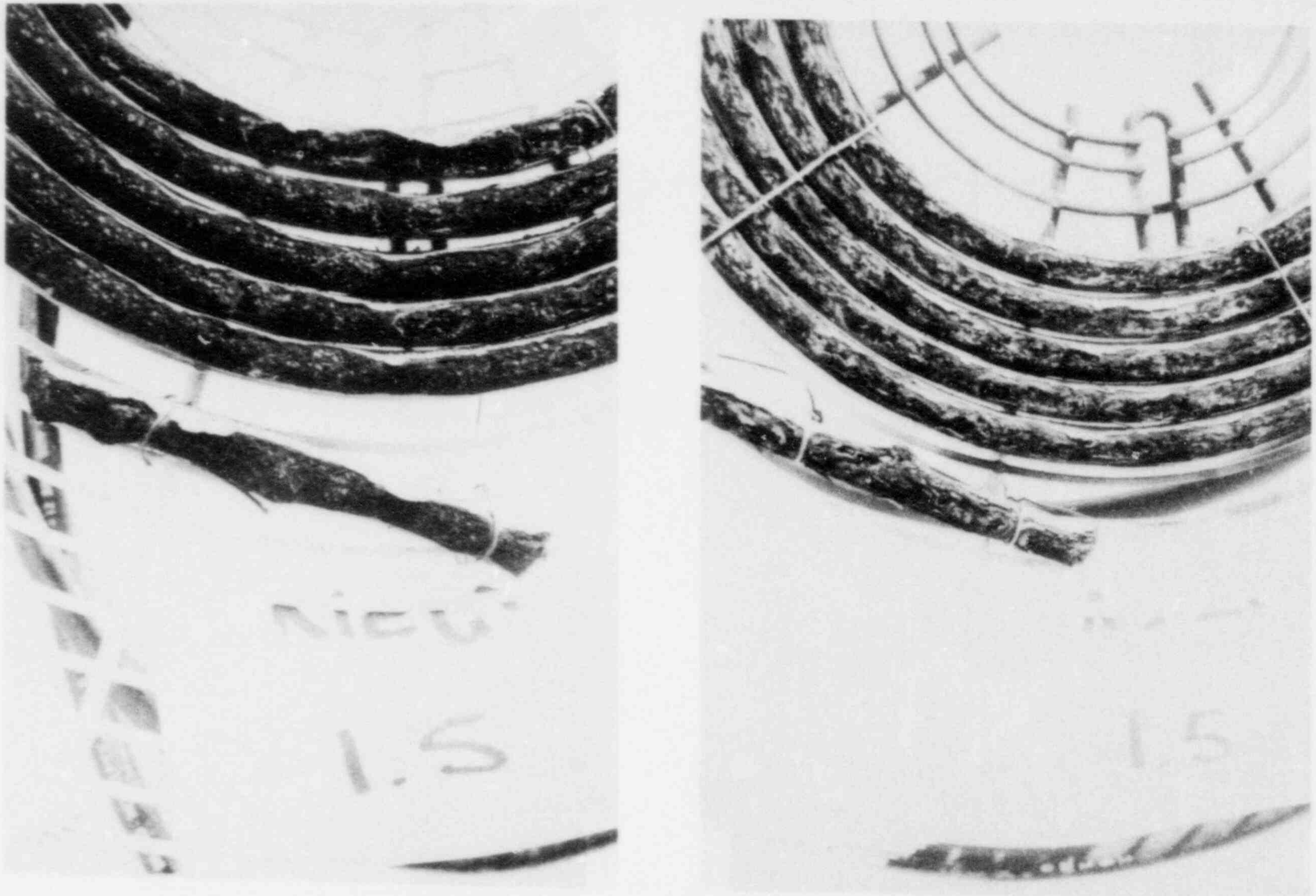

Unaged

Aged

Figure 4-2. Factor 1.5 Cables After Exposure

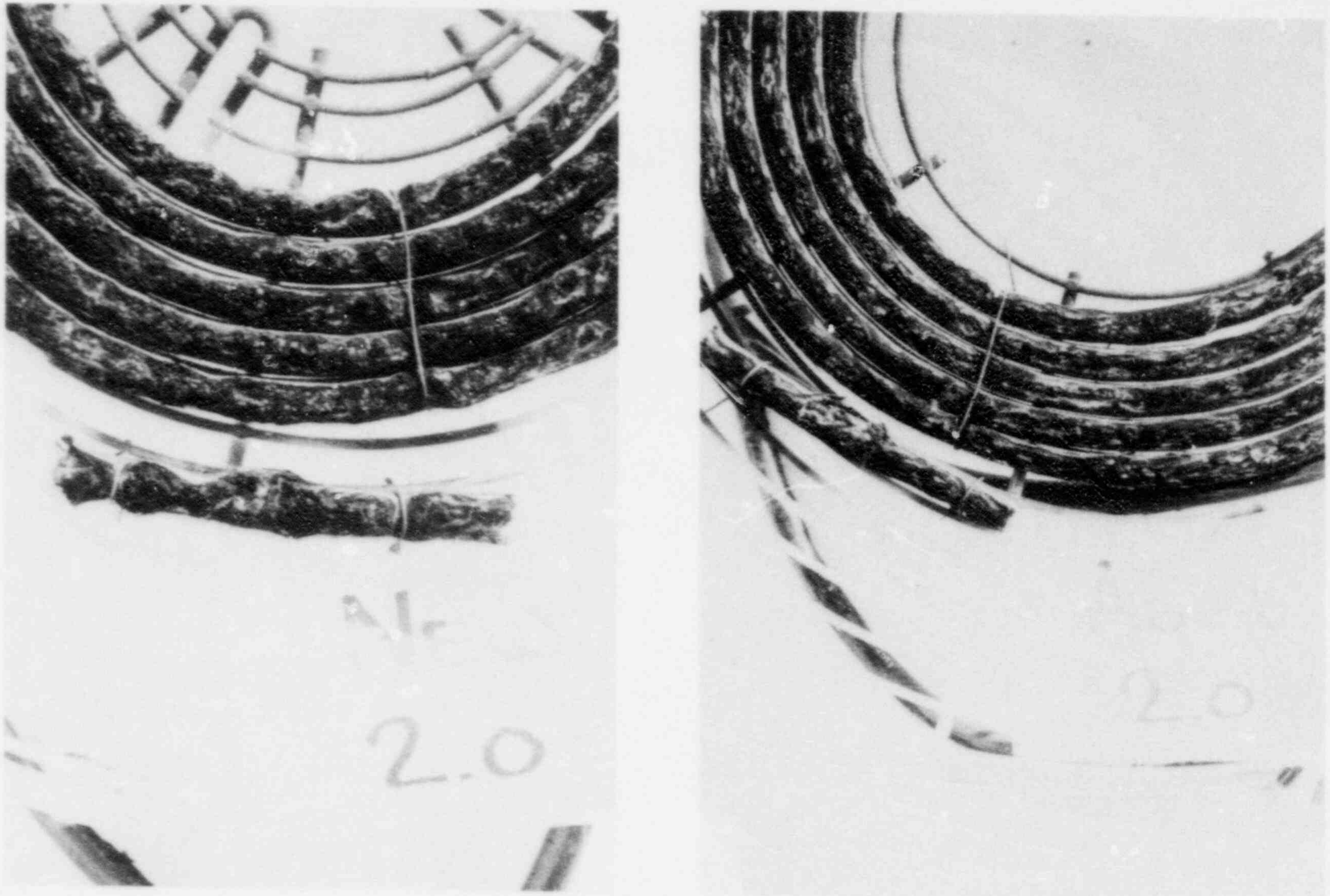

Unaged

Aged

Figure 4-3. Factor 2.0 Cables After Exposure

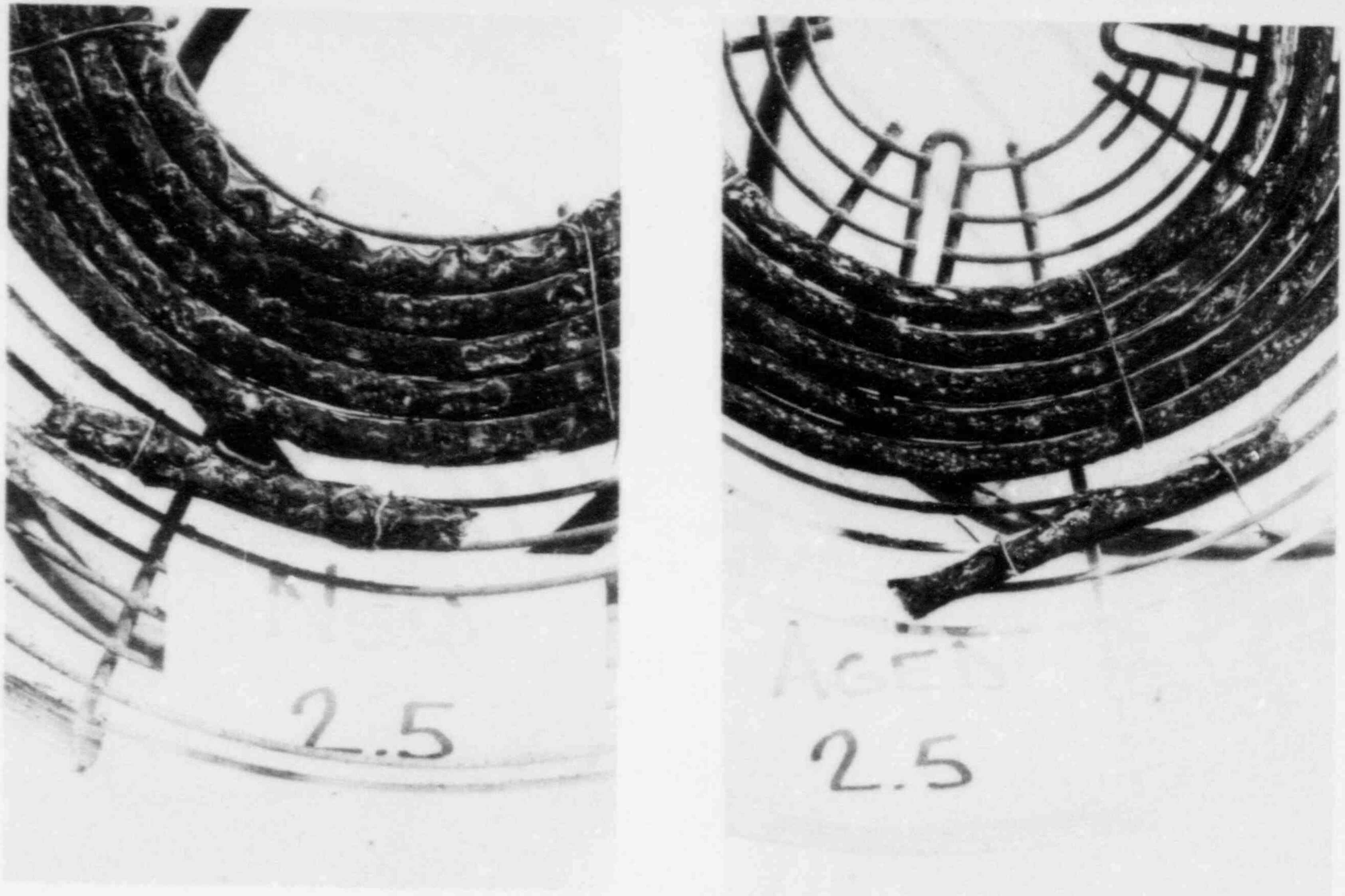

Unaged

Aged

Figure 4-4. Factor 2.5 Cables After Exposure

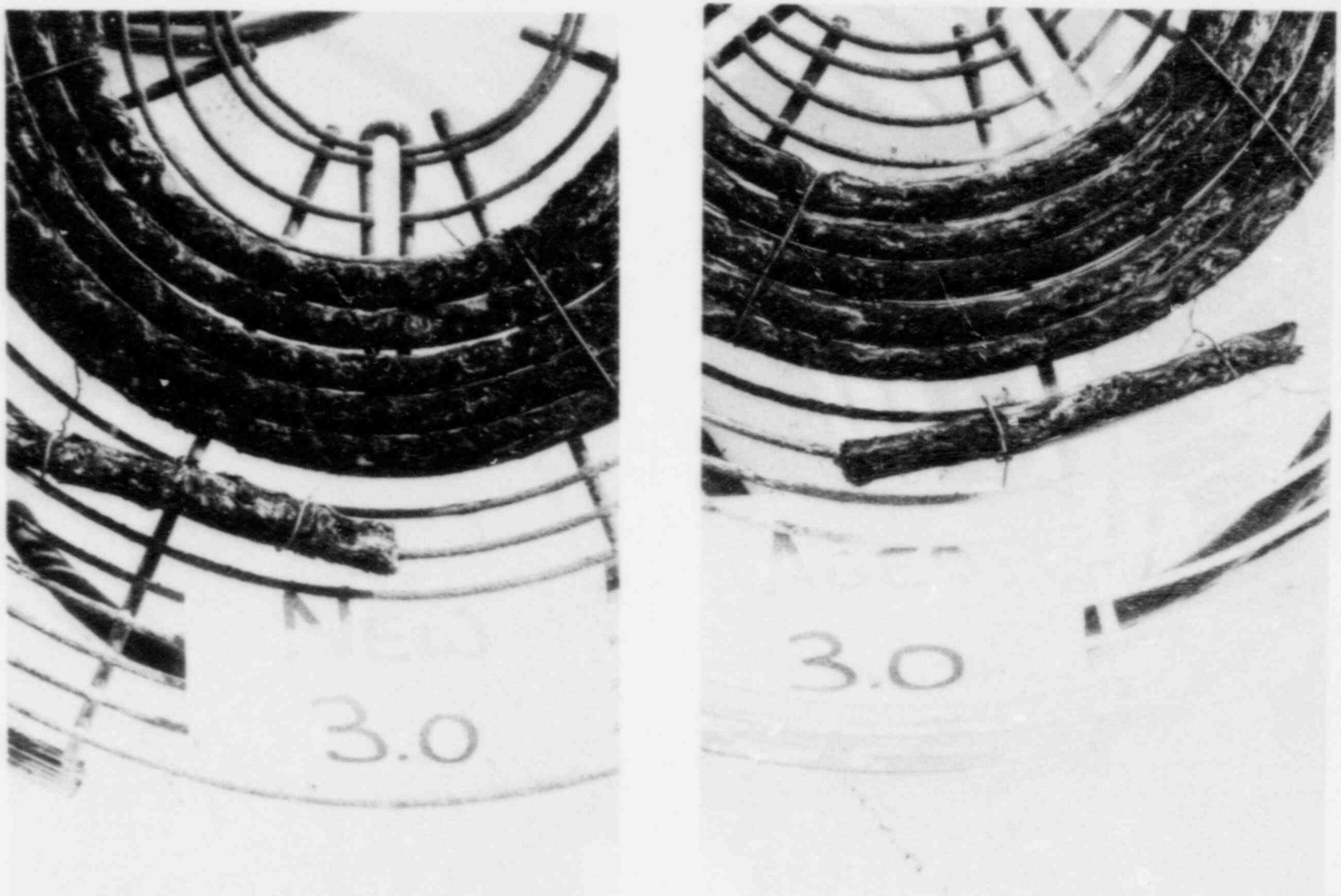

Unaged

Aged

Figure 4-5. Factor 3.0 Cables After Exposure

radius was approximately 4 inches for the inner loop of the cable samples. None of the aged samples displayed this scallop pattern.

As a result of the exposure to the heat flux pulses, all samples became charred. The char on the unaged samples had a powder-like consistency. The aged sample also had a powdery consistency but this was accompanied by flaking of the cable jacket.

In cases where the jacket was breached and the insulation of the conductors was exposed, the insulation remained intact. No copper conductors were exposed. Some of the exposed insulation experienced a slight flattening.

Some filler material melting was evident in samples whose jacket was breached. The white, fibrous, polymeric filler material inside the cables melted around some of the interior wires and refroze. No melting of the conductor insulation was evident in any of the samples.

Temperature traces for the unaged 2.5 sample are given in Figure 4-6 and peak temperatures for all samples measured during the 120 second test period are given in Table 4-2. Additional cable temperature plots are given in Appendix A.

Table 4-2

Maximum Measured Cable Temperatures

Cable Specimen (Unaged/Aged-Factor)	Max Jacket Temp. (°F)	Max Centerline Temp. (°F)
Unaged 1.0	470	233
Aged 1.0	338	208
Unaged 1.5*	323	225
Aged 1.5*	671	361
Unaged 2.0	582	325
Aged 2.0	827	403
Unaged 2.5	601	418
Aged 2.5	679	409
Unaged 3.0	**	**
Aged 3.0	721	458

*Tests exhibited erratic thermocouple signals.
**Jacket split, directly exposing thermocouples to heat flux. Recorded temperatures were not indicative of cable temperatures.

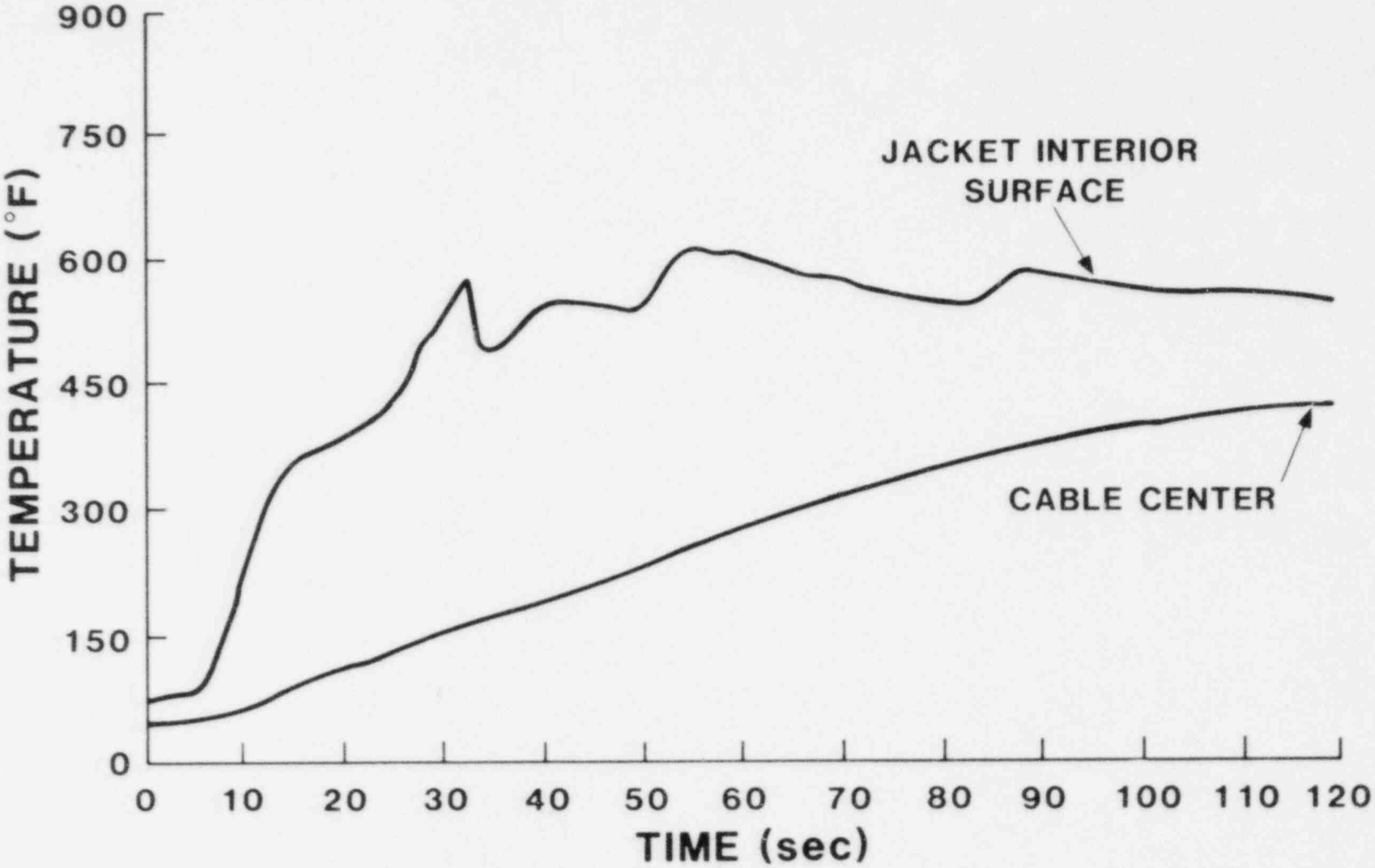

Figure 4-6. Factor 2.5 Unaged Cable Temperatures

All temperature traces for both unaged and aged samples exhibit similar characteristics. The inner surface of the jacket experienced a rapid temperature rise when exposure to the heat flux pulse was initiated and ignition occurred. After the initial rapid temperature increase the temperature continued to increase but in an irregular fashion. Toward the end of the pulse, as incident flux decreased to the lowest levels and combustion subsided, the temperature of the inside surface of the jacket started a steady decline.

With the exception of the unaged and aged factor 1.5 samples, which exhibited signal anomalies, the centerline temperatures exhibited steady rises throughout the exposures. At the end of the 120 second data acquisition run the centerline temperatures of all samples were all increasing very slowly or had leveled off.

Table 4-2 compares the maximum cable temperatures measured during the 120 second data acquisition time period. The lower jacket temperature for the aged 1.0 sample accounts for the less severe damage to that sample than was experienced by the unaged 1.0 sample. Subsequent tests at higher factors resulted in the aged sample jackets reaching considerably higher temperatures than the unaged samples tested at the same flux levels. Yet, posttest visual inspection of the samples indicated that, in general, the visible damage to the unaged samples was slightly more severe than the visible damage to the aged samples. Jacket temperatures for the unaged 3.0 sample are unavailable. Immediately upon exposure to the simulated hydrogen burn, the jacket of the unpowered specimen split, exposing the thermocouples to the incident heat flux. As a result, the indicated temperatures followed the flux profile and not the cable temperatures. Temperatures at the cable centerline follow the same pattern by flux factor as the jacket inside surface temperatures.

4.1.2 Effects on Cable Electrical Performance

As stated earlier, the cable samples were powered during testing and monitored for open circuits, for short circuits between individual conductors, and for short circuits between conductors and the sample mount. No short or open circuits were detected in any sample during exposure to the heat flux pulses.

After exposure to the simulated hydrogen burns, all cable samples were subjected to high-potential withstand (hi-pot) testing and insulation resistance (IR) testing. Both postexposure tests were conducted with the cable specimens submerged in water. In addition to the exposed specimens, the hi-pot and IR tests were also performed on aged and unaged unexposed samples of the same cable. These unexposed cables served as control samples.

The high-potential withstand testing was conducted using a Hipotronics HD103 hi-pot tester. The insulation resistance testing was done using a Hewlett Packard 4329A High Resistance meter. The setup for both tests is shown schematically in Figure 4-7. For the hi-pot tester, the meter was a milliammeter and testing was conducted at three voltages: 600, 1200, and 2400 Vac. For the HP high resistance meter, the meter was an ohmmeter and the voltage was set to 50 Vdc. After the initial application of the voltage in each test a two-minute waiting period was observed before any readings were taken.

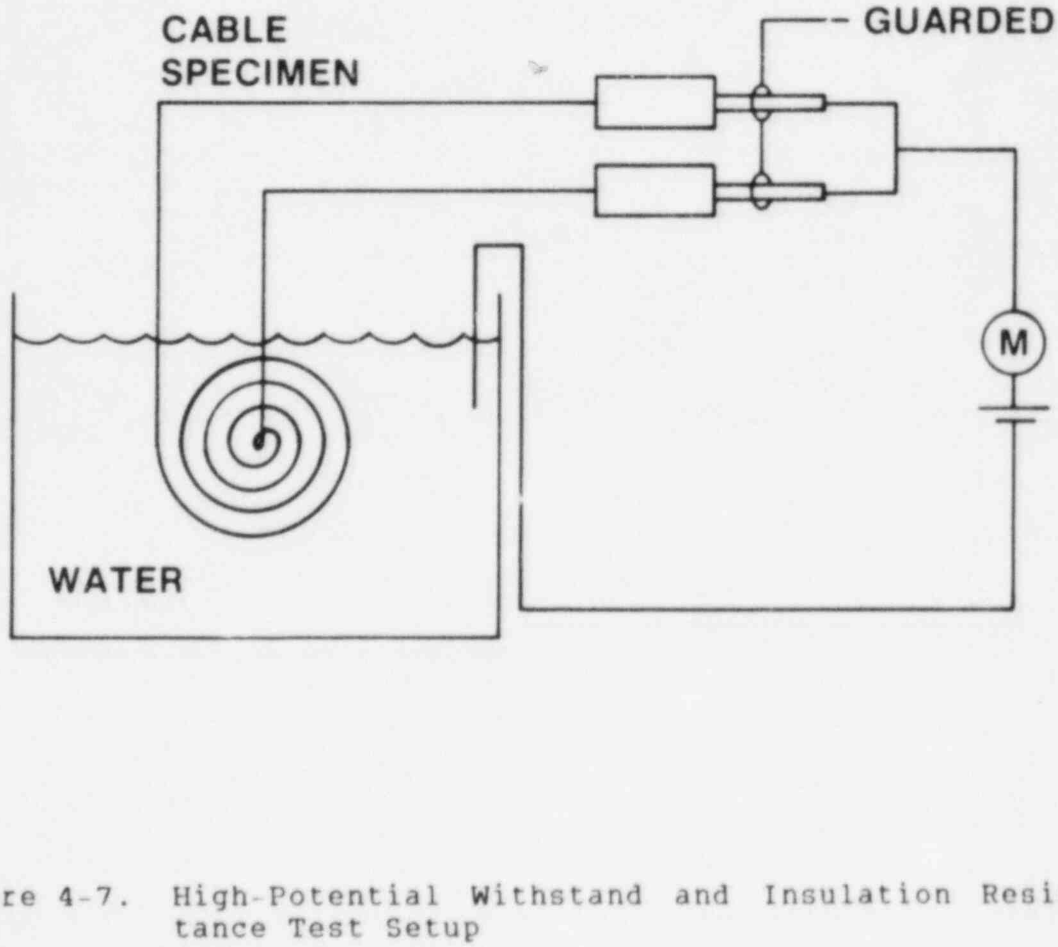

Figure 4-7. High-Potential Withstand and Insulation Resistance Test Setup

High-potential withstand test results are given in Table 4-3. Table 4-4 gives the percent difference in leakage current between the exposed cable specimens and the appropriate (aged or unaged) control sample. The percent difference was determined using the equation:

$$\% \text{ Diff} = \frac{\text{(Exposed - Control) Leakage Current}}{\text{Control Leakage Current}} \times 100\% \quad (4\text{-}1)$$

for each applied voltage.

The parenthetical values for the aged specimens are the leakage current percent differences between the aged cables and the unaged control sample.

Generally, the exposed aged samples exhibited less of a difference with the aged control than did the unaged samples with the unaged control. It is also noted that leakage currents from the aged control sample are only slightly higher than from the unaged control (see Table 4-3).

At the 600 Vac hi-pot test voltage the differences between the aged and unaged exposed samples and their respective control samples are generally less than 20 percent. The one exception to this is the unaged 3.0 sample. The three conductor average percent difference for that sample is 27 percent.

Both the unaged and aged cables show the greatest difference with their respective control samples starting at the factor 2.5 exposure and the 1200 Vac hi-pot test voltage. Larger differences are evident at the 2400 Vac test voltage.

With respect to all exposed cable samples, the largest differences are apparent at 1200 Vac and 2400 Vac for the unaged 3.0 sample. Interestingly, the two conductors that exhibited the largest difference at 1200 volts in this sample (white and pink) maintained that difference at 2400 volts. The black conductor, which differed with the unaged control black conductor by 33 percent at 1200 Vac, broke down within seconds of the application of the 2400 Vac hi-pot voltage.

The aging process had a slight effect on the leakage current of the aged specimens. The percent differences in leakage currents (Table 4-4) between the aged control and unaged control samples show that aging had approximately the same effect on leakage current as did exposure of an unaged sample to the factor 1.0 simulated hydrogen burn. Comparison of the leakage current percent differences between the unaged cables and unaged control and the aged cables and unaged control shows that aging plus exposure resulted in slightly higher leakage currents than did exposure alone with one

Table 4-3

Cable High-Potential Withstand Leakage Currents

Sample and Conductor	Leakage Current (mA/ft and mA/m) at 600 Vac	1200 Vac	2400 Vac
Unaged Control			
White	0.012/0.041	0.023/0.076	0.046/0.152
Black	0.013/0.044	0.024/0.080	0.049/0.160
Pink	0.012/0.041	0.023/0.074	0.046/0.152
Unaged 1.0			
White	0.013/0.044	0.026/0.086	0.052/0.171
Black	0.014/0.046	0.027/0.088	0.052/0.171
Pink	0.014/0.046	0.026/0.086	0.052/0.171
Unaged 1.5			
White	0.014/0.046	0.028/0.091	0.053/0.174
Black	0.013/0.044	0.027/0.088	0.053/0.174
Pink	0.013/0.044	0.027/0.088	0.052/0.170
Unaged 2.0			
White	0.012/0.041	0.025/0.081	0.049/0.162
Black	0.012/0.041	0.025/0.081	0.049/0.162
Pink	0.012/0.041	0.025/0.081	0.049/0.162
Unaged 2.5			
White	0.013/0.044	0.030/0.097	0.061/0.199
Black	0.013/0.044	0.030/0.097	0.061/0.199
Pink	0.013/0.044	0.028/0.093	0.058/0.190
Unaged 3.0			
White	0.016/0.051	0.034/0.112	0.068/0.222
Black	0.015/0.049	0.032/0.105	Broke Down
Pink	0.016/0.051	0.034/0.112	0.068/0.222
Aged Control			
White	0.013/0.042	0.027/0.087	0.053/0.175
Black	0.013/0.042	0.029/0.094	0.053/0.175
Pink	0.013/0.042	0.027/0.087	0.053/0.175
Aged 1.0			
White	0.013/0.042	0.028/0.092	0.056/0.185
Black	0.013/0.042	0.028/0.092	0.056/0.185
Pink	0.013/0.042	0.027/0.087	0.054/0.179
Aged 1.5			
White	0.015/0.049	0.030/0.097	0.059/0.194
Black	0.015/0.049	0.030/0.097	0.059/0.194
Pink	0.015/0.049	0.030/0.097	0.059/0.194

Table 4-3 (continued)

Cable High-Potential Withstand Leakage Currents

Sample and Conductor	Leakage Current (mA/ft and mA/m) at 600 Vac	1200 Vac	2400 Vac
Aged 2.0			
White	0.015/0.049	0.029/0.095	0.058/0.191
Black	0.015/0.049	0.030/0.097	0.059/0.194
Pink	0.015/0.049	0.029/0.095	0.058/0.191
Aged 2.5			
White	0.014/0.047	0.031/0.101	0.062/0.203
Black	0.014/0.047	0.030/0.097	0.061/0.200
Pink	0.014/0.047	0.030/0.097	0.062/0.203
Aged 3.0			
White	0.014/0.047	0.030/0.097	0.060/0.195
Black	0.014/0.047	0.030/0.097	0.057/0.187
Pink	0.014/0.047	0.028/0.092	0.056/0.183

Table 4-4

Leakage Current Deviation From Control Samples

Sample and Conductor	Leakage Current Percent Difference (%) at 600 Vac	1200 Vac	2400 Vac
Unaged 1.0			
White	8.33	13.04	13.04
Black	7.69	12.50	6.12
Pink	16.67	13.04	13.04
Unaged 1.5			
White	16.67	21.74	15.22
Black	0.00	12.50	8.16
Pink	8.33	17.39	13.04
Unaged 2.0			
White	0.00	8.70	6.52
Black	-7.69	4.17	0.00
Pink	0.00	8.70	6.52
Unaged 2.5			
White	8.33	30.43	32.61
Black	0.00	25.00	24.49
Pink	8.33	21.74	26.09
Unaged 3.0			
White	33.33	47.83	47.83
Black	15.38	33.33	Broke Down
Pink	33.33	47.83	47.83
Aged Control			
White	--- (8.33)*	--- (17.39)	--- (15.22)
Black	--- (0.00)	--- (20.83)	--- (8.16)
Pink	--- (8.33)	--- (17.39)	--- (15.22)
Aged 1.0			
White	0.00 (8.33)	3.70 (21.74)	5.66 (21.74)
Black	0.00 (0.00)	-3.45 (16.67)	5.66 (14.29)
Pink	0.00 (8.33)	0.00 (17.4)	1.89 (17.39)
Aged 1.5			
White	15.38 (25.00)	11.11 (30.43)	11.32 (28.26)
Black	15.38 (15.38)	3.45 (25.00)	11.32 (20.41)
Pink	15.38 (25.00)	11.11 (30.43)	11.32 (28.26)
Aged 2.0			
White	15.38 (25.00)	7.41 (26.09)	9.43 (26.09)
Black	15.38 (15.38)	3.45 (25.00)	11.32 (20.41)
Pink	15.38 (25.00)	7.41 (26.09)	9.43 (26.09)

Table 4-4 (continued)

Leakage Current Deviation From Control Samples

Sample and Conductor	Leakage Current Percent Difference (%) at 600 Vac	1200 Vac	2400 Vac
Aged 2.5			
White	7.69 (16.67)	14.81 (34.78)	16.98 (34.78)
Black	7.69 (17.69)	3.45 (25.00)	15.09 (24.49)
Pink	7.69 (16.67)	11.11 (30.43)	16.98 (34.78)
Aged 3.0			
White	7.69 (16.67)	11.11 (30.43)	13.21 (30.43)
Black	7.69 (7.69)	3.45 (25.00)	7.55 (16.33)
Pink	7.69 (16.67)	3.70 (21.74)	5.66 (21.74)

*Values in parentheses are percent differences of aged samples with the unaged control sample.

significant exception. At the factor 3.0 exposure level, the leakage current percent differences between the exposed aged sample and the unaged control are consistently lower than the percent differences between the exposed unaged sample and the unaged control. Thus, the aged cable was better able to withstand the most severe pulse than was the unaged cable.

In terms of withstanding the effects of exposure to the simulated hydrogen burn, one other factor may be significant. The results in Table 4-4 indicate that both the unaged and aged black conductors consistently exhibited smaller percent differences with the unaged black control conductor than did the other two conductors with their respective unaged control. Thus, pigmentation, which may affect material formulation, may play a role in determining an insulation material's resistance to degradation.

Insulation resistance (IR) testing at 50 Vdc was conducted after hi-pot testing. Measured insulation resistances are given in Table 4-5. The insulation resistances are given in units of ohm-ft and ohm-m. The derivation of this resistance-length unit is given in Appendix B. Insulation resistance percent differences between exposed specimens and their respective control samples are given in Table 4-6. The parenthetical values for the aged cables are the percent differences between the aged specimens and the unaged control cable. The IR percent differences were determined using the equation:

$$\% \text{ Diff} = \frac{\text{IR (Exposed Sample)} - \text{IR (Control)}}{\text{IR (Control)}} \times 100\% \quad . \qquad (4\text{-}2)$$

Table 4-6 shows the unaged samples experienced reductions in insulation resistance compared with the unaged control sample. Reductions in the IR of the exposed aged specimens as compared with the aged control were not as great. However, comparison of the IR percent differences between the exposed aged specimens and the unaged control shows that the combination of aging and exposure to the simulated hydrogen burns resulted in roughly the same decrease in IR as exposure to the simulated burns alone at all flux levels with one exception. At the 1.0 flux level the reduction in the aged specimen IR below that of the unaged control cable is significantly less than for the unaged 1.0 sample. Unlike the hi-pot results, the black conductors were no less prone to IR reduction than were the white or pink wires.

Table 4-5

Cable Sample Insulation Resistance

Sample	White	Black	Pink
	Conductor Insulation Resistance (10^{12} ohm-ft/10^{11} ohm-m)		
Unaged Control	1.36/4.13	1.38/4.20	1.38/4.20
1.0	0.751/2.29	0.751/2.29	0.778/2.37
1.5	0.762/2.32	0.762/2.32	0.804/2.45
2.0	0.873/2.66	0.876/2.67	0.941/2.87
2.5	0.771/2.35	0.771/2.35	0.771/2.35
3.0	0.771/2.35	*	0.785/2.39
Aged Control	0.930/2.84	1.27/3.89	0.930/2.84
1.0	0.978/2.98	0.978/2.98	1.02/3.11
1.5	0.825/2.51	0.840/2.56	0.810/2.47
2.0	0.825/2.51	0.798/2.43	1.23/3.77
2.5	0.807/2.46	0.779/2.38	0.785/2.39
3.0	0.951/2.90	0.935/2.85	0.935/2.85

*The unaged 3.0 black conductor broke down during hi-pot testing; as a result this conductor had no detectible IR.

Table 4-6

Insulation Resistance Deviation From Control Samples

Sample	White	Black	Pink
	Conductor IR Percent Difference (%)		
Unaged			
1.0	-44.78	-45.58	-43.62
1.5	-43.97	-44.78	-41.74
2.0	-35.81	-36.52	-31.81
2.5	-43.31	-44.13	-44.13
3.0	-43.31	*	-43.12
Aged Control	--- (-31.62)**	--- (-7.97)	--- (-32.61)
1.0	5.16(-28.09)	-22.99(-29.13)	9.68(-26.09)
1.5	-11.29(-39.34)	-33.86(-39.13)	-12.90(-41.30)
2.0	-11.29(-39.34)	-37.17(-42.17)	32.26(-10.86)
2.5	-13.23(-40.66)	-38.66(-43.55)	-15.59(-43.12)
3.0	2.26(-30.07)	-26.38(-32.25)	0.54(-32.25)

*Unaged 3.0 black conductor insulation failed during hi-pot testing.

**Values in parentheses are percent differences of aged samples with the unaged control sample.

4.2 Barton Transmitters

4.2.1 Temperature Response

A typical maximum qualification temperature for class 1E equipment is 340°F (171°C). During the course of the testing this temperature was exceeded several times by the transmitter case of both the aged and unaged samples. However, due to the transient nature of the heat input, none of the interior electronics reached this temperature. The temperature responses of both transmitters were similar with slight differences occurring as a result of air currents in the open test bay during the unaged, factor 3.0 exposure. The maximum measured temperatures from the transmitter tests are given in Table 4-7. Electrical components reached their highest temperature after exposure was completed, as heat from the casing was transferred to the interior of the instruments.

The only damage observed during these tests was the melting of insulation on two data lines which were installed in one transmitter to monitor aspects of its electrical performance. The data lines were not part of the transmitter. Their sole purpose was to monitor transmitter performance during testing. Thus, the melting of the insulation should not be taken to reflect upon the performance of the transmitter.

Table 4-7

Barton Transmitter Maximum Measured Component Temperatures

Component	Maximum Temperature (°F)
Front Plate	498
Rear of Case	260
Inside Air	336
Potentiometer Bracket	258*
Capacitor	287*
Current Amp Transistor	291*
Voltage Ref Transistor	284*

*These temperatures were reached after exposure to the simulated hydrogen burn was completed.

Temperature profiles for the casing and some of the interior electronics at the 3.0 exposures are given in Figures 4-8 through 4-11 for unaged and aged specimens. Temperature profiles for other exposures are given in the appendices.

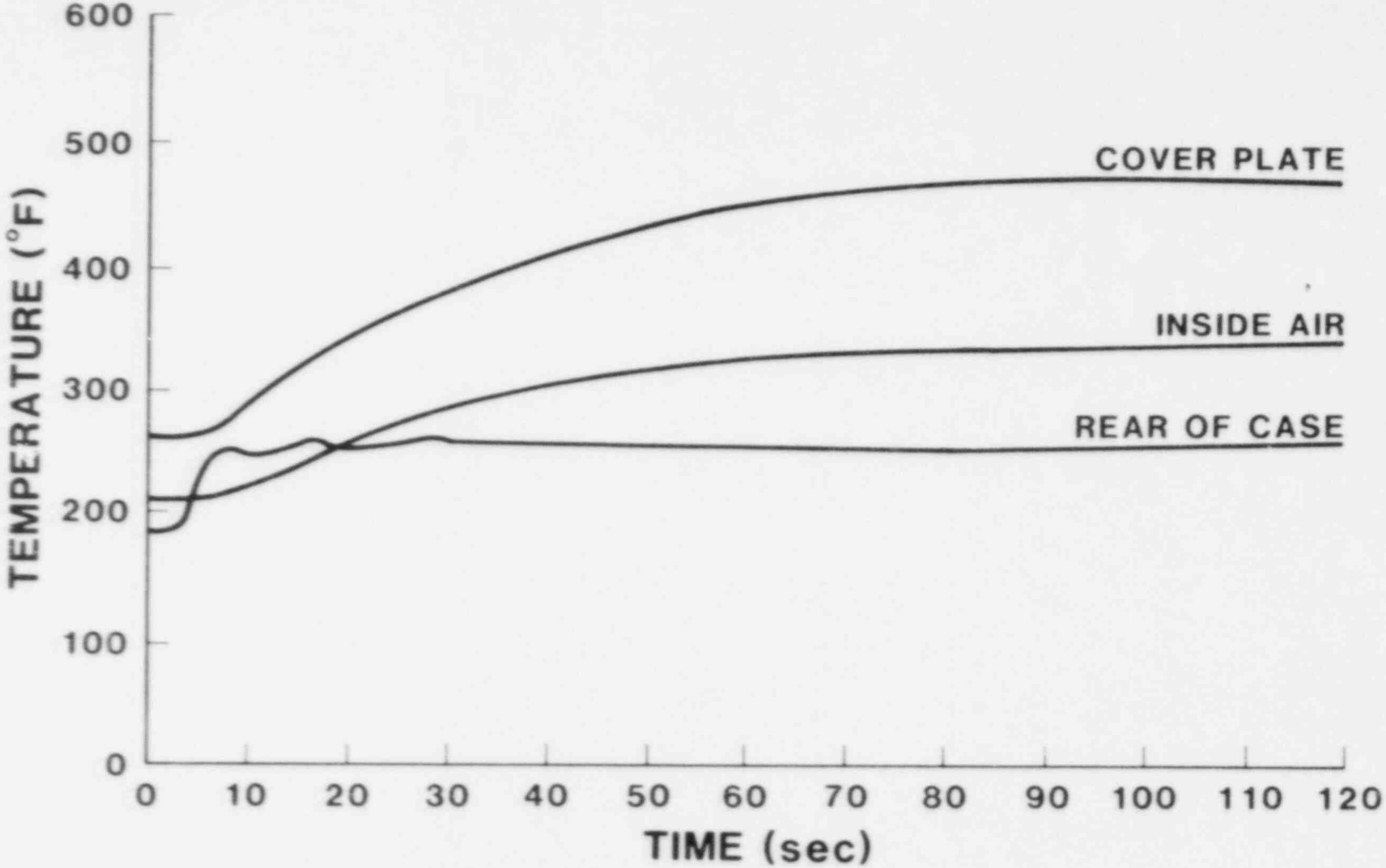

Figure 4-8. Unaged Transmitter Casing Temperatures for the Factor 3.0 Exposure

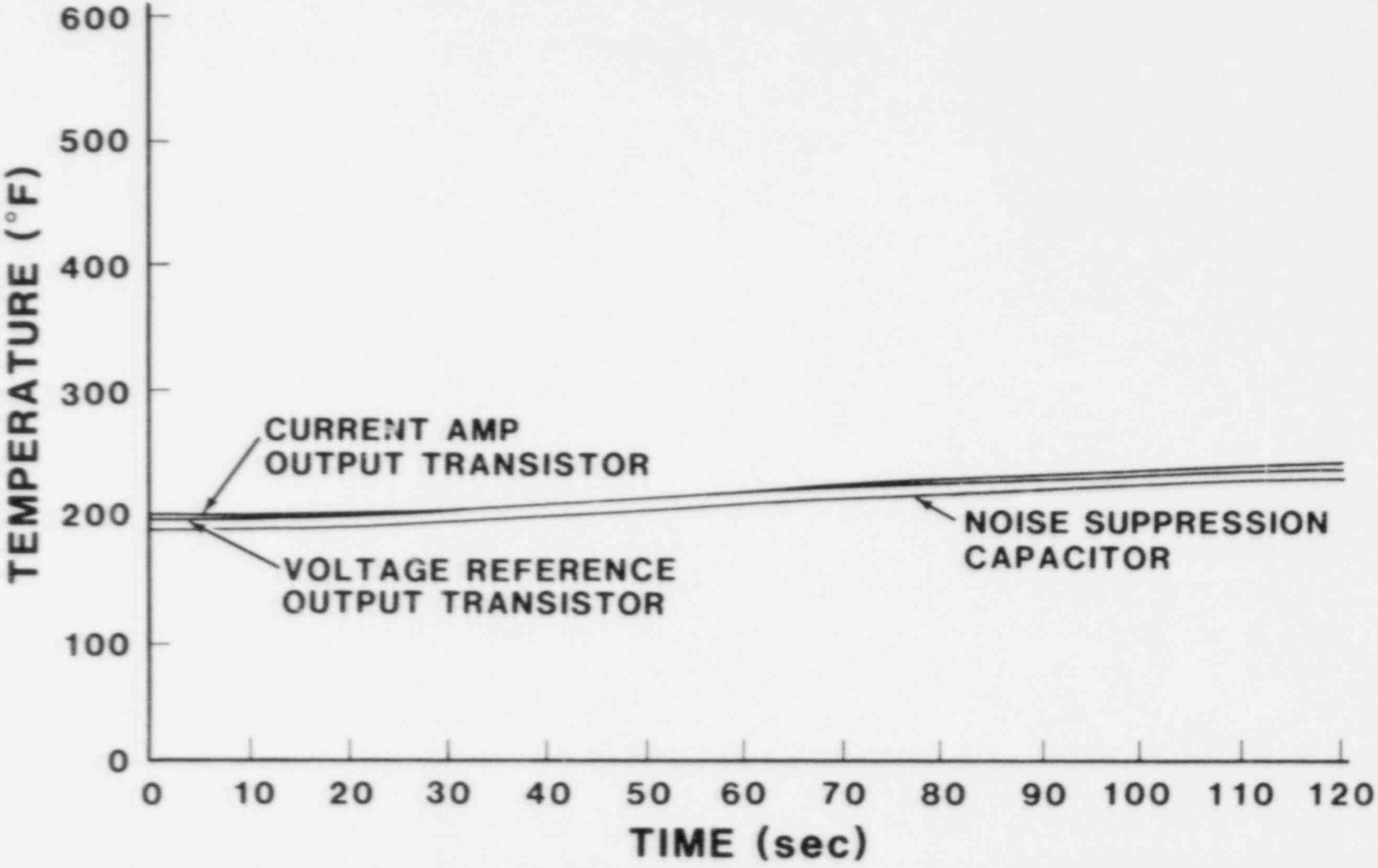

Figure 4-9. Unaged Transmitter Electronics Temperatures for the Factor 3.0 Exposure

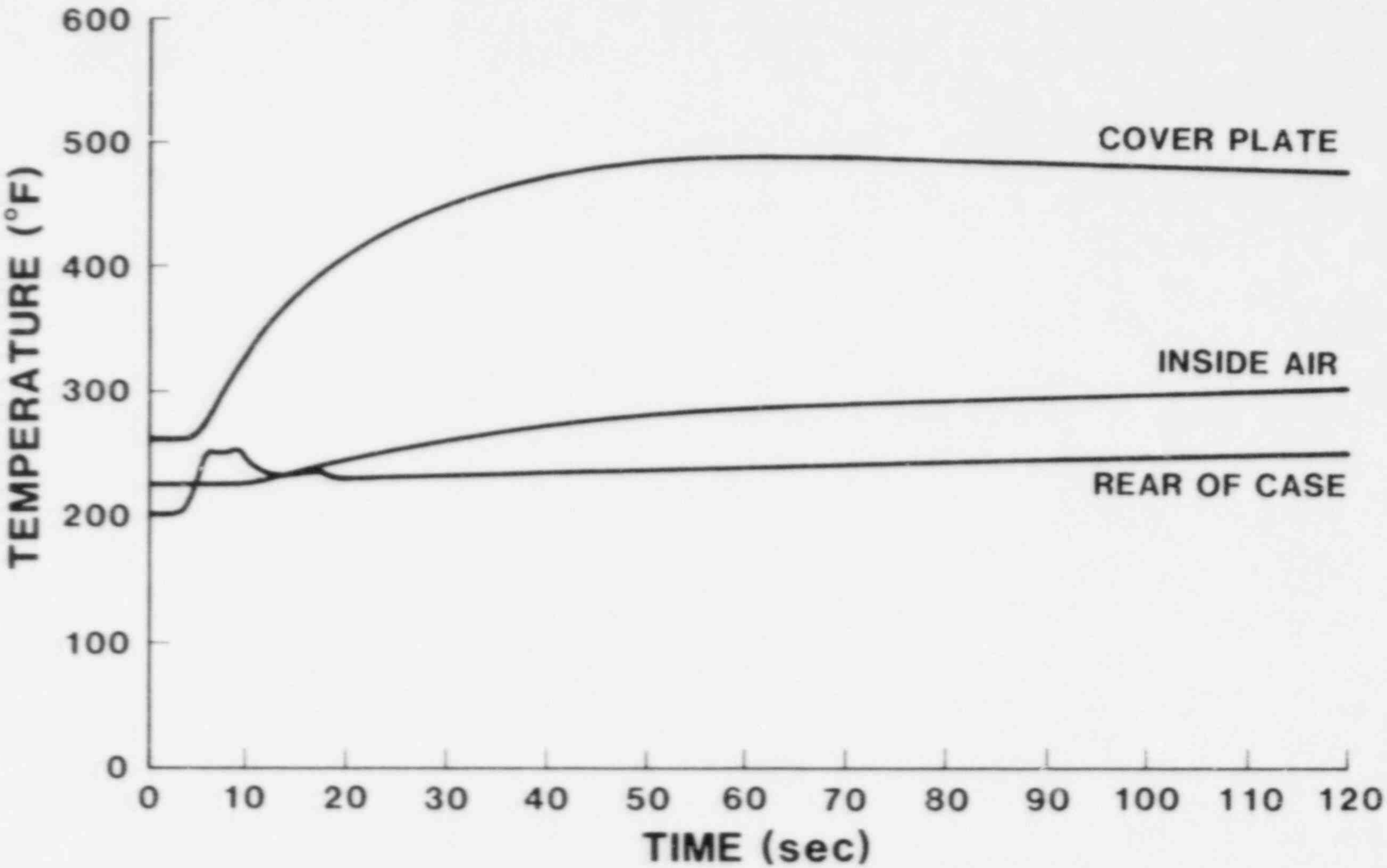

Figure 4-10. Aged Transmitter Casing Temperatures for the Factor 3.0 Exposure

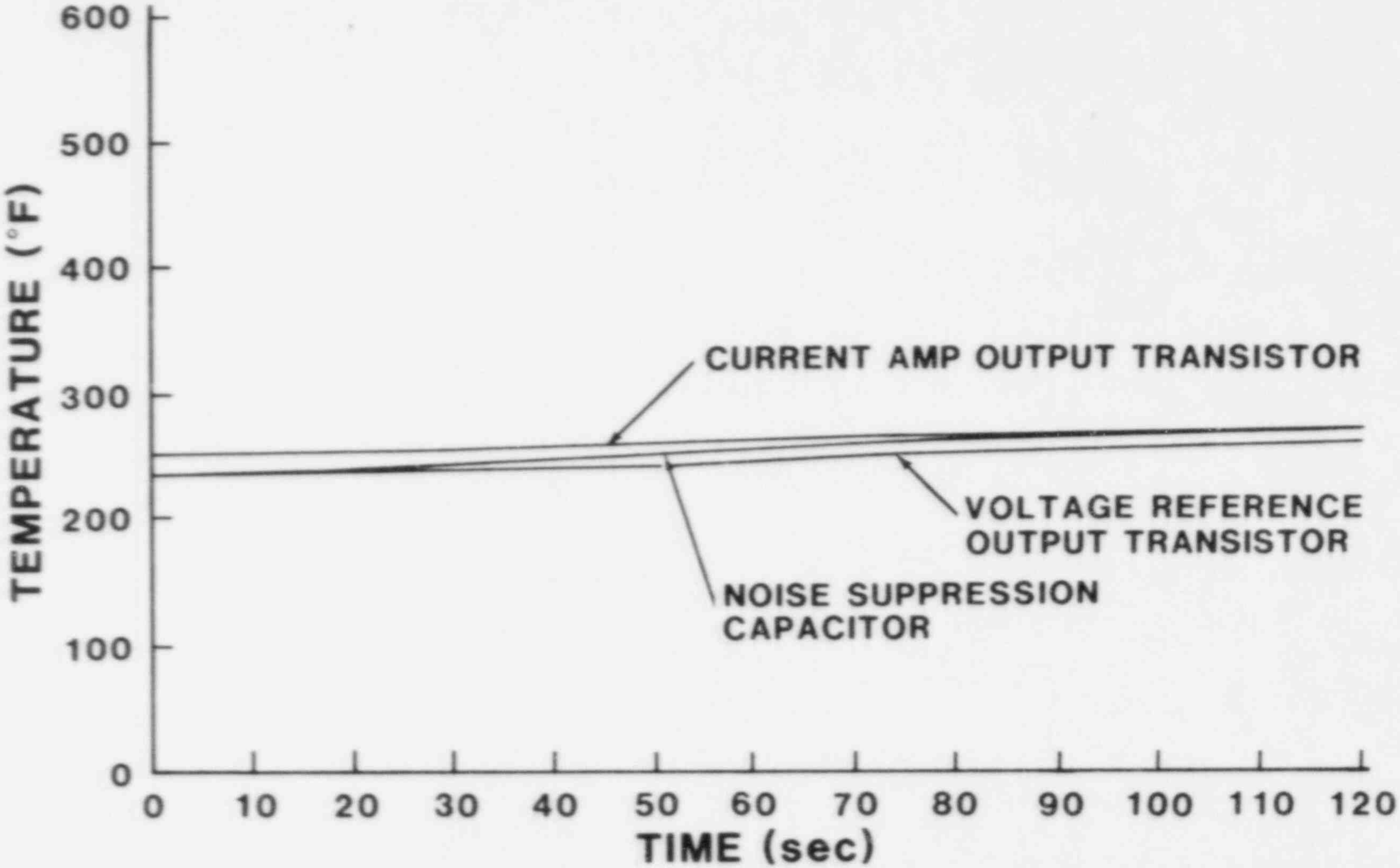

Figure 4-11. Aged Transmitter Electronics Temperatures for the Factor 3.0 Exposure

The pattern of temperature rises is the same in all cases. The front plate rises to a maximum in approximately 30 seconds and then starts a gradual decline. The inside air in all cases shows a very gradual increase over the duration of the pulse.

The back of the transmitter case shows a rapid rise and small drop at the beginning of the exposure before leveling out. The rapid rise is due to solar flux that was reflected from the back of the test stand and onto the rear case thermocouple (the thermocouple was mounted to the outside of the rear of the case). When the first group of heliostats was removed the thermocouple response was dominated by the casing temperature rather than the reflected solar flux and the temperature reading stabilized.

4.2.2 Transmitter Performance During Testing

Both the unaged and aged transmitters performed properly during and immediately after exposure to the simulated hydrogen burns. Measured signal voltages (voltage drops across the parallel 1000 ohm resistors--see Section 3.2) for the factor 3.0 exposures of the unaged and aged transmitters are given in Figures 4-12 and 4-13 respectively.

The high casing temperatures reached during the factor 2.0, 2.5, and 3.0 exposures of the unaged transmitter caused some melting of data line insulation which had come into contact with the case. This caused these lines to short circuit to the case and to each other resulting in some signal fluctuation. In each case the data lines were repaired and a normal signal was then monitored. Data line routing for the aged transmitter was modified and this problem was eliminated. As stated earlier, these data lines were not part of the transmitter as manufactured and the melting of the insulation should not be construed as reflecting transmitter performance.

4.2.3 Posttest Transmitter Calibrations

Two sets of calibration checks were run on each of the transmitters. During the course of the tests the calibration was checked prior to the first exposure while the transmitters were at ambient temperature and immediately after each exposure to the heat flux pulses while the transmitters were at elevated temperatures. These checks are referred to in this report as the "Tower Checks." Another set of precise calibration checks was performed in the pressure lab of Sandia's Test Measurements and Mechanical Design Division using a King Nutronics Gauge Calibration Station, Model 3692 (S/N 7894). These calibrations are referred to in this report as the "Lab Checks." The lab checks consisted

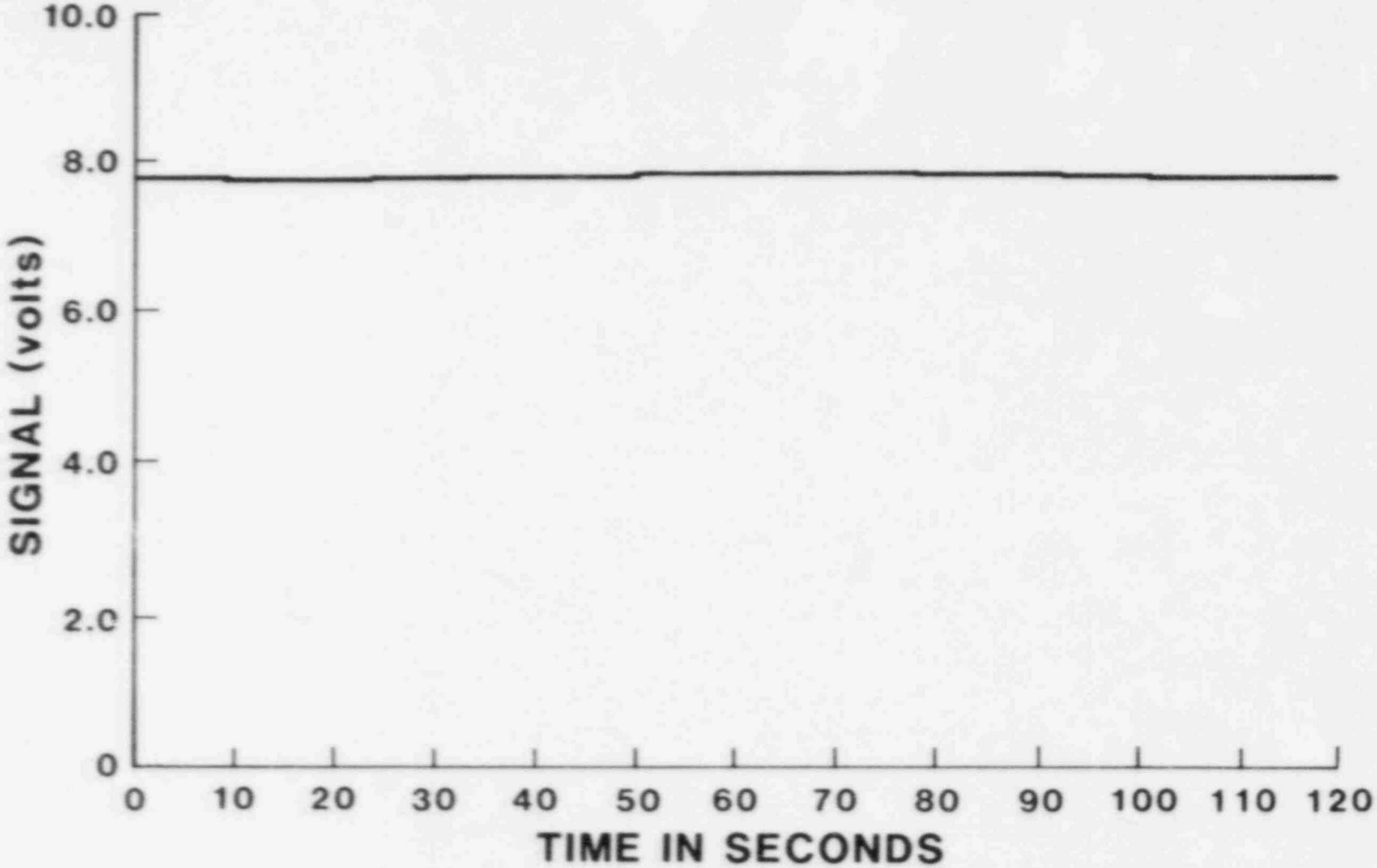

Figure 4-12. Unaged Transmitter Signal at Factor 3.0 Exposure

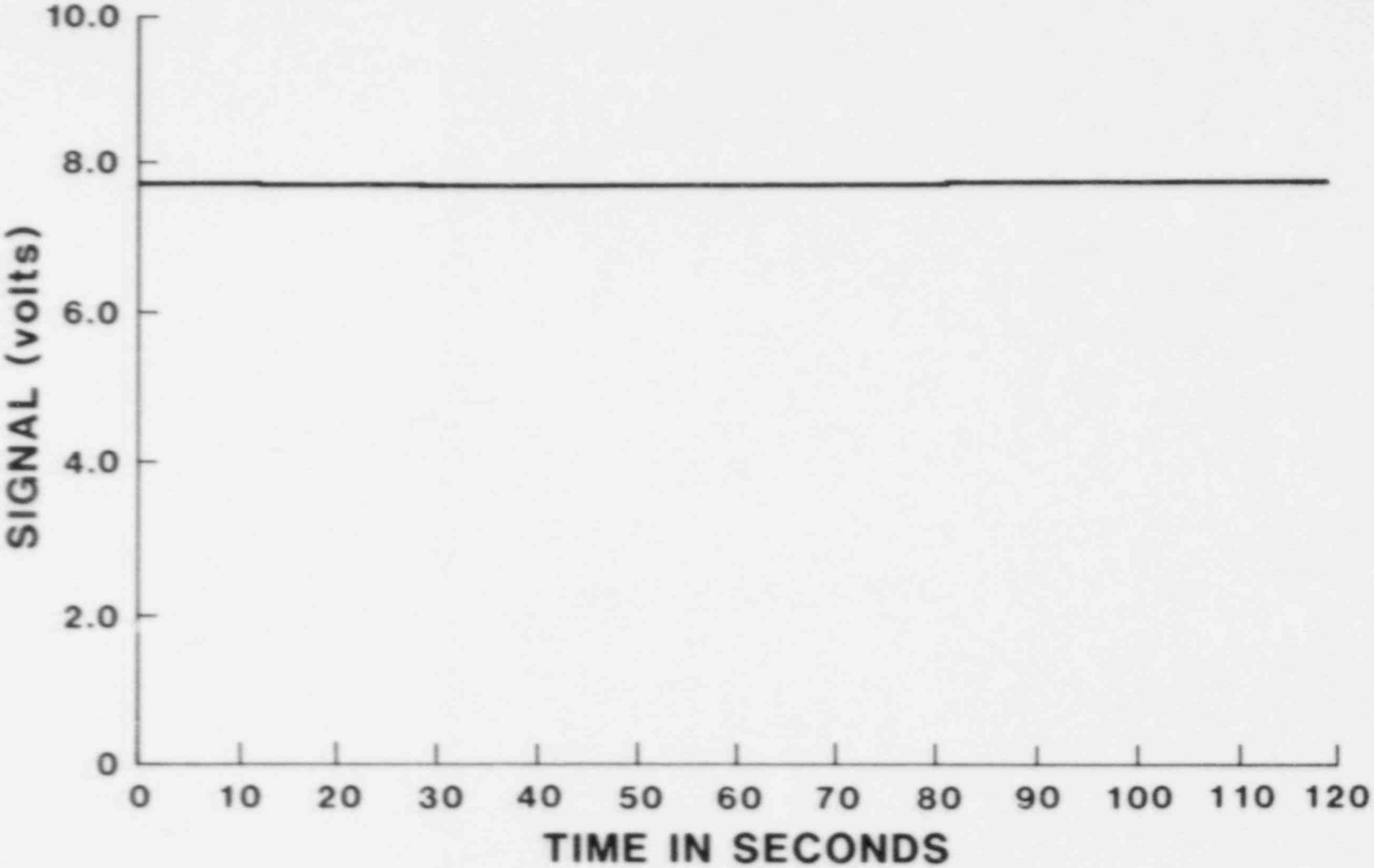

Figure 4-13. Aged Transmitter Signal at Factor 3.0 Exposure

of two calibration runs. The first was done prior to any aging or testing. The instruments' zero and span were set per the manufacturers instructions[13] and the instrument signal was checked over the 0-1000 psig operating span in 100 psig increments. One transmitter was then placed in the aging oven. The second lab check was performed after all testing was completed. No zero or span adjustments were made prior to the second lab calibration check.

The tower checks were made by increasing the applied pressure from 0 to 1000 psig in 200 psig increments and measuring the signal voltage (across the 500-ohm resistance) using the CRTF data acquisition system. These calibration checks were performed to monitor the overall condition of the transmitters throughout the test series and to assess test-to-test changes in the instruments. In all, six tower calibration checks were made for each transmitter. Since the results, when plotted, overlay each other they are given in equation form in Tables 4-8 and 4-9 for the unaged and aged transmitters respectively. The equations were determined by entering the applied pressures and corresponding measured voltages into a linear regression program. The equations in parentheses in the tables are the milliamp equivalents for the voltage signals which were measured.

The optimum calibration curve is given by

$$V = 2.0 + 0.008P \qquad (4\text{-}1)$$

where V = voltage drop of the signal current across the 500-ohm resistance (volts)

P = applied pressure (psig).

Alternatively, the calibration equation may be written as

$$S = 4.0 + 0.016P$$

where S = signal current (mA)

P = applied pressure (psig).

This latter equation corresponds to the 4-20 mA output signal range over the 0-1000 psig operating span of the transmitters.

The tower checks showed that the calibrations of both the unaged and the aged transmitters changed little throughout the test series. The aged specimen was the more consistent of the two. Over the exposures, the calibration equations

Table 4-8

Unaged Transmitter Tower Calibration Checks

When Checked	Calibration Equation*
Initial Pretest	V = 2.03 + 0.00779P (S = 4.06 + 0.01558P)
After 1.0 Exposure	V = 1.99 + 0.00748P (S = 3.98 + 0.01496P)
After 1.5 Exposure	V = 2.09 + 0.00736P (S = 4.18 + 0.01472P)
After 2.0 Exposure	V = 2.02 + 0.00744P (S = 4.04 + 0.01488P)
After 2.5 Exposure	V = 2.20 + 0.00741P (S = 4.40 + 0.01482P)
After 3.0 Exposure	V = 2.23 + 0.00724P (S = 4.46 + 0.01448P)

*V, P, and S as previously defined.

Table 4-9

Aged Transmitter Tower Calibration Checks

When Checked	Calibration Equation*
Initial Pretest	V = 1.99 + 0.00766P (S = 3.98 + 0.01532P)
After 1.0 Exposure	V = 2.11 + 0.00760P (S = 4.22 + 0.01520P)
After 1.5 Exposure	V = 2.13 + 0.00758P (S = 4.26 + 0.01516P)
After 2.0 Exposure	V = 2.09 + 0.00755P (S = 4.18 + 0.01510P)
After 2.5 Exposure	V = 2.11 + 0.00761P (S = 4.22 + 0.01522P)
After 3.0 Exposure	V = 2.12 + 0.00763P (S = 4.24 + 0.01526P)

*V, P, and S as previously defined.

of both transmitters exhibited changes in intercept and slope from the pretest equations.

For the unaged transmitter, the largest difference in the intercept with the pretest value occurred after the factor 3.0 exposure. After this exposure, it was 9.9 percent higher than the pretest value. After each exposure, the slope of the unaged transmitter calibration equation was lower than the pretest value. Its lowest value was also after the 3.0 exposure where it was 7.06 percent lower than the pretest slope.

For the aged transmitter, all posttest intercepts were higher than the pretest intercept. The largest difference occurred after the factor 1.5 exposure. During this calibration check the intercept was 6.2 percent higher than the pretest value. Posttest slopes for the aged transmitter calibration equation were all lower than the pretest value. The largest difference in the slope occurred after the factor 2.0 exposure when the slope was 1.4 percent lower than the pretest slope.

The effects of each individual pulse can be assessed by considering the test-to-test changes in the calibration equation. The percent changes in the slope and intercept of this equation are given in Table 4-10.

Table 4-10

Test-to-Test Changes in Calibration Equation Slope and Intercept

Test-to-Test (By Exposure Factor)	Intercept Change (%)		Slope Change (%)	
	Unaged	Aged	Unaged	Aged
Pretest - 1.0	-1.97	6.03	-3.98	-0.78
1.0 - 1.5	5.03	0.95	-1.60	-0.26
1.5 - 2.0	-3.35	-1.88	1.09	-1.88
2.0 - 2.5	8.91	0.96	-0.40	0.96
2.5 - 3.0	1.36	0.47	-2.29	0.47

With the exception of the large rise in the intercept of the aged transmitter after the 1.0 exposure, the largest changes in the slope and intercept generally occurred in the unaged transmitter. In the two other instances where the aged transmitter had the larger change (intercept change after the 2.0 and 2.5 exposures), the differences with the changes for the unaged transmitter were small.

The lab checks were performed to determine the combined effects of aging and the entire test series on the Barton Model 763 pressure transmitters. Calibration equations established during these checks gave indicated pressure as a function of the signal current. Changes in instrument performance were characterized by comparing the pretest and posttest percent of full-scale deviation (PFSD) of the transmitter signal from the pretest (and preaging) calibration equations. Details of the percent of full-scale deviation calculation are given in Appendix D.

The percent of full-scale deviations of the unaged transmitter from its pretest calibration equation are given in Figure 4-14. The technical specifications[13] of the Barton Model 763 pressure transmitter state that the reference accuracy is ±0.5 percent of the maximum span and thermal effects are ±1.0 percent of the maximum span per 100°F change from 40°F to 150°F. Taking the pressure lab temperature as 70°F, the sum of the reference accuracy and thermal effects projects a possible deviation of ±0.8 percent.

Applying this criteria to the unaged transmitter performance during the lab checks, Figure 4-14 shows that, prior to testing, the unaged instrument was well within specification over its full range of operation. After completion of the entire test series the deviation of the unaged transmitter fell outside the 0.8 percent range for applied pressures above approximately 300 psig. The maximum PFSD for the unaged instrument was -2.85 percent at 1000 psig applied pressure. The magnitude of this deviation is comparable to that of another unaged Barton Model 763 tested previously.[9] That specimen was exposed to four simulated hydrogen burns whose severity was equal to a factor 1.0 exposure in the present test series. The largest deviation in that series was 2.4 percent at 1000 psig. Thus, though the present series of endurance tests was, in toto, much more severe than those described in Reference 9, the effect on the calibration of the unaged Barton Model 763 transmitter was about the same.

The PFSD results for the aged Barton transmitter are shown in Figure 4-15. Prior to aging and testing, the PFSD characteristics of the sample were the same as those of the sample that was not aged. After testing the PFSD characteristics were different from those of the unaged sample. The aged transmitter was outside the ±0.8 percent criterion over the entire range of operation. However, the magnitude of the largest PFSD is somewhat less than that of the unaged transmitter. The aged transmitter's largest posttest deviation is also at 1000 psig but it is only -2.15 percent as opposed to the -2.85 percent for the unaged instrument.

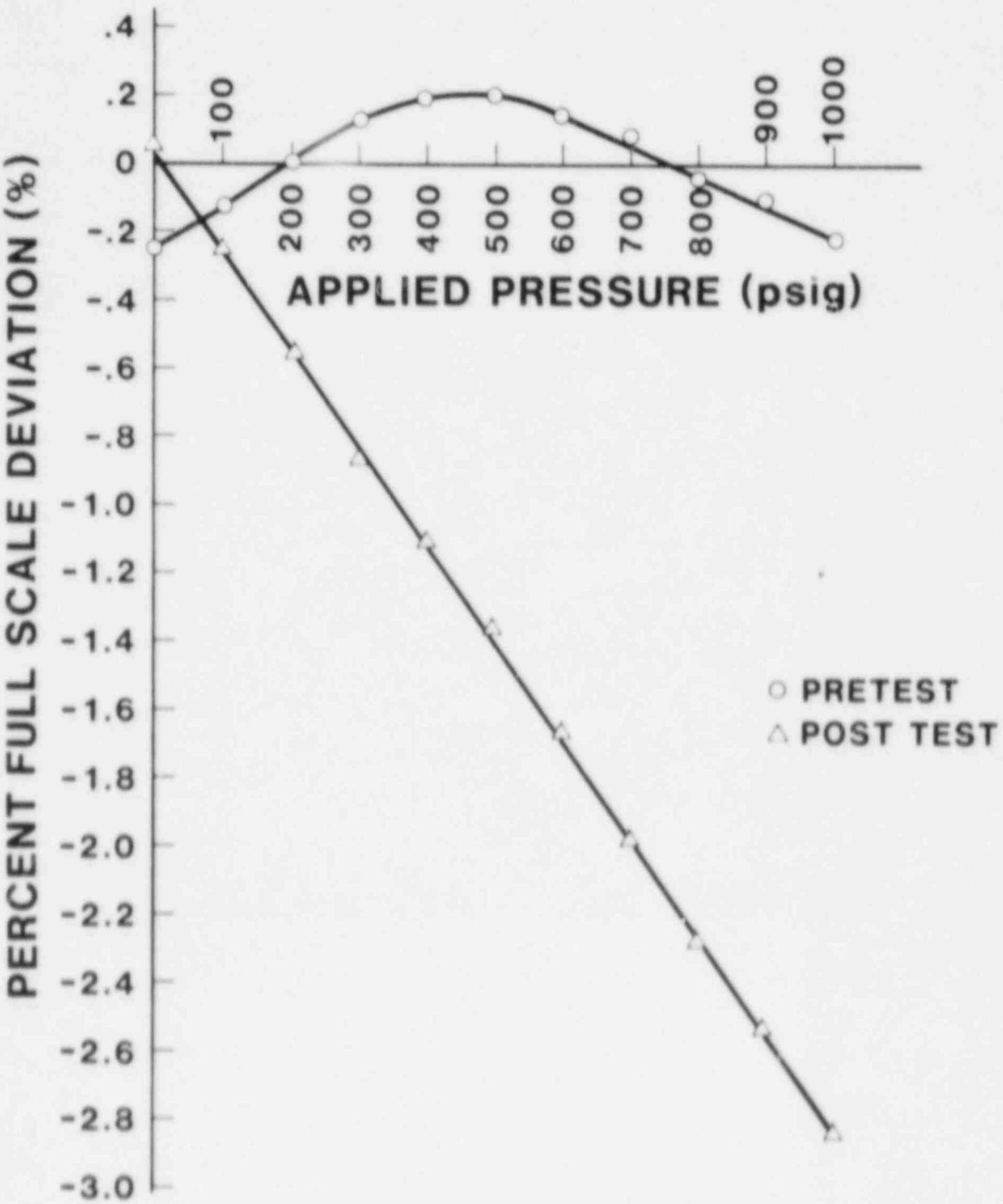

Figure 4-14. Unaged Transmitter Percent of Full-Scale Deviation From Pretest Calibration (Lab Check Results)

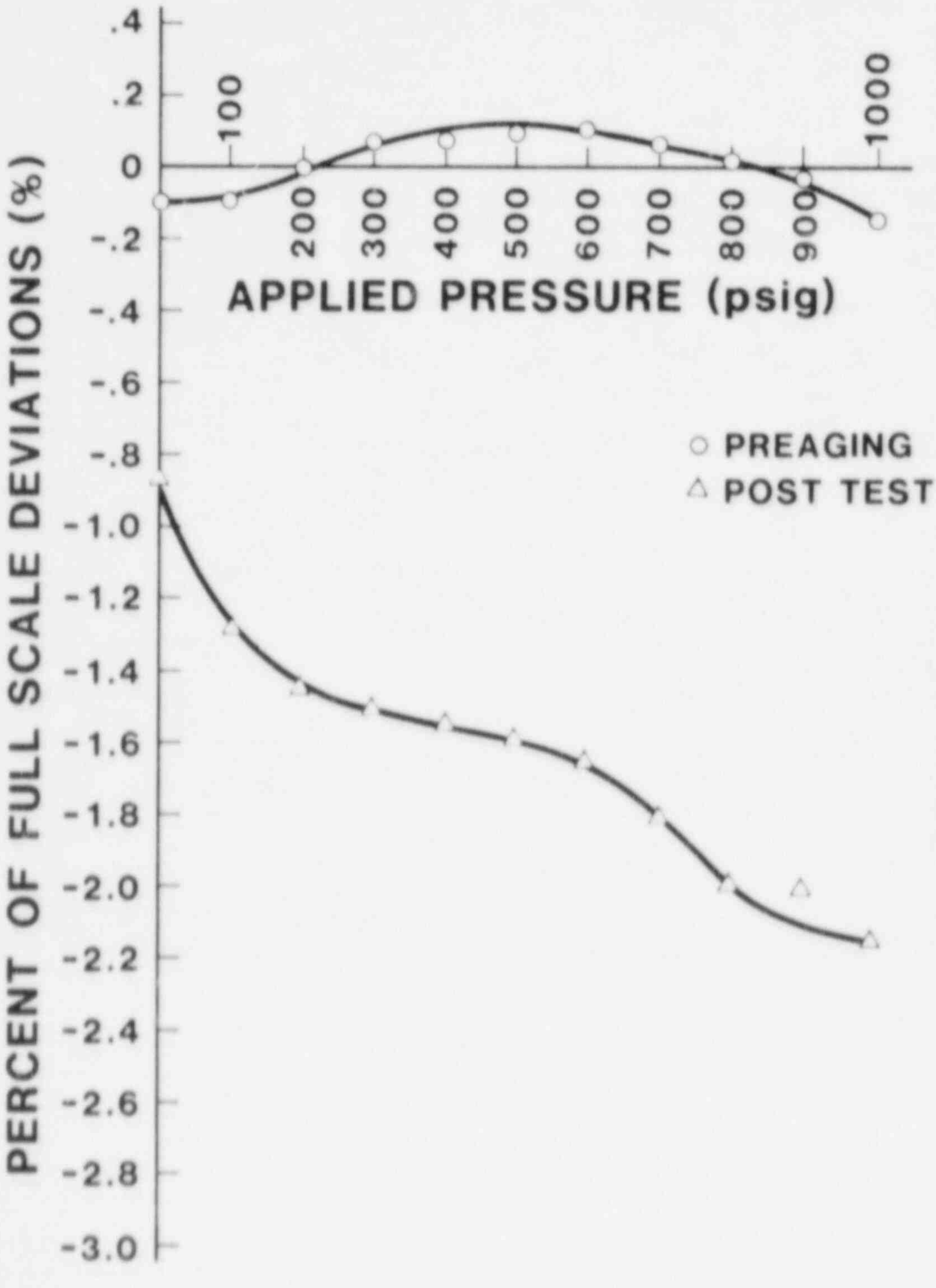

Figure 4-15. Aged Transmitter Percent of Full-Scale Deviation From Preaging Calibration (Lab Check Results)

The aged transmitter's posttest PFSD curve is also different. The unaged transmitter's posttest deviation curve is a straight line. The aged transmitter's deviation curve is not linear. It is, however, approximately piecewise linear over two sections, 0 to 200 psig and 200 to 600 psig.

The calibration equations, as determined by the pressure lab, gave pressure as a function of the signal current (see Appendix D). These equations were converted to the form of those obtained in the tower checks (signal voltage drop across a 500-ohm resistance) and are given in Table 4-11.

Table 4-11

Converted Lab Check Calibration Equations

Sample (Before/After Testing)	Calibration Equation
Unaged Before	V = 2.0203 + 0.007998P
Unaged After	V = 2.0232 + 0.007768P
Aged Before	V = 2.00866 + 0.007988P
Aged After	V = 1.9215 + 0.007902P

The slope and intercept changes for the unaged transmitter were -2.88 percent and 0.144 percent, respectively. The changes for the aged transmitter were 1.08 percent and -4.34 percent for the slope and intercept, respectively.

5.0 SUMMARY AND CONCLUSIONS

Several specimens of artificially aged and unaged Brand Rex XLP/CU 12 AWG three conductor nuclear qualified cable and one unaged and one artificially aged Barton Model 763 pressure transmitter have been exposed to simulated hydrogen burns of increasing severity at Sandia's Central Receiver Test Facility.

The heat flux pulses simulating the hydrogen burns were based on the heat flux profile resulting from a 13 volume percent premixed hydrogen deflagration which was one of the tests conducted during the EPRI hydrogen combustion experiments at the Nevada Test Site. This profile, which served as the base case for these tests, was determined to be very similar in peak flux and pulse duration to the pulse which would result from the deflagration of hydrogen from a 75 percent core metal-water reaction in a reactor in a large, dry containment building.

Starting with the base heat flux pulse, test specimens were exposed to pulses whose flux levels were increased in 50 percent increments of the base pulse. The flux levels of the most severe pulse were 300 percent of the flux levels of the base pulse. Each cable sample was exposed to only one pulse so that the effects of each individual pulse could be studied. The transmitters were exposed to each of the pulses from the base pulse (factor 1.0) through the most severe (factor 3.0) and their performance was checked before, during, and after each exposure.

Visible damage to the cables increased with the severity of the pulse to which they were exposed. Generally, the aged cables experienced less severe visible damage than the unaged samples at each flux level. The differences were less pronounced as the severity of the pulses increased. All cable samples showed evidence of combustion. At the factor 1.0 and 1.5 flux levels the sample mounts exhibited scorch marks. Above the 1.5 level the mounts became coated with soot. Blistering was common to all cable jackets.

Starting with the factor 1.5 exposures, cracks penetrated the cable jackets. The cracking exposed the insulation of the interior conductors. This insulation remained intact during all tests. The only interior cable constituent that experienced significant damage was the fibrous, white polymeric filler material packed between the cable wires and the jacket. When exposed, this material melted and refroze around the insulation.

The cables were electrically powered during exposure to the heat flux pulses. All samples were monitored for short circuits from the conductors to the sample mounting fixture and from conductor to conductor. The cables were also monitored for open circuits. No shorts or open circuits were detected during the test exposure.

After exposure, all cables were subjected to high potential withstand (hi-pot) testing at 600, 1200, and 2400 Vac and insulation resistance (IR) was measured at 50 Vdc. These tests included one aged and one unaged sample of Brand Rex cable that had not been exposed to the hydrogen burn simulations. These unexposed cables served as control samples for comparison with the hi-pot and IR results of the exposed specimens.

With one exception, all insulation maintained its integrity during the hi-pot testing. The exception was the black conductor from the unaged cable, which had been exposed to the factor 3.0 pulse. The insulation broke down within seconds after the application of the 2400 Vac test voltage. Leakage currents for all other samples remained on the order of 10^{-1} to 10^{-2} mA/ft for all test voltages.

Aging had a slight effect on the hi-pot leakage current results. The differences in leakage current between the aged cables and unaged control were consistently greater than the differences between the unaged cables and the unaged control. Thus, thermal aging plus exposure to the simulated hydrogen burns increased leakage currents by a greater amount than exposure to the simulated burns alone. There was one exception to this trend. At the factor 3.0 exposure level, the leakage current differences between the aged sample and the unaged control were consistently lower than the differences between the unaged sample and the unaged control.

Aging did not have as great an effect on the insulation resistance measurements. All measured insulation resistances were on the order of 10^{12} ohm-ft. Generally, the IR differences between the aged samples and the unaged control were approximately the same as those between the unaged samples and unaged control.

The metal case of both the unaged and aged Barton Model 763 transmitters reached very high temperatures during testing. Casing temperatures approached 500°F during exposure to the most severe pulses and interior electronics temperatures approached 300°F shortly after the most severe tests were completed. Despite the high temperatures, both transmitters performed properly during and after testing.

Calibration checks conducted immediately after each exposure to the heat flux pulses, using the experimental facility data acquisition system, indicated slight changes in the calibration equations of both transmitters from test to test. Generally these changes were slightly more pronounced for the unaged transmitter.

Calibration checks conducted in a pressure lab at the completion of the entire test series, when the transmitters had returned to ambient temperature, indicate a slight departure from the instrument's technical specifications at the laboratory temperature. The specifications indicate that the maximum percent of full-scale deviation (PFSD) should have been ±0.8 percent. The maximum PFSD for the unaged transmitter at the completion of the test series (compared with its pretest calibration) was -2.85 percent at 1000 psig (the upper end of its operating range). The maximum PFSD for the aged transmitter was -2.15 percent, also at 1000 psig.

Several conclusions can be drawn from these tests. First, unaged and thermally aged Brand Rex XLP/CU three-conductor cable was found to function during exposure to a heat flux pulse whose heat flux levels were 300 percent of those postulated to result from the combustion of hydrogen produced by a 75 percent core metal-water reaction in a reactor housed in a large dry containment building. With one exception, the cable samples displayed no significant insulation degradation in postexposure testing.

Second, thermal aging only slightly affects the degree to which Brand Rex insulation electrical properties change when exposed to a severe heat flux pulse. In quantitative terms, the leakage currents measured during high potential withstand tests following test exposure were low for both unaged and aged samples (except for the unaged sample exposed to the factor 3.0 pulse whose black wire insulation broke down during the most severe hi-pot test). The changes in insulation resistance as measured at 50 Vdc were about the same for the unaged and aged samples.

Third, both the unaged and thermally aged Barton Model 763 pressure transmitters withstood heat flux pulses considerably more severe than those anticipated for the 75 percent core metal-water event and continued to function.

Exposure to these severe heat flux pulses, individually and <u>in toto</u>, produced only small changes in transmitter calibration. Results of these tests indicate that, while changes were quite small, the changes in the thermally aged transmitter were smaller than those of the unaged transmitter.

REFERENCES

1. H. Alvares, D. Bearson, and G. Eidem, Investigation of Hydrogen Burn Damage in the Three Mile Island Unit 2 Reactor Building, GEND-INF-023, Vol. 1, U.S. Department of Energy, June 1982.

2. A. Camp, M. Wester, and S. Dingman, HECTR Version 1.0 User's Manual, Sandia National Laboratories, NUREG/CR-3913, SAND84-1522, February 1985.

3. D. B. King et al., The Hydrogen Burn Equipment Response Algorithm (HYBER) User's Guide, Sandia National Laboratories, NUREG/CR-3779, SAND84-0160, Vol. 1, August 1984.

4. E. H. Richards and J. J. Aragon, Hydrogen Burn Survival Experiments at the Fully Instrumented Test Site (FITS), Sandia National Laboratories, NUREG/CR-3521, SAND83-1715, August 1984.

5. J. A. Achenbach et al., Large Scale Hydrogen Burn Experiments, Westinghouse Electric Corporation, In Preparation.

6. V. J. Dandini and J. J. Aragon, Testing of Safety-Related Nuclear Power Plant Equipment at the Central Receiver Test Facility, Sandia National Laboratories, NUREG/CR-3776, SAND83-1960, July 1984.

7. J. Walker (Ed.), Reactor Safety Research Quarterly Report July-September 1984, Vol 31, Sandia National Laboratories, NUREG/CR-3816, SAND84-1072 (3 of 4), May 1985.

8. W. H. McCulloch et al., Hydrogen Burn Survival: Preliminary Thermal Model and Test Results, Sandia National Laboratories, NUREG/CR-2730, SAND82-1150, August 1982.

9. V. J. Dandini and J. J. Aragon, Simulation of an EPRI-Nevada Test Site (NTS) Hydrogen Burn Test at the Central Receiver Test Facility, Sandia National Laboratories, NUREG/CR-4146, SAND85-0205, August 1985.

10. D. B. King, Report on Results of HECTR Analyses of Hydrogen Burns in a Large-Dry Containment Building, In Preparation.

11. Letter to W. S. Farmer (USNRC/EEB) from J. H. Linebarger (SNLA/6445), Subject: Progress on NTS Data Analysis Work, dated August 13, 1984.

12. Qualification Tests of Electrical Cables in a Simulated Steam Line Break (SLB) and Loss of Coolant Accident (LOCA) Environment, FRC Final Report F-C5120-1, Franklin Research Center, August 1980.

13. Technical Manual, Model 763 Gauge Pressure Electronic Transmitter, Manual No. 83C3(A), ITT Barton, 1983.

14. Qualification Test Report for the Barton Model 763 Gage Pressure Electronic Transmitter Report No. R3-763-6, ITT Barton, September 1982.

15. IEEE Standard For Qualifying Class 1E Equipment for Nuclear Power Generating Stations, IEEE Std. 323-1974, Institute of Electrical and Electronics Engineers, 1974.

Appendix A

Additional Cable Temperature Profiles

NOTE

This appendix contains temperature plots of the unaged factor 1.0 and 2.0 cable samples and all aged cable samples. During testing spurious signals from the unaged 1.5 and 3.0 samples were recorded. The temperature plots from those tests are not included here. The unaged, factor 2.5 cable temperature trace is given in the body of the report.

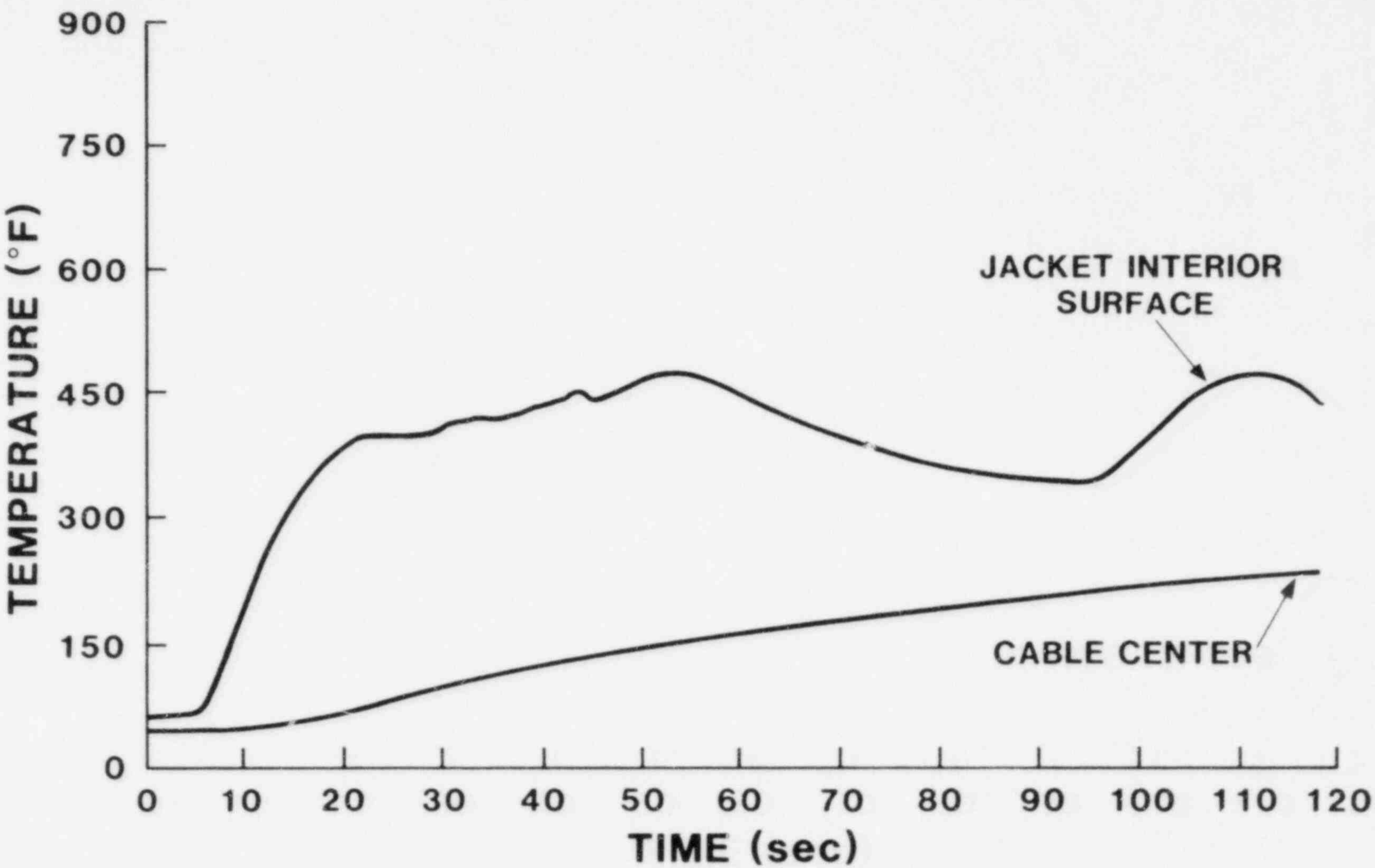

Figure A-1. Unaged Cable Temperatures (Factor 1.0)

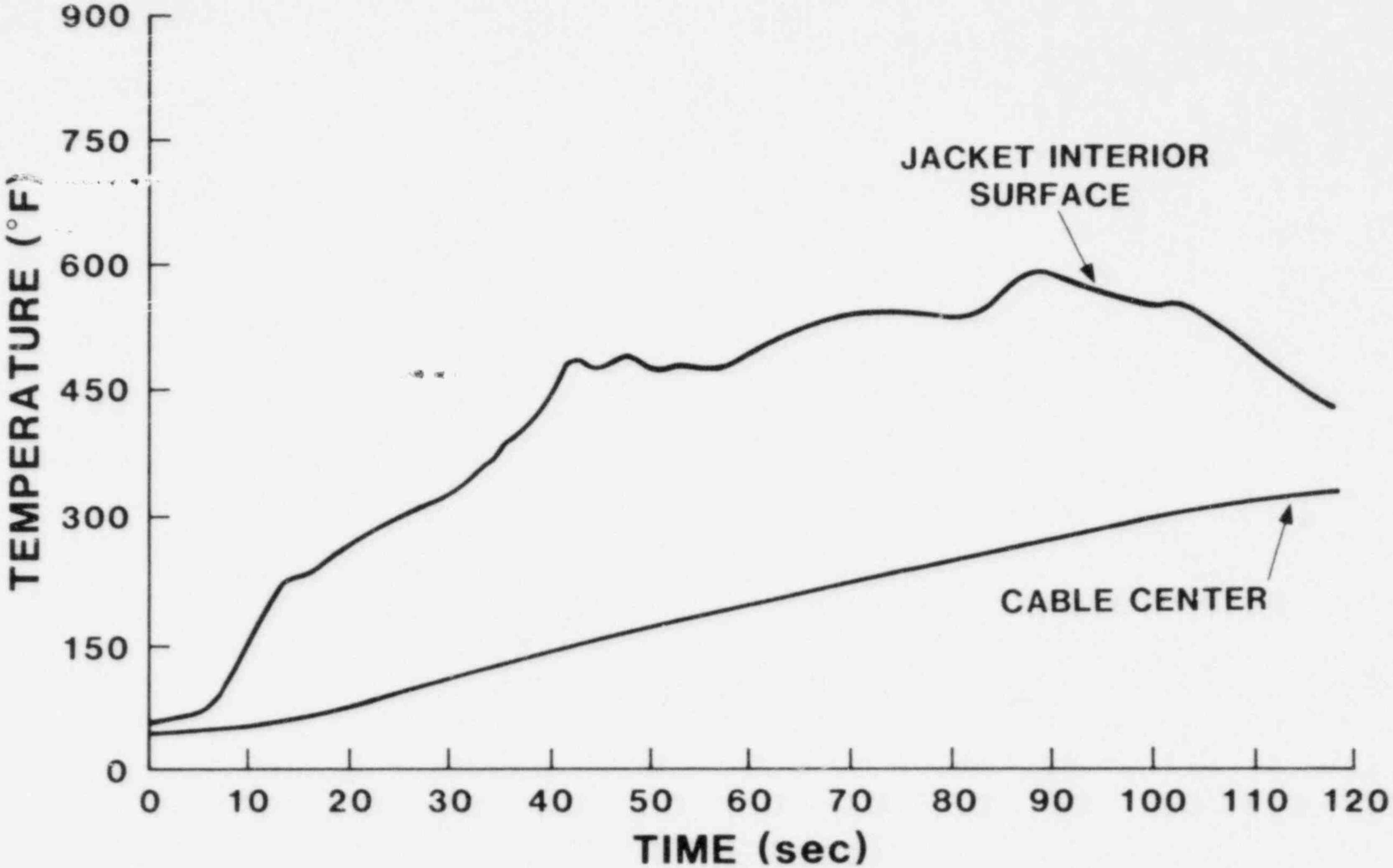

Figure A-2. Unaged Cable Temperatures (Factor 2.0)

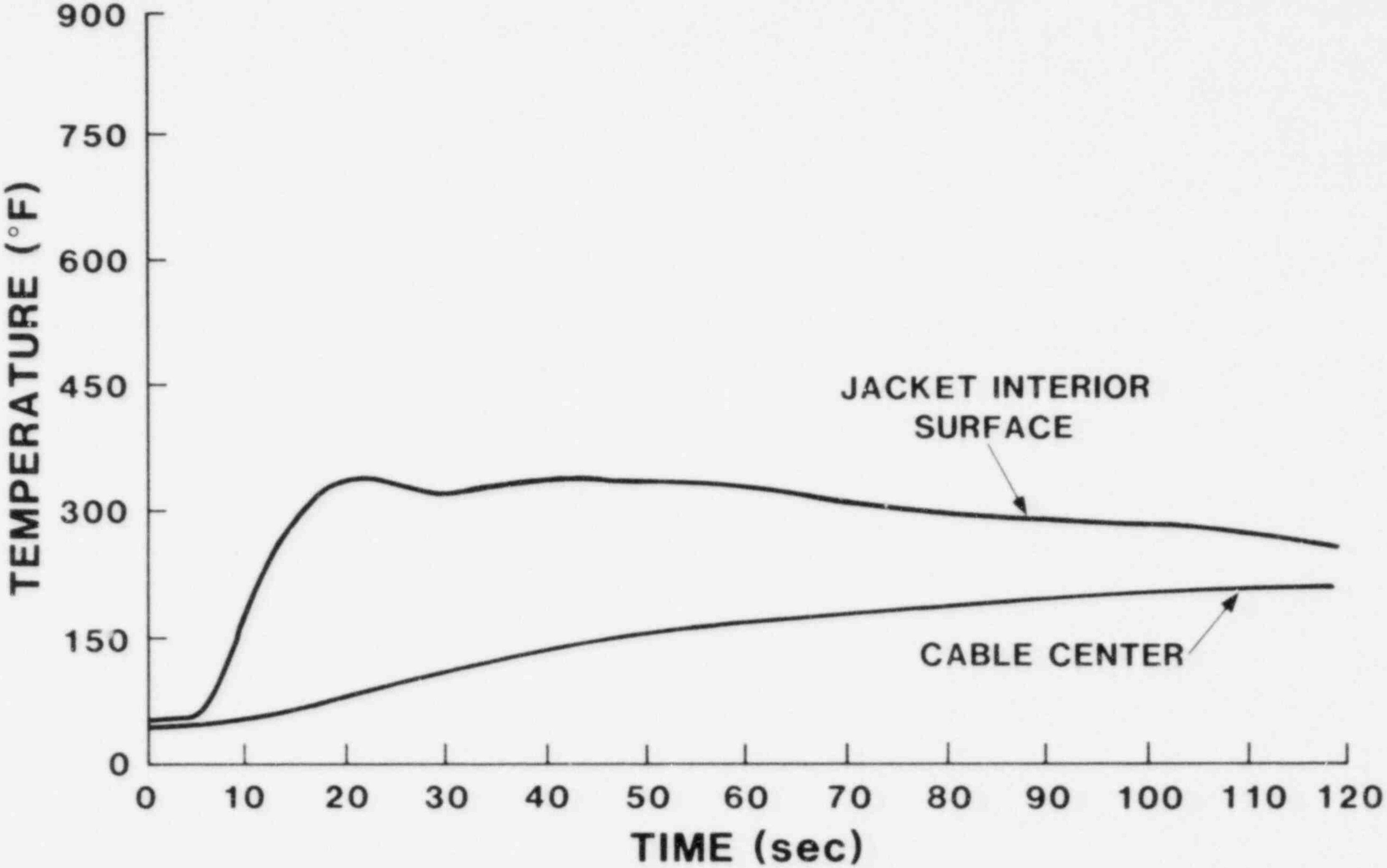

Figure A-3. Aged Cable Temperatures (Factor 1.0)

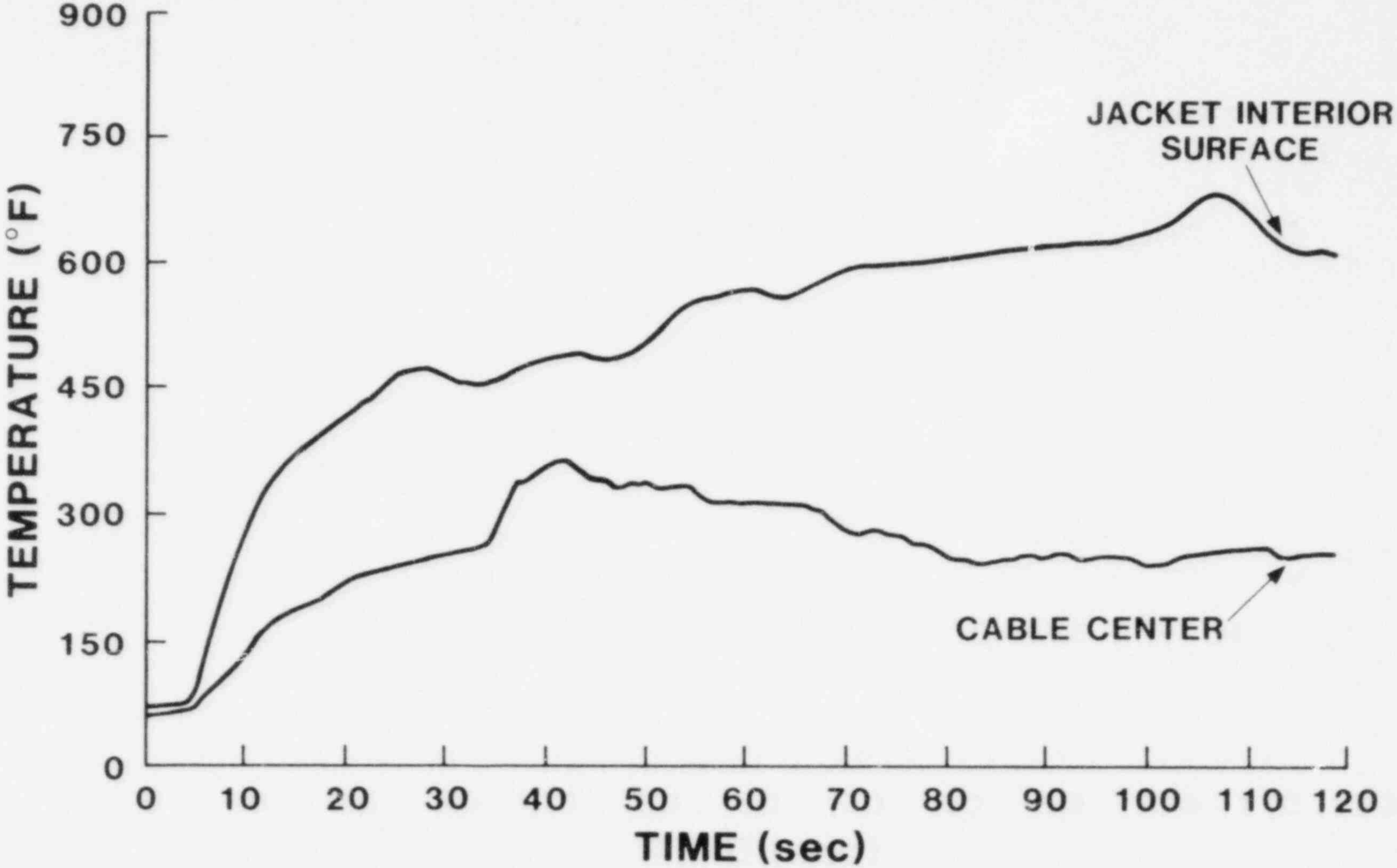

Figure A-4. Aged Cable Temperatures (Factor 1.5)

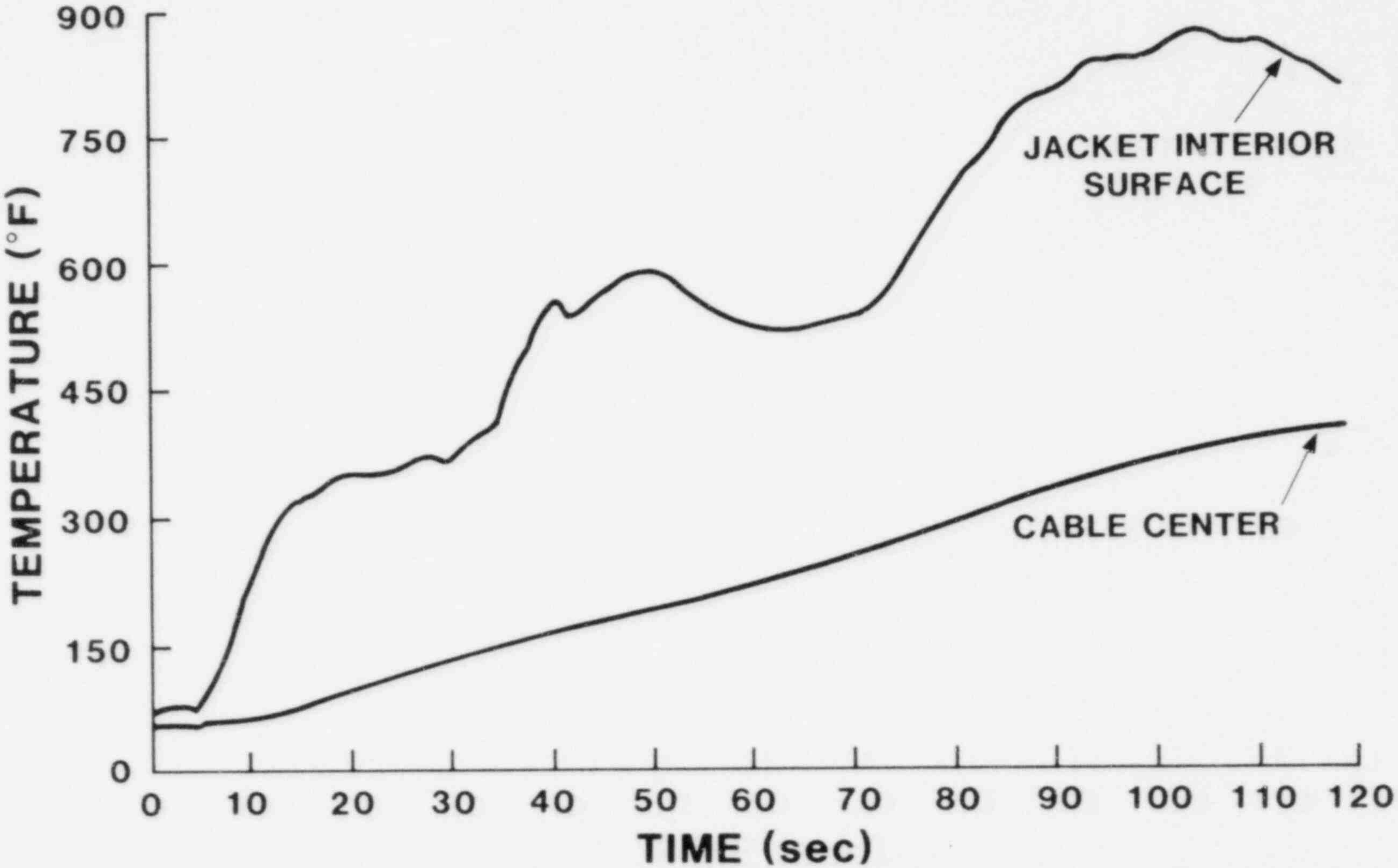

Figure A-5. Aged Cable Temperatures (Factor 2.0)

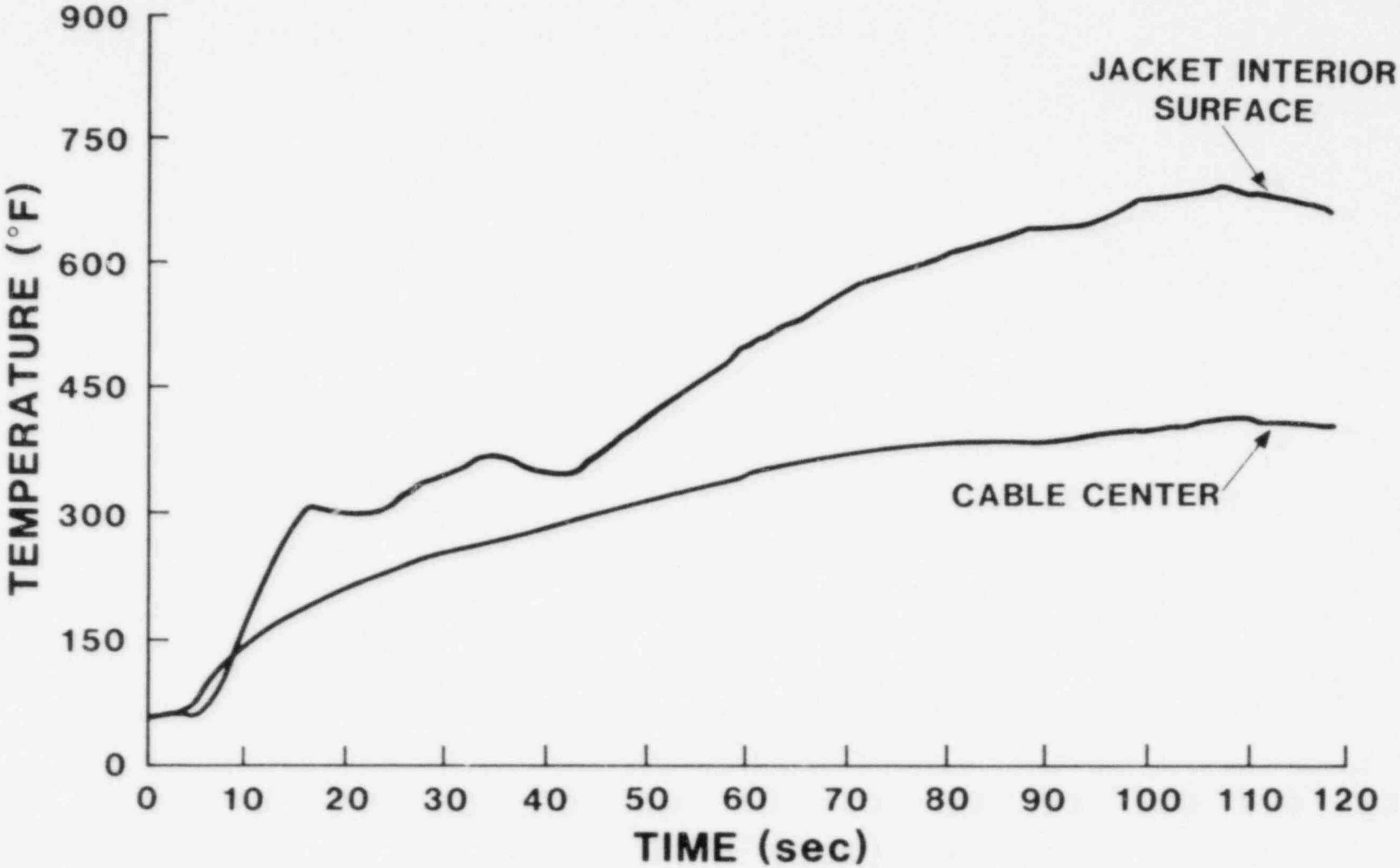

Figure A-6. Aged Cable Temperatures (Factor 2.5)

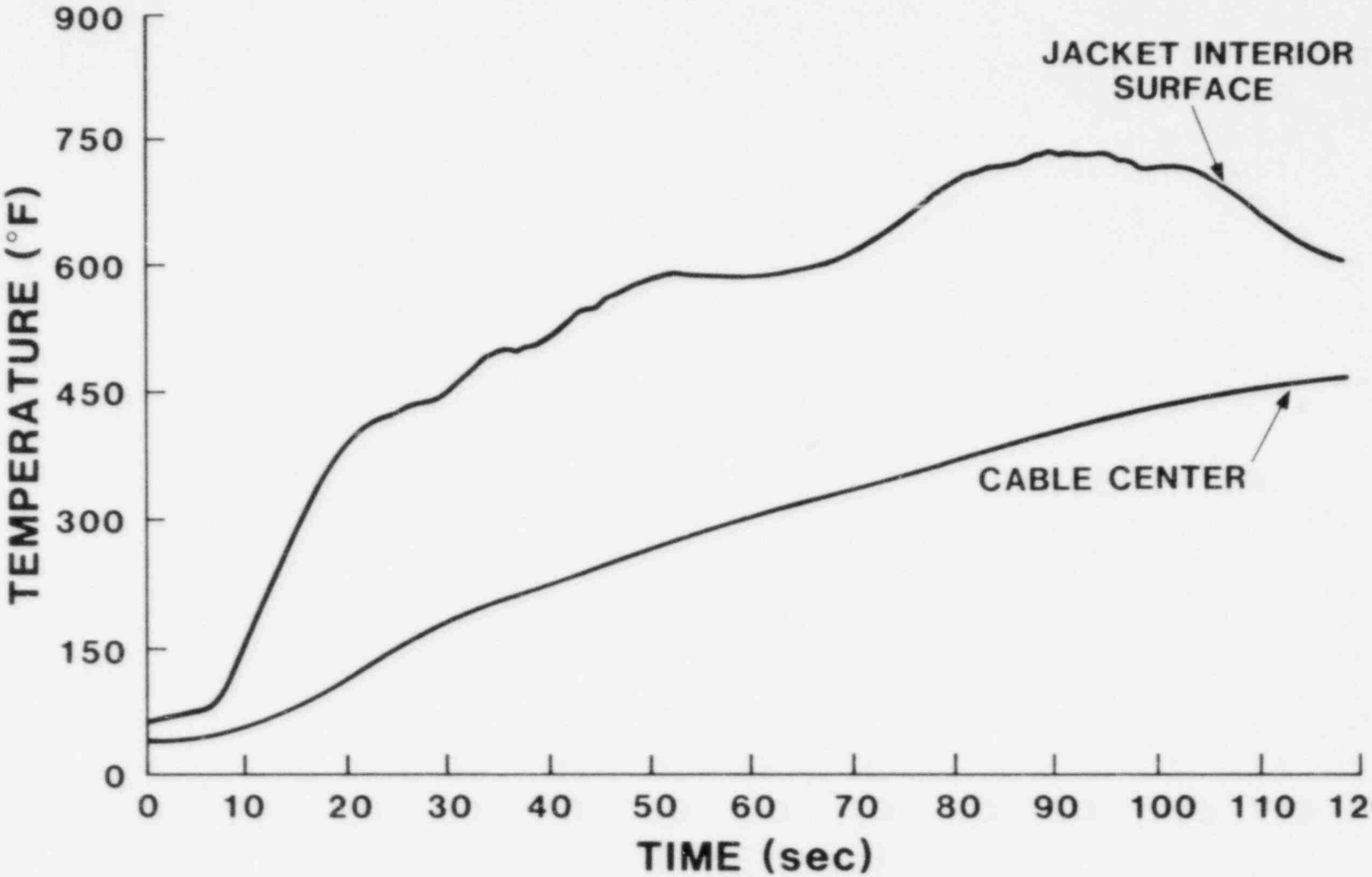

Figure A-7. Aged Cable Temperatures (Factor 3.0)

Appendix B

The Ohm-Ft Dimension of Insulation Resistance

Given the insulation resistance measurement setup as shown in Figure 4-7, the leakage current across the cable-water system will increase linearly with the submerged length of the cable. If n feet of cable are submerged, and the resistance of i^{th} foot is R_i, the cable-water circuit can be characterized as having n resistances in parallel. Any resistance, R_m, measured by the megohmmeter will be given by

$$\frac{1}{R_m} = \frac{1}{R_1} + \frac{1}{R_2} + \ldots + \frac{1}{R_n} = \sum_{i=0}^{n} \frac{1}{R_i} \quad . \qquad \text{(B-1)}$$

If $R_1 = R_2 = \ldots = R_n = R$, then

$$\frac{1}{R_m} = \frac{n}{R}$$

where R = the resistance of each foot of cable insulation.

Thus the insulation resistance of each section of the cable sample is given by

$$R(\text{ohm-ft}) = n(\text{ft}) \times R_m(\text{ohm}) \quad . \qquad \text{(B-2)}$$

R in ohm-m is given by

$$R(\text{ohm-m}) = 0.3048n(\text{ft}) \times R_m(\text{ohm}) \quad . \qquad \text{(B-3)}$$

Appendix C

Transmitter Temperature Profiles
Flux Factors 1.0 - 2.5

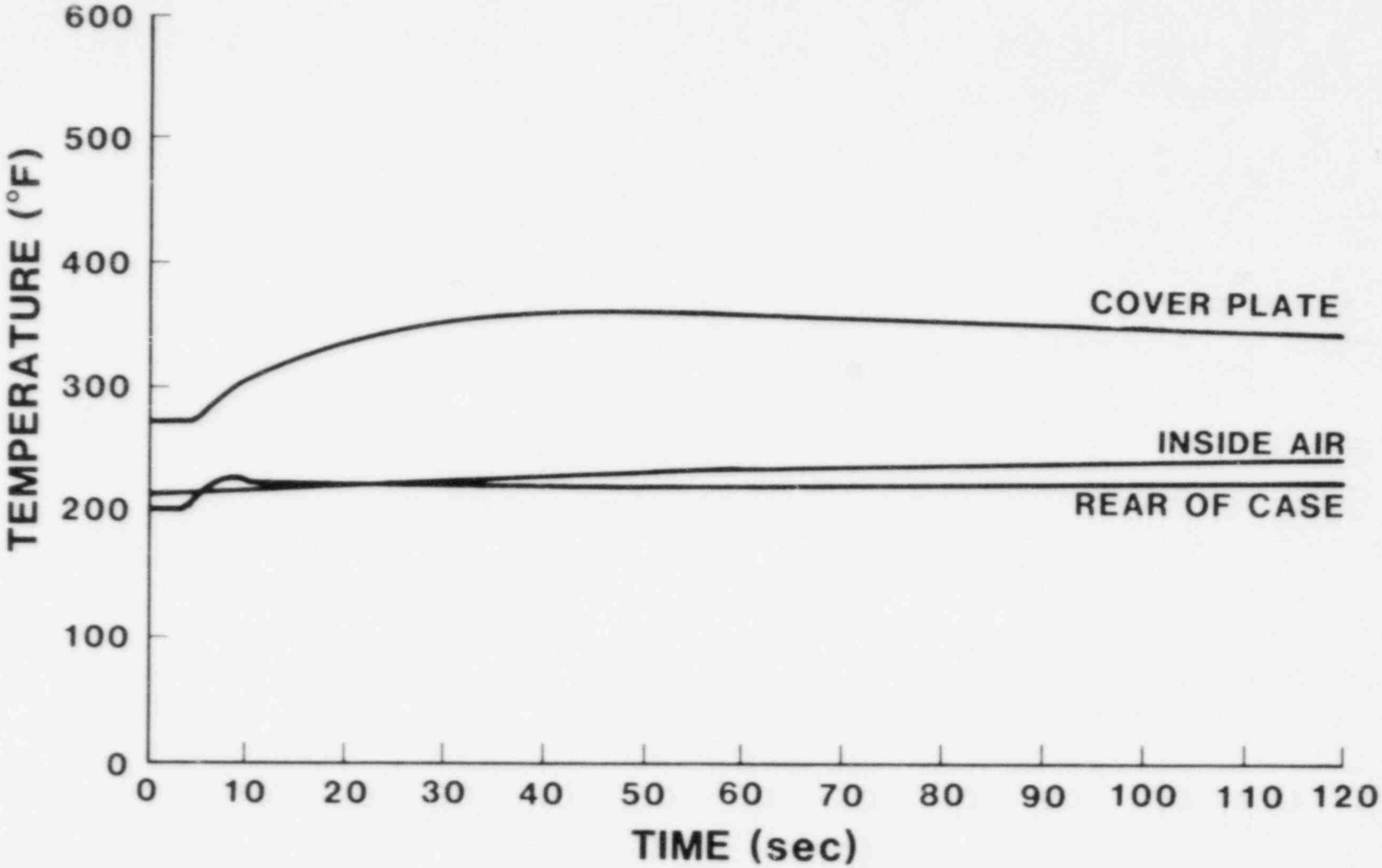

Figure C-1. Unaged Transmitter Casing Temperatures (Factor 1.0)

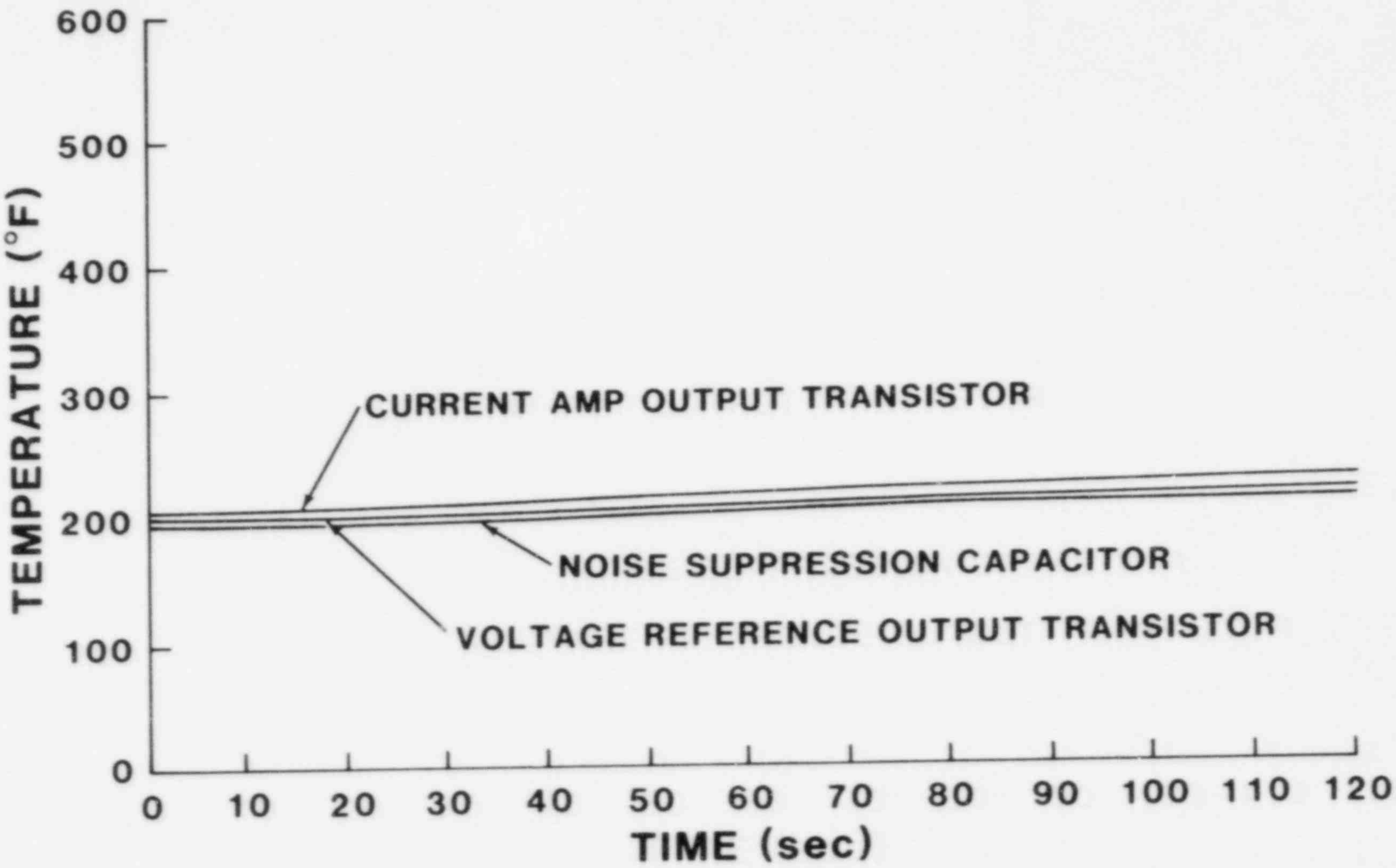

Figure C-2. Unaged Transmitter Electronic Temperatures (Factor 1.0)

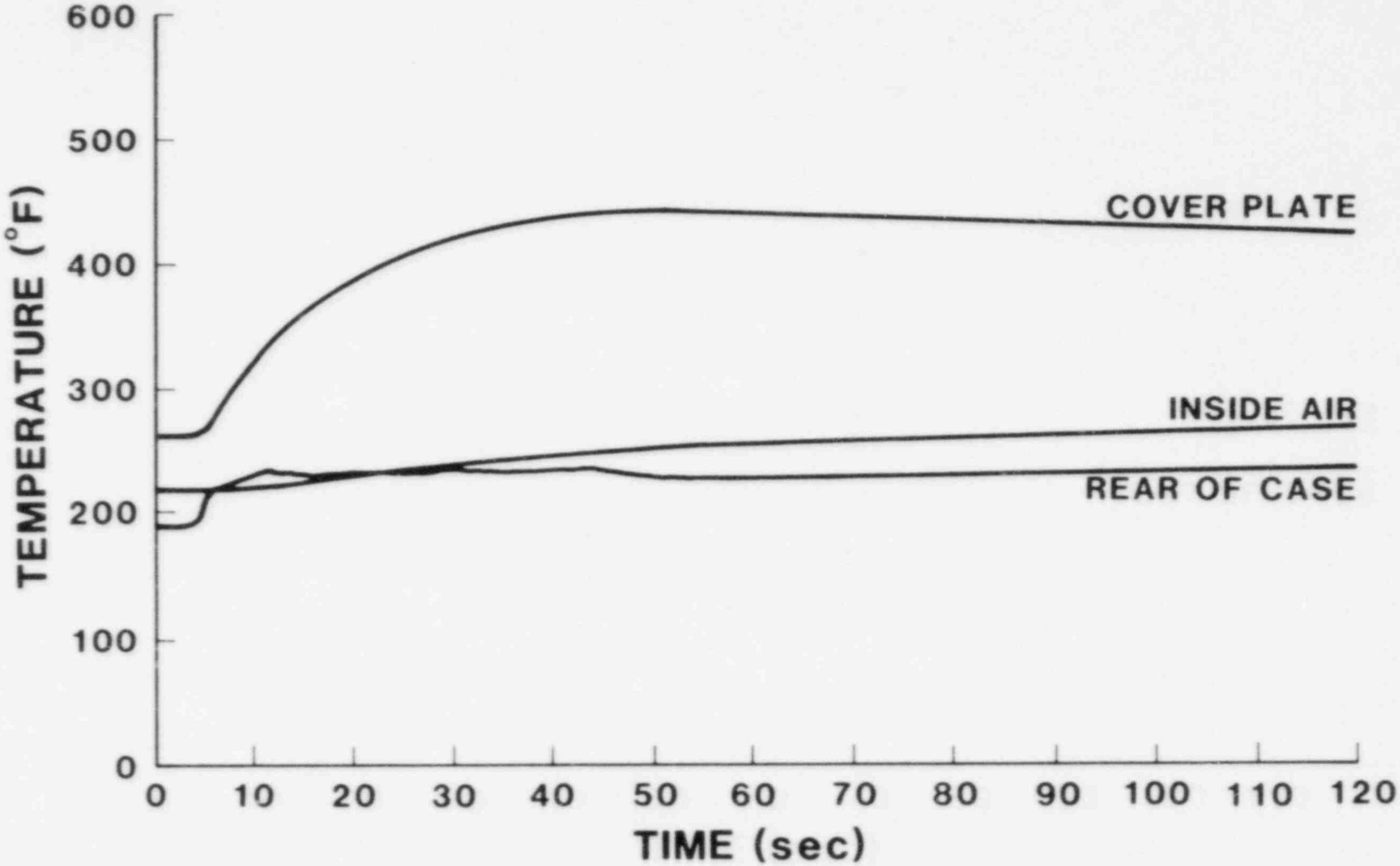

Figure C-3. Unaged Transmitter Casing Temperatures (Factor 1.5)

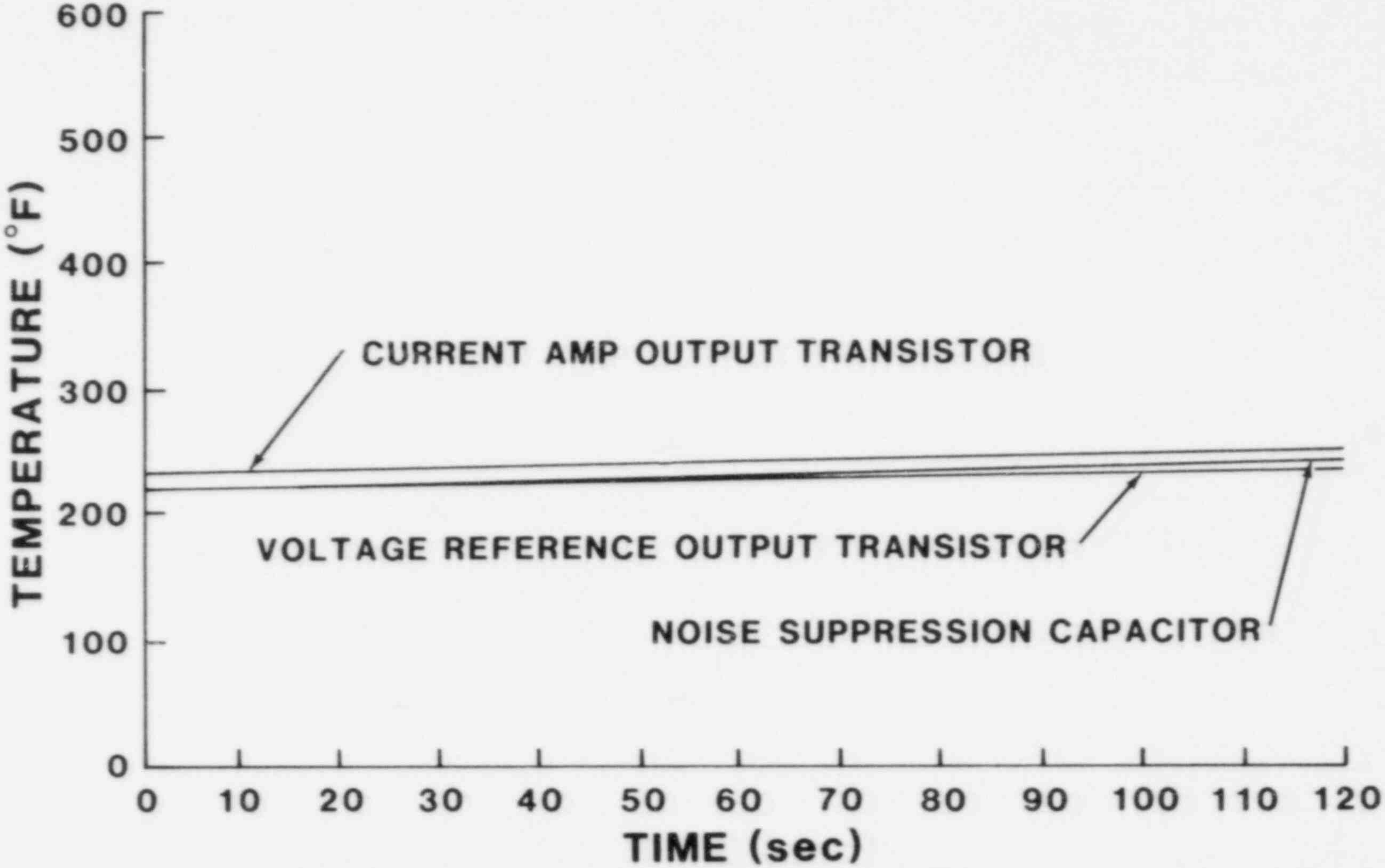

Figure C-4. Unaged Transmitter Electronic Temperatures (Factor 1.5)

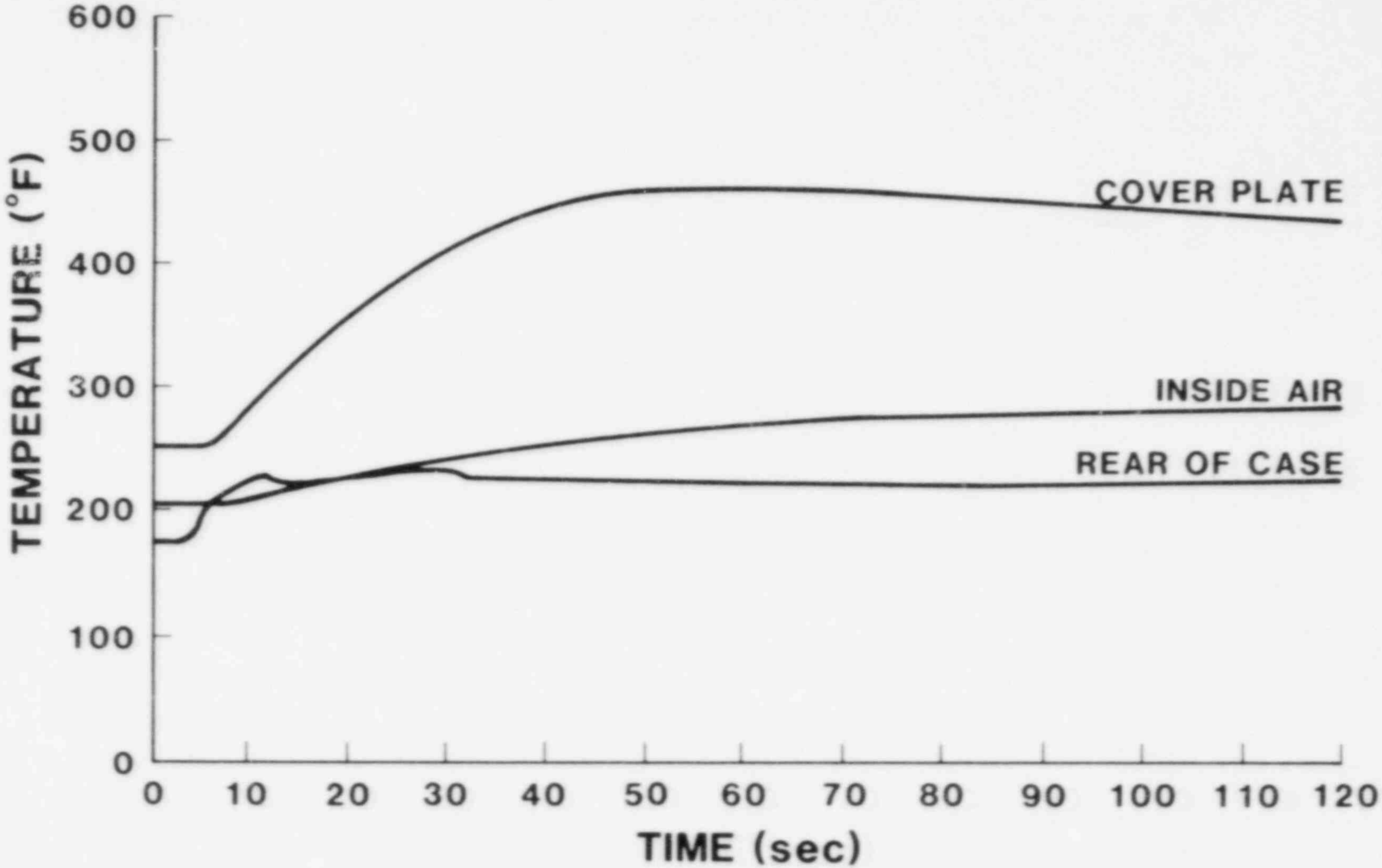

Figure C-5. Unaged Transmitter Casing Temperatures (Factor 1.5)

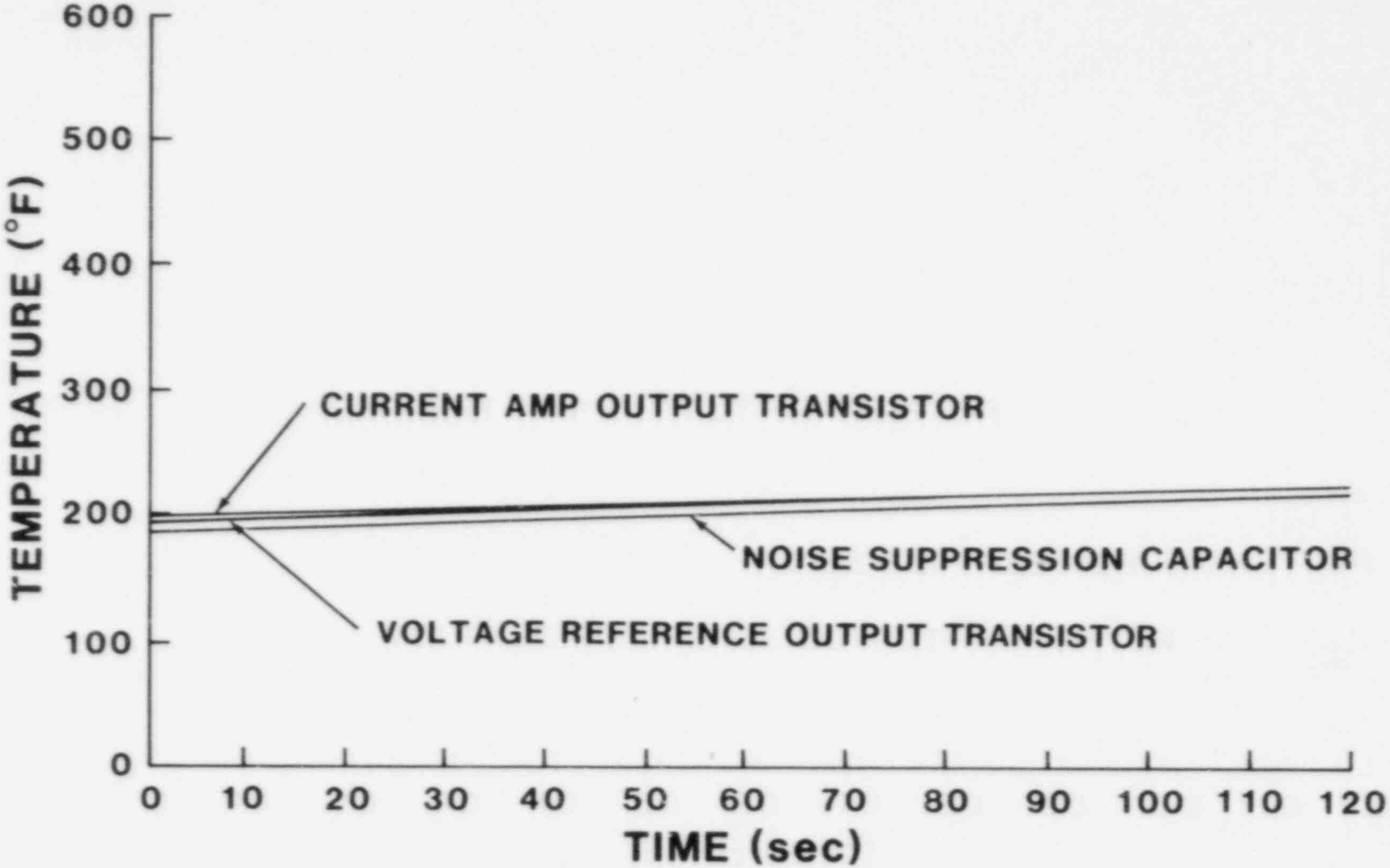

Figure C-6. Unaged Transmitter Electronic Temperatures (Factor 2.0)

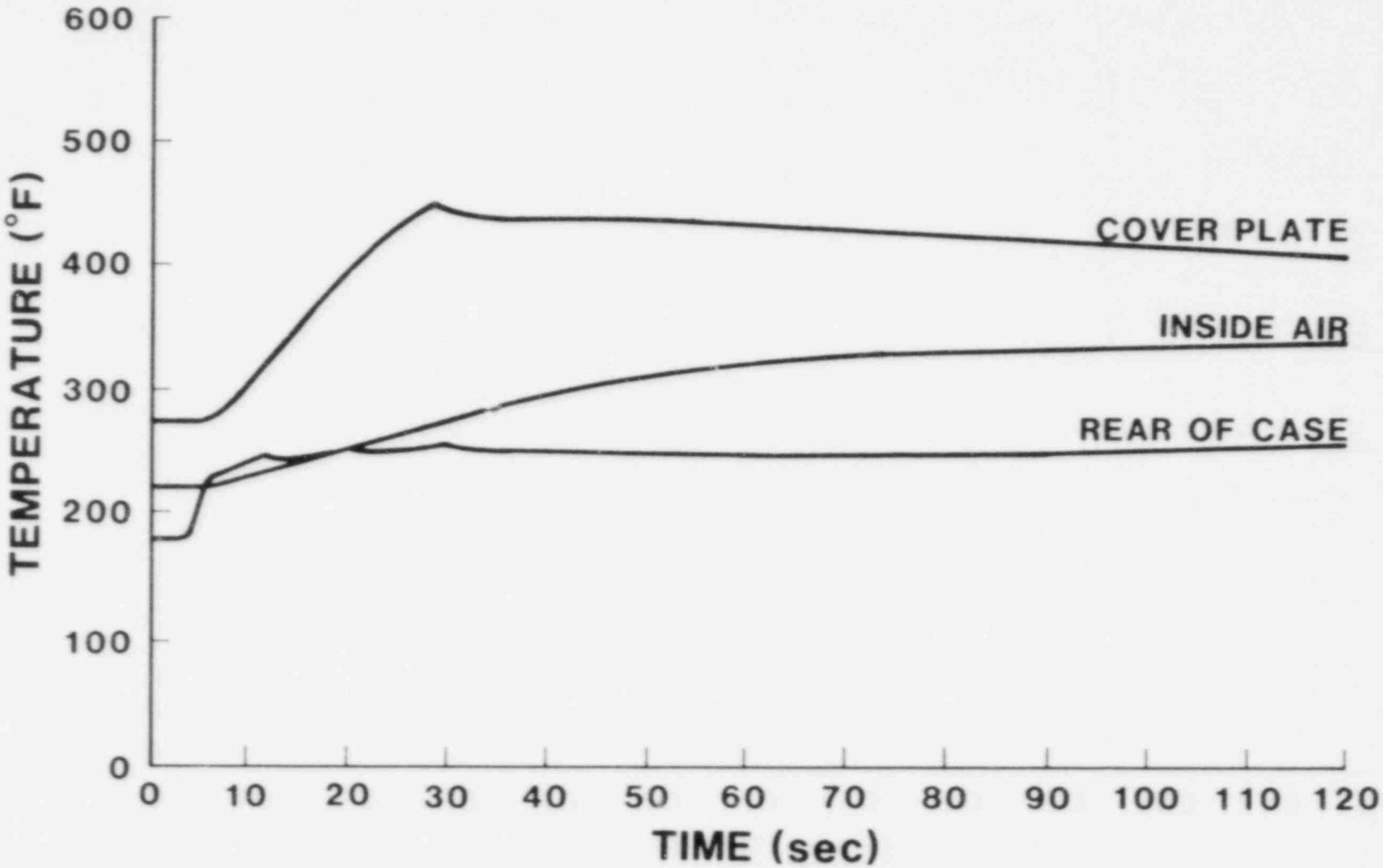

Figure C-7. Unaged Transmitter Casing Temperatures (Factor 2.5)

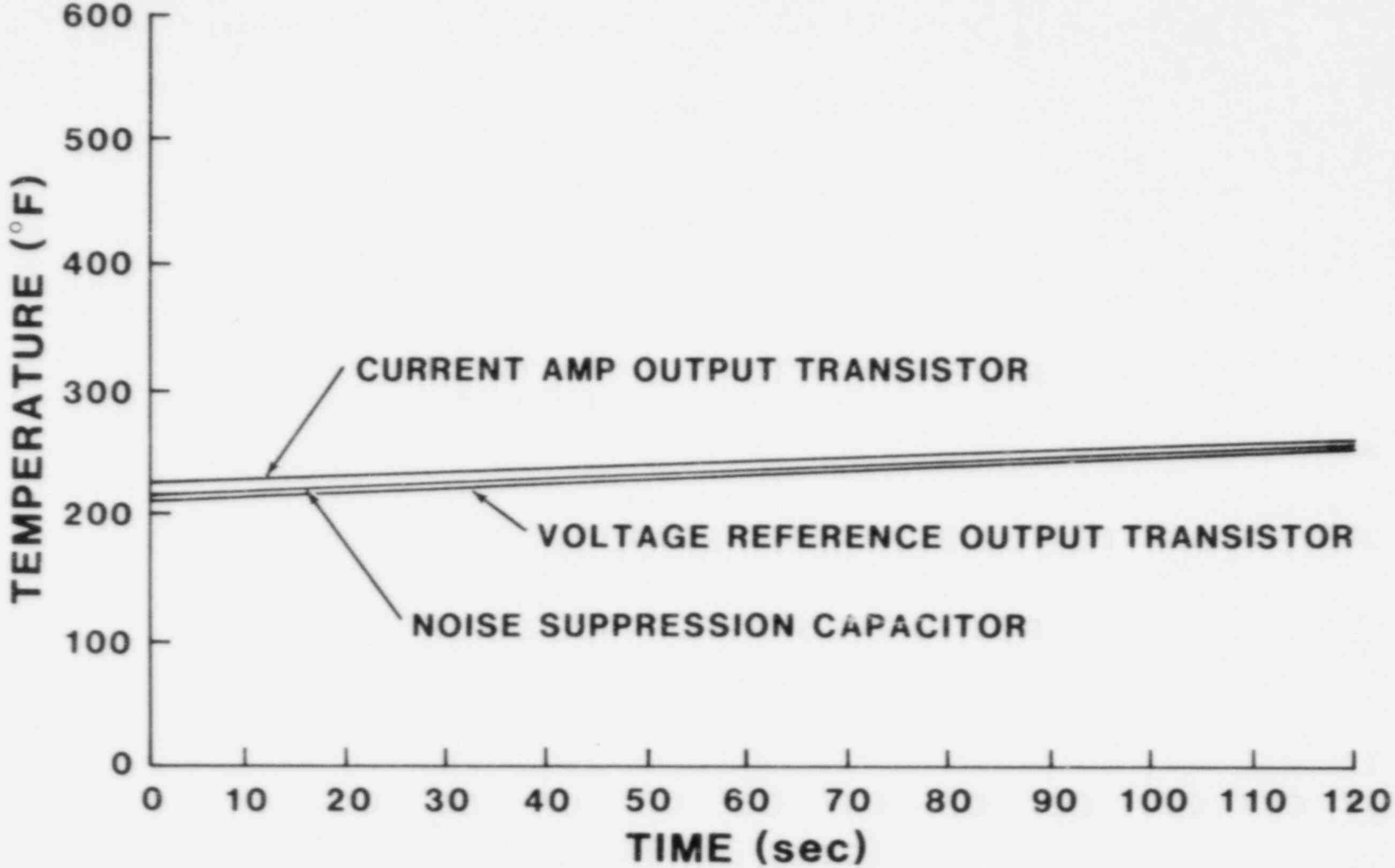

Figure C-8. Unaged Transmitter Electronic Temperatures (Factor 2.5)

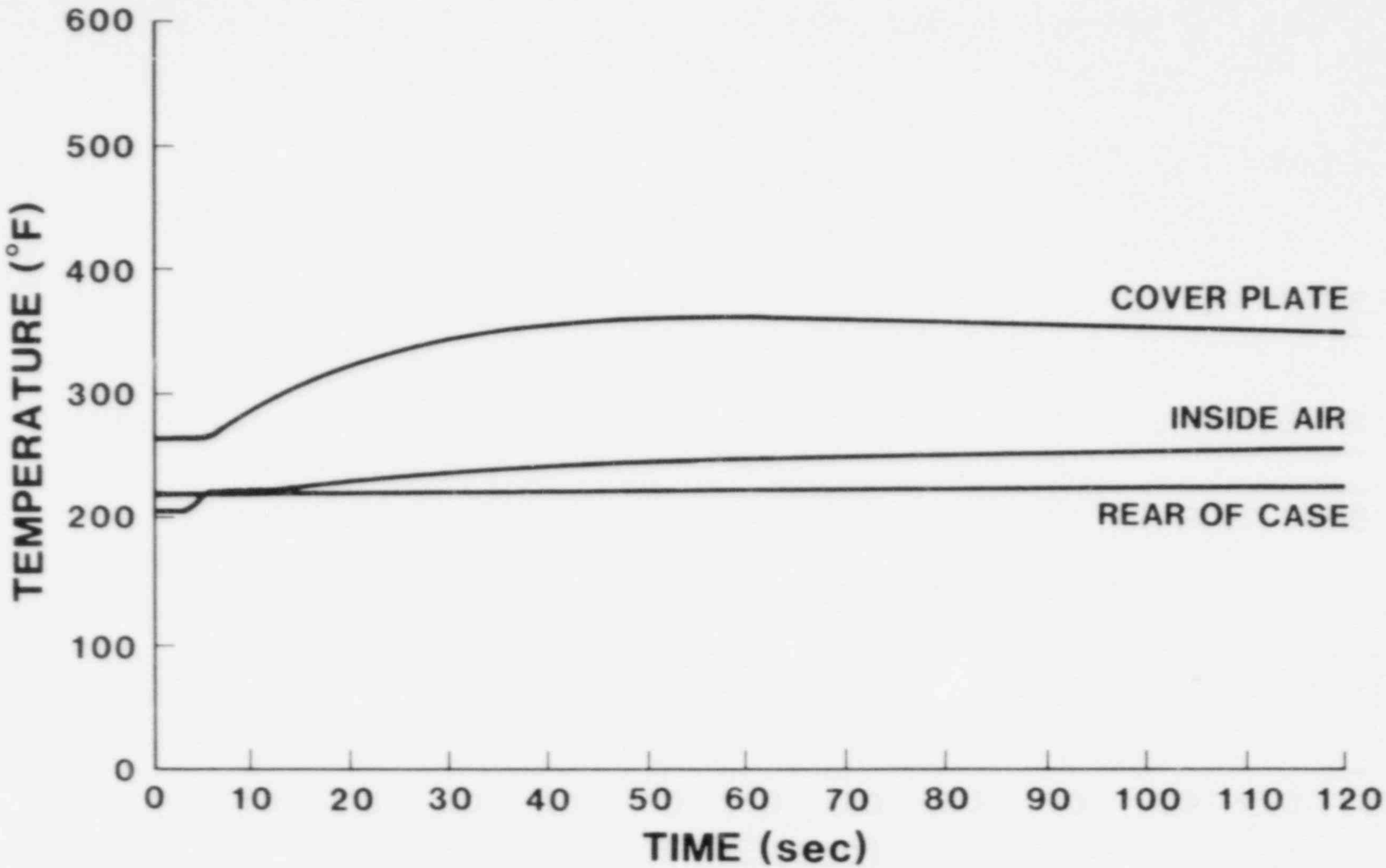

Figure C-9. Aged Transmitter Casing Temperatures (Factor 1.0)

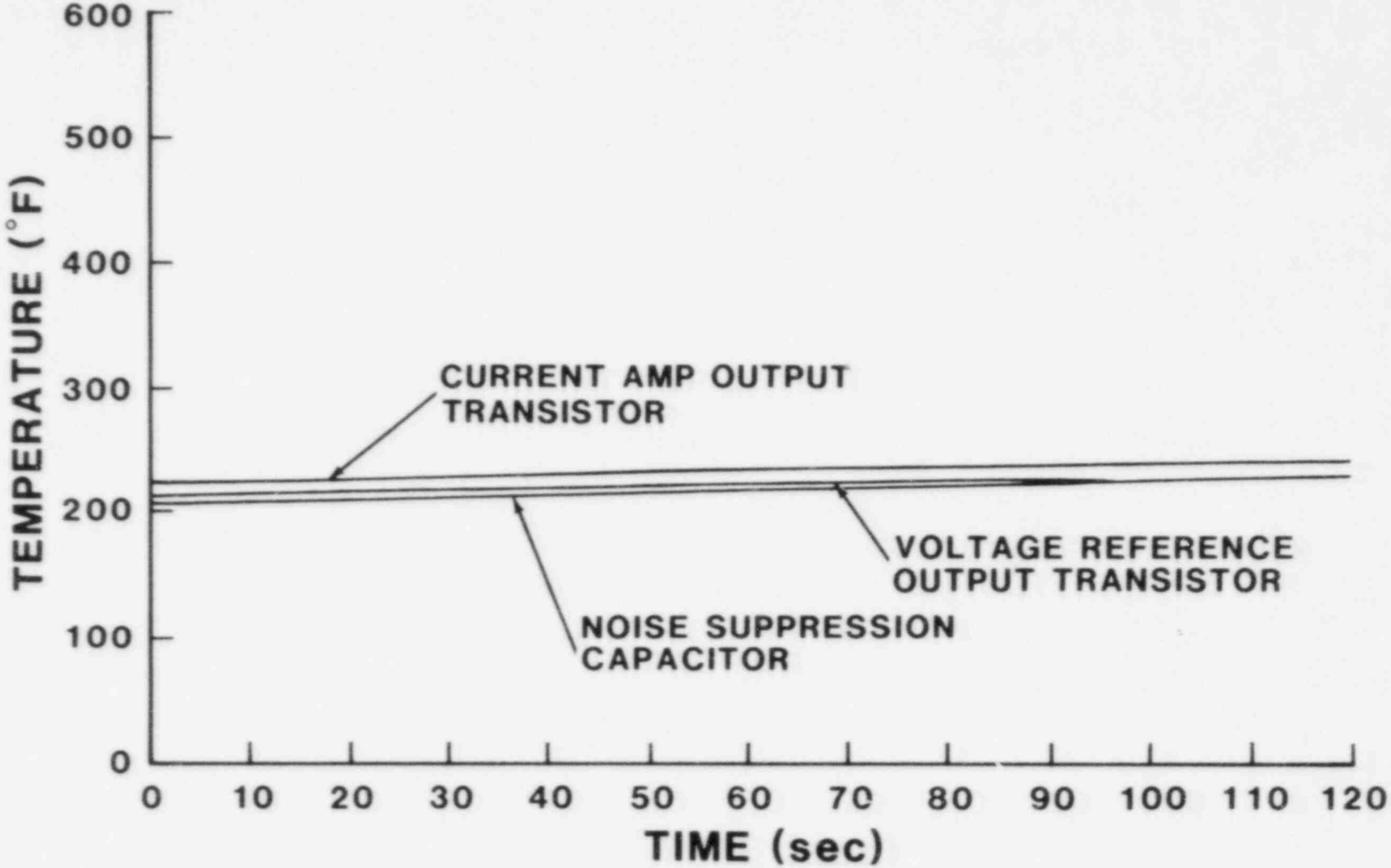

Figure C-10. Aged Transmitter Electronic Temperatures (Factor 1.0)

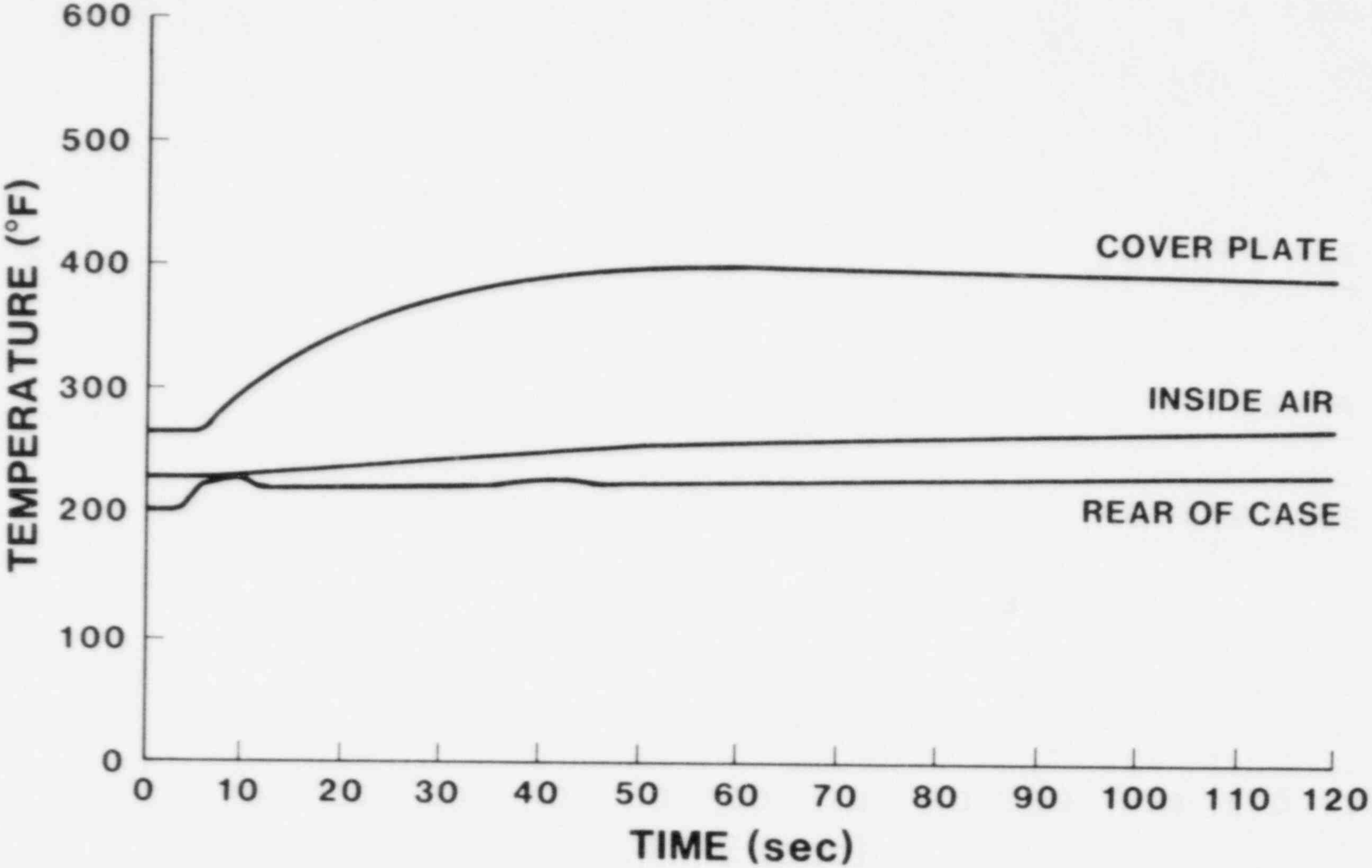

Figure C-11. Aged Transmitter Casing Temperatures (Factor 1.5)

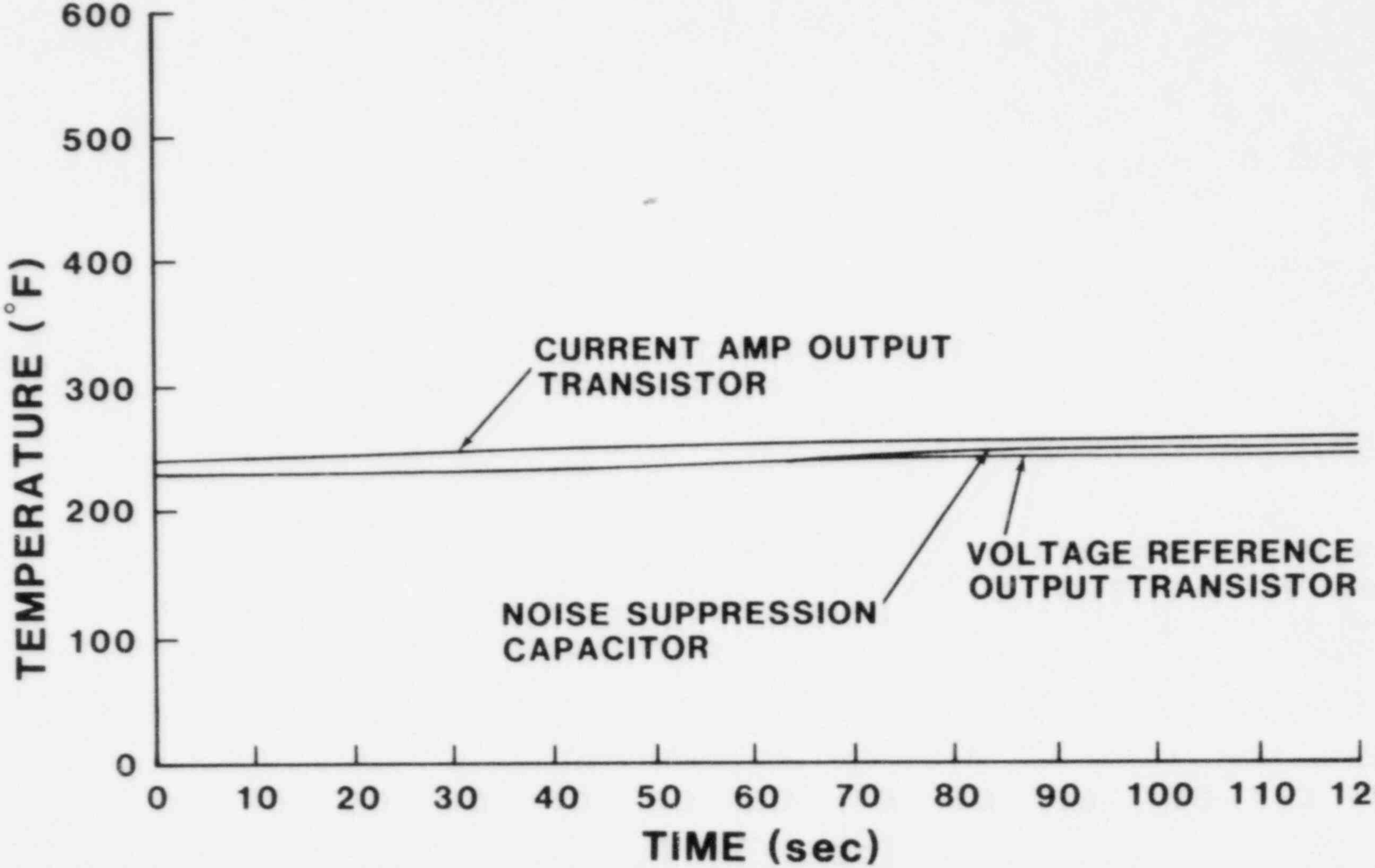

Figure C-12. Aged Transmitter Electronic Temperatures (Factor 1.5)

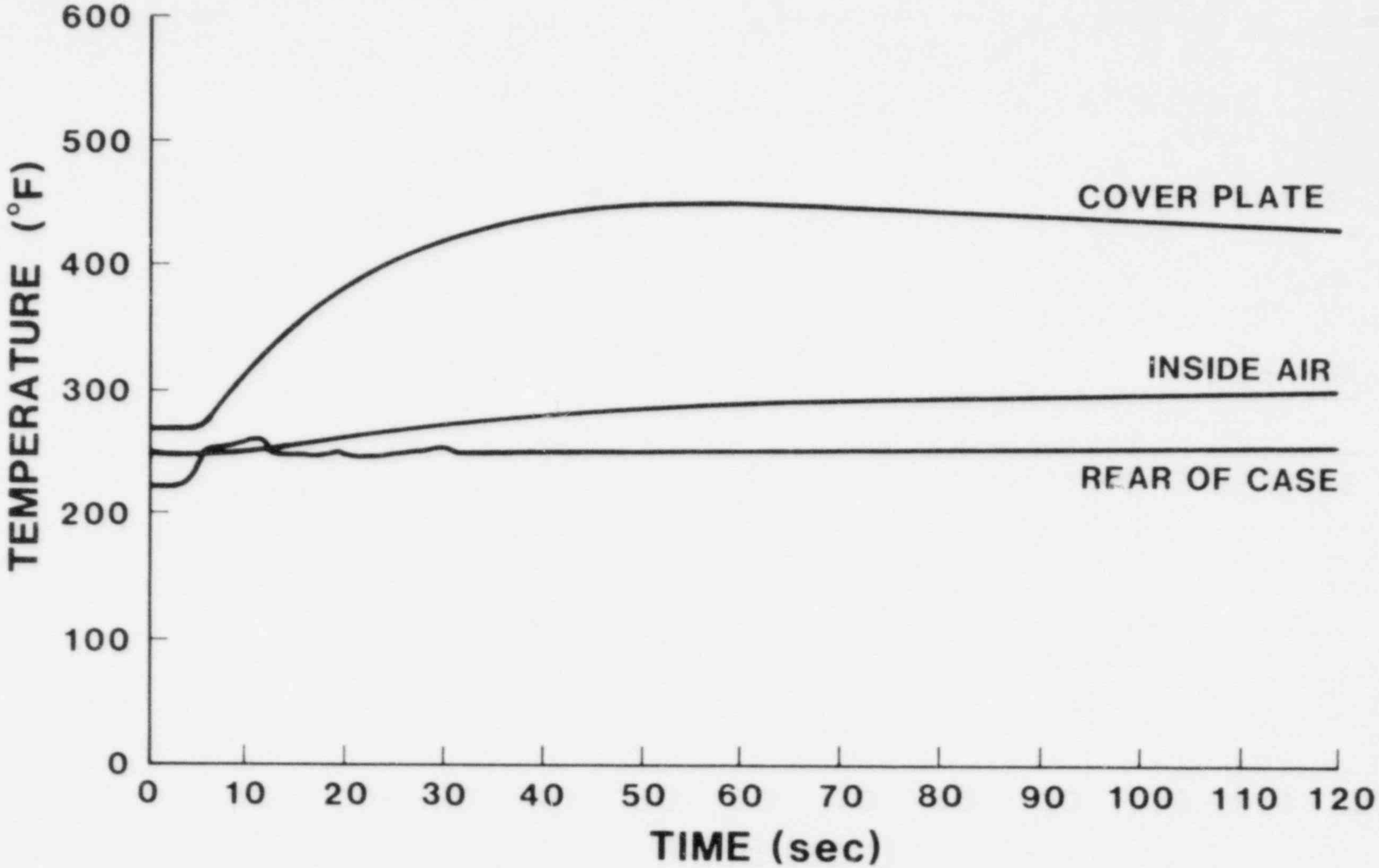

Figure C-13. Aged Transmitter Casing Temperatures (Factor 2.0)

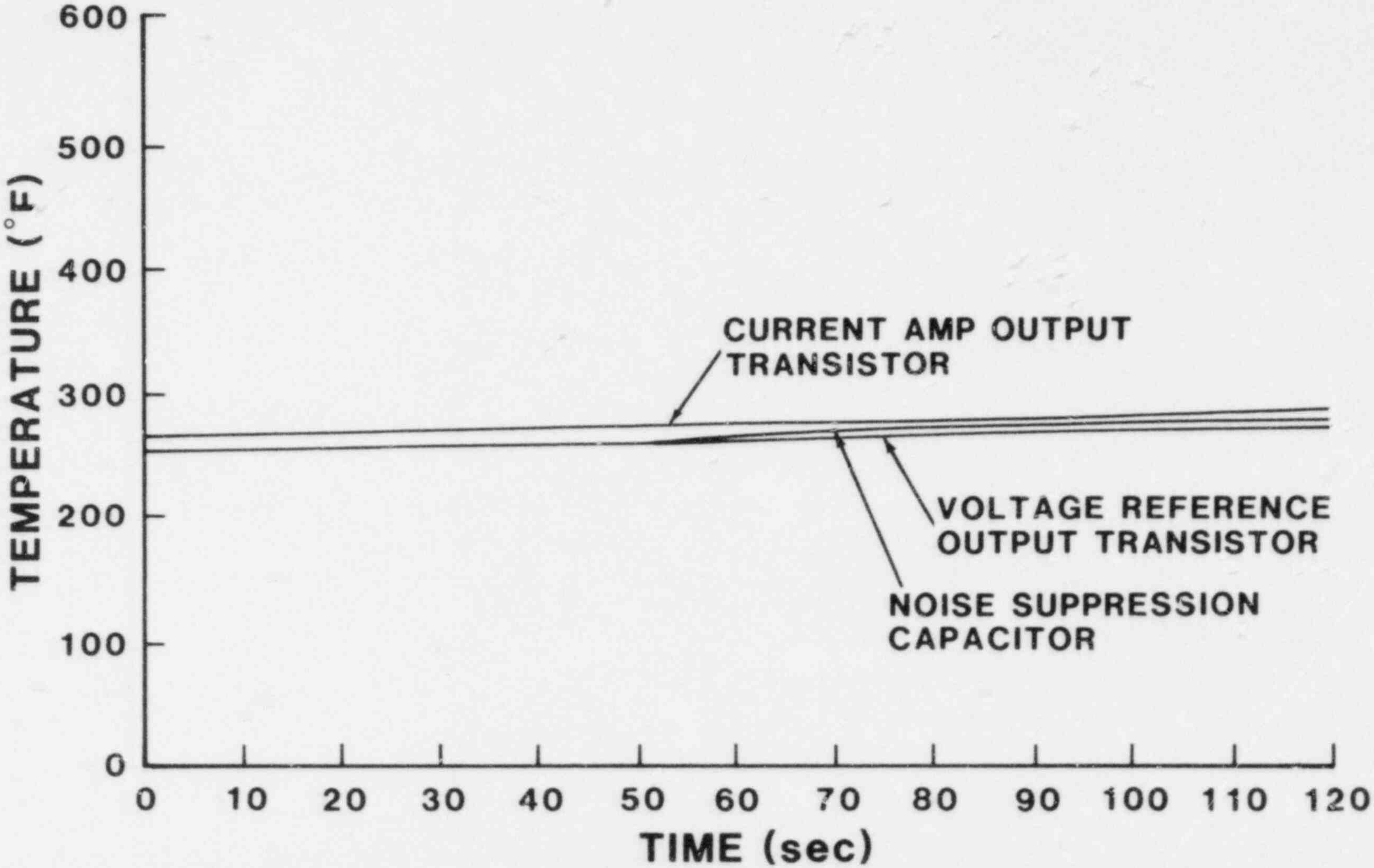

Figure C-14. Aged Transmitter Electronic Temperatures (Factor 2.0)

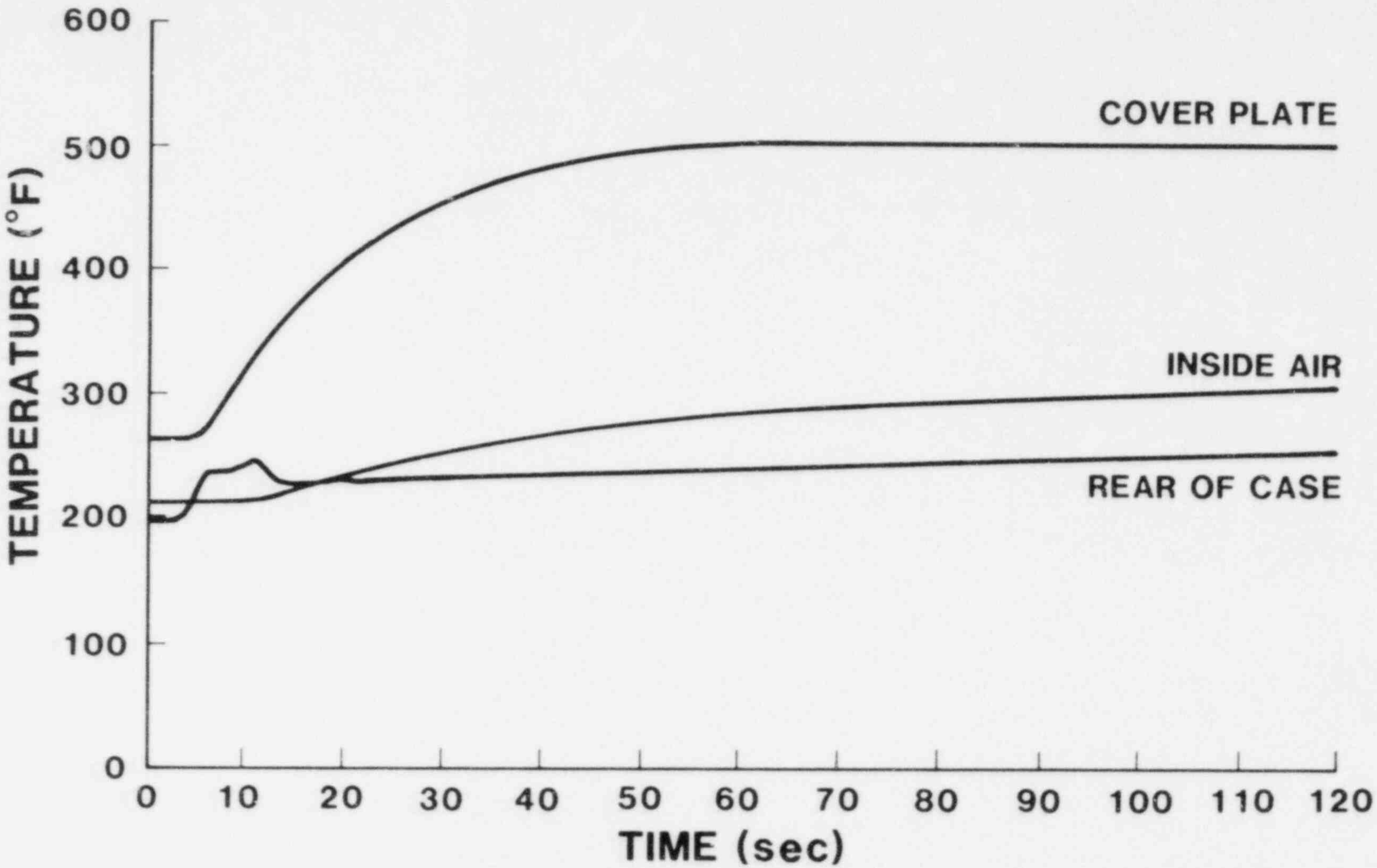

Figure C-15. Aged Transmitter Casing Temperatures (Factor 2.5)

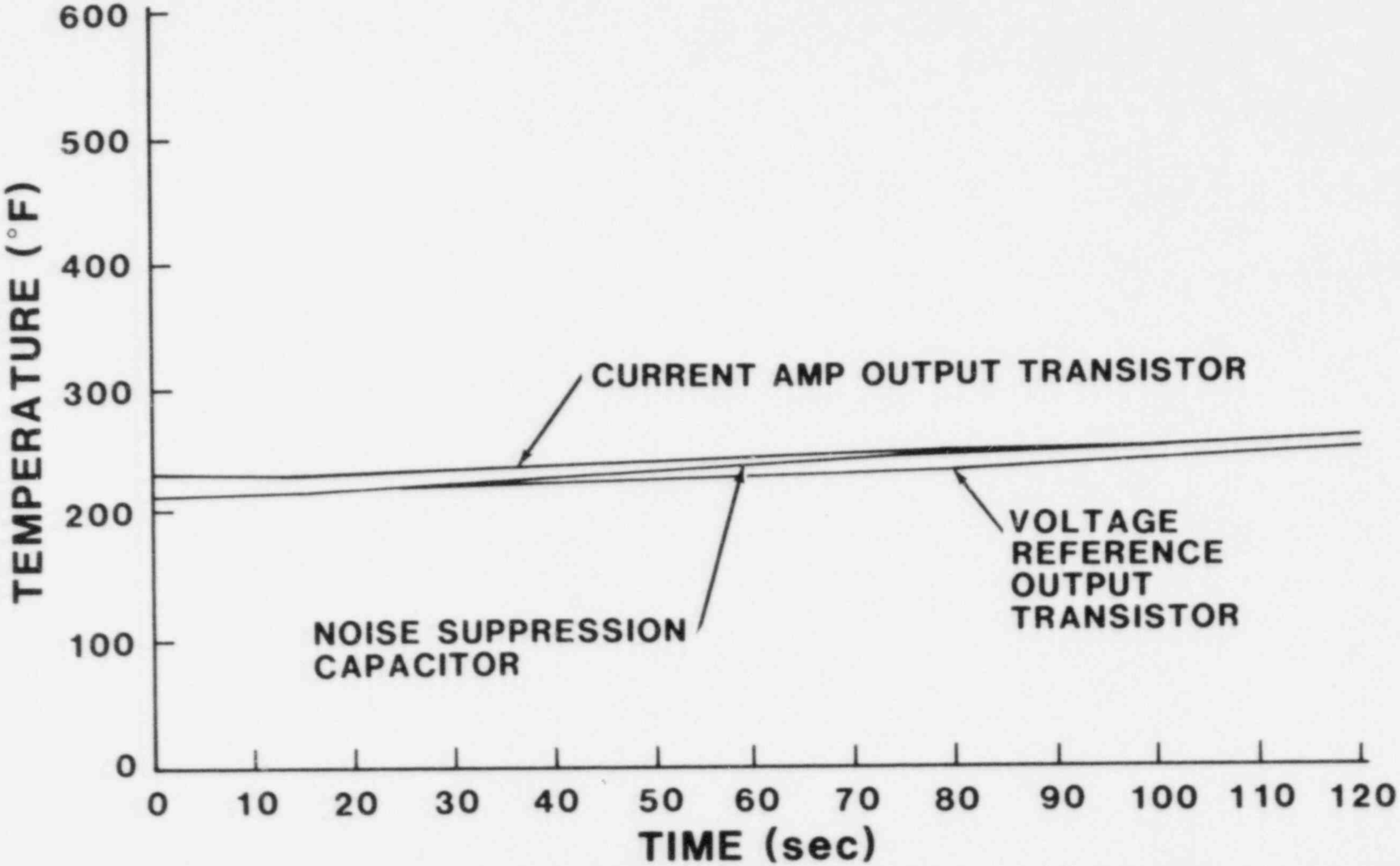

Figure C-16. Aged Transmitter Electronic Temperatures (Factor 2.5)

Appendix D

Pressure Lab Calibrations
and
Percent of Full-Scale Deviation Calculations

D.1 Pretest Calibration

Pretest calibrations were set in the Sandia Test Measurement and Design Division pressure lab according to the manufacturers instructions (Reference 13) prior to any testing or aging. The instrument signal was then read at 100 psi steps over the operational span of the transmitters (0-1000 psig). The data are given in Table D-1. the "Aged" designation refers to the transmitter which was thermally aged after this calibration check. Signals for pressures above 0 psig are truncated to two decimal places.

Table D-1

Pretest Transmitter Calibration Data

Applied Pressure (psig)	Unaged Transmitter Signal (mA)	Aged Transmitter Signal (mA)
0	3.999	4.003
100	5.62	5.60
200	7.24	7.21
300	8.86	8.82
400	10.47	10.42
500	12.07	12.02
600	13.66	13.62
700	15.25	15.21
800	16.83	16.80
900	18.42	18.39
1000	20.00	19.97

Using the results of Table D-1, calibration equations were determined by pressure lab personnel for each transmitter. The unaged transmitter calibration equation, which stated the pressure (P) as a function of the measured signal current (S), was found by the pressure lab to be

$$P = 62.518S - 252.518 \quad . \tag{D-1}$$

The corresponding equation for the sample that was subsequently aged was

$$P = 62.5939S - 251.460 \quad . \tag{D-2}$$

D.2 Percent of Full-Scale Deviation

Data systems which convert signals from instruments such as the Barton Model 763 pressure transmitter into readings of actual conditions do so by means of calibration equations having the form of Equations (D-1) and (D-2). Since these equations are based on best-fit approximations, the pressures indicated by the equation may not exactly match the actual pressures applied during the calibration of the instruments. Specifications are established which limit this deviation so as to insure confidence in instrument readings. These specifications for instrument deviation are often stated in terms of Percent of Full-Scale Deviation (PFSD) given by

$$\text{PFSD} = \frac{\text{Indicated Pressure} - \text{Actual Pressure}}{\text{Instrument Operating Pressure Span}} \times 100\% \qquad \text{(D-3)}$$

where the indicated pressure is that determined by Equation (D-1) or (D-2). The operating pressure span for the transmitters used during these tests was 1000 psig.

In order to examine the changes in transmitter calibration characteristics resulting from aging and exposure to the entire series of simulated hydrogen burns, the PFSD based on Equations (D-1) and (D-2) was determined for both transmitters while both were in unaged condition and at the completion of testing. The results are given in Tables D-2 and D-3 for the unaged and aged transmitters respectively and are plotted in Figures 4-14 and 4-15.

Transmitter calibration equations based on the after test lab checks were also determined. The after test calibration equation for the unaged transmitter was

$$P = 64.3726S - 260.475 \quad . \qquad \text{(D-4)}$$

The calibration equation for the aged transmitter after aging and testing was

$$P = 63.2705S - 243.135 \quad . \qquad \text{(D-5)}$$

Table D-2

Unaged Transmitter Percent of Full-Scale Deviations

Applied Pressure (psig)	Before Testing: Signal (mA)	Before Testing: Indicated Pressure (psig)	Before Testing: PFSD (%)	After Testing: Signal (mA)	After Testing: Indicated Pressure (psig)	After Testing: PFSD (%)
0	3.999	-2.59	-0.259	4.050	0.60	0.060
100	5.62	98.75	-0.125	5.60	97.50	-0.250
200	7.24	200.03	0.003	7.15	194.40	-0.560
300	8.86	301.31	0.131	8.70	291.30	-0.870
400	10.47	401.97	0.197	10.26	388.84	-1.116
500	12.07	501.99	0.199	11.82	486.37	-1.363
600	13.66	601.40	0.140	13.37	583.26	-1.674
700	15.25	700.80	0.080	14.92	680.17	-1.983
800	16.83	799.58	-0.042	16.47	777.07	-2.293
900	18.42	898.98	-0.102	18.03	874.60	-2.540
1000	20.00	997.76	-0.224	19.58	971.51	-2.849

Table D-3

Aged Transmitter Percent of Full Scale Deviations

	Before Testing			After Aging and Testing		
Applied Pressure (psig)	Signal (mA)	Indicated Pressure (psig)	PFSD (%)	Signal (mA)	Indicated Pressure (psig)	PFSD (%)
0	4.003	-0.897	-0.090	3.879	-8.66	-0.866
100	5.60	99.07	-0.093	5.41	87.17	-1.283
200	7.21	199.84	-0.016	6.98	185.45	-1.456
300	8.82	300.62	0.062	8.57	284.97	-1.503
400	10.42	400.77	0.077	10.16	384.49	-1.551
500	12.02	500.92	0.092	11.75	484.02	-1.598
600	13.62	601.07	0.107	13.34	583.54	-1.646
700	15.21	700.59	0.059	14.91	681.82	-1.818
800	16.80	800.12	0.012	16.48	780.09	-1.991
900	18.39	899.64	-0.036	18.07	879.61	-2.038
1000	19.97	998.54	-0.146	19.65	978.51	-2.149

DISTRIBUTION

U.S. Government Printing Office
Receiving Branch (Attn: NRC Stock)
8610 Cherry Lane
Laurel, MD 20707
275 copies for R3

W. S. Farmer (5)
U.S. Nuclear Regulatory Commission
Office of Nuclear Regulatory Research
Division of Engineering Technology
Washington, DC 20555

J. T. Larkins
U.S. Nuclear Regulatory Commission
Office of Nuclear Regulatory Research
Division of Accident Evaluation
Washington, DC 20555

K. I. Parczewski
U.S. Nuclear Regulatory Commission
Office of Nuclear Regulatory Regulation
Division of Engineering
Washington, DC 20555

F. G. Hudson
Duke Power Company
Design Engineering Department
P.O. Box 33189
Charlotte, NC 28242

C. Moser
Energy Incorporated
1 Energy Drive
Box 736
Idaho Falls, ID 83402

Dr. S. F. Hall
Safety and Reliability Directorate
United Kingdom Atomic Energy Authority
Wigshaw Lane
Culcheth
Warrington WA3 4NE, Cheshire
GREAT BRITAIN

P. Holzman
Engineering Planning and Management
298 Boston Post Road
Wayland, MA 01778

Dr. S. Turner
Southern Science Applications
P.O. Box 10
Dunedin, FL 33528

L. Reiman
Department of Reactor Safety
Institute of Radiation Protection
P.O. Box 268
00101 Helsinki 10
FINLAND

Dr. M. McIntyre
Technical Department
Rolls-Royce & Associates, Ltd.
P.O. Box 31
Derby, DE2 8BJ
GREAT BRITAIN

Dr. W. Baukal
Battelle-Institut e.V.
Am Rowershof 35
D-6000 Frankfurt am Main 90
FEDERAL REPUBLIC OF GERMANY

6400 A. W. Snyder
6411 S. E. Dingman
6425 W. Frid
6427 M. Berman
6427 B. Marshall
6433 J. J. Aragon
6440 L. D. Buxton
6442 W. A. von Riesemann
6444 L. D. Buxton
6446 L. L. Bonzon
6446 D. T. Furgal
6446 E. H. Richards
6447 D. L. Berry
6447 V. J. Dandini (25)
6447 D. B. King
6449 K. D. Bergeron
3141 S. A. Landenberger (5)
3151 W. L. Garner
8024 P. W. Dean

NRC FORM 335
(2-84)
NRCM 1102,
3201, 3202

U.S. NUCLEAR REGULATORY COMMISSION

BIBLIOGRAPHIC DATA SHEET

SEE INSTRUCTIONS ON THE REVERSE

1. REPORT NUMBER (Assigned by TIDC, add Vol. No., if any)
NUREG/CR-4324
SAND85-1481

2. TITLE AND SUBTITLE
Testing of Nuclear Qualified Cables and Pressure Transmitters in Simulated Hydrogen Deflagrations to Determine Survival Margins and Sensitivities

3. LEAVE BLANK

4. DATE REPORT COMPLETED

MONTH	YEAR
August	85

5. AUTHOR(S)
Vincent J. Dandini

6. DATE REPORT ISSUED

MONTH	YEAR
December	85

7. PERFORMING ORGANIZATION NAME AND MAILING ADDRESS (Include Zip Code)
Sandia National Laboratories
P.O. Box 5800
Albuquerque, NM 87185

8. PROJECT/TASK WORK UNIT NUMBER
N/A

9. FIN OR GRANT NUMBER
A-1270

10. SPONSORING ORGANIZATION NAME AND MAILING ADDRESS (Include Zip Code)
Division of Engineering Technology
Office of Nuclear Regulatory Research
U. S. Nuclear Regulatory Commission
Washington, DC 20555

11a. TYPE OF REPORT
Final, Technical

b. PERIOD COVERED (Inclusive dates)

12. SUPPLEMENTARY NOTES

13. ABSTRACT (200 words or less)

A series of tests was conducted at Sandia National Laboratories Central Receiver Test Facility that addressed the margin for survival of nuclear reactor safety equipment in hydrogen burns. The tests Exposed aged and unaged specimens of nuclear qualified electrical cable and pressure transmitters to simulated hydrogen burns of increasing severity. Starting with a base heat flux pulse corresponding to that resulting from a 75 percent core metal-water reaction in a large dry containment, the heat flux levels of each successive pulse increased in increments of 50 percent of the base pulse. The heat flux levels of the most severe pulse were 300 percent of the base pulse.

All specimens functioned properly during exposure to all of the simulated hydrogen burns. Cables maintained a constant applied potential; no shorts or open circuits were detected. The pressure transmitters delivered steady signals indicating no significant degradation in performance.

Post exposure tests indicated slight differences between the aged and unaged cable insulation characteristics. The insulation of one cable failed during the 2400 Vac high potential withstand test.

Transmitter calibration checks performed between exposures and after completion of the test series indicated slight changes in calibration for both the aged and unaged transmitter.

14. DOCUMENT ANALYSIS — a. KEYWORDS/DESCRIPTORS
Reactor Instrumentation, Reactor Accidents

b. IDENTIFIERS/OPEN ENDED TERMS
Hydrogen Burn, Equipment Survivability, Pressure Transmitters, Electrical Cables

15. AVAILABILITY STATEMENT
NTIS
GPO Sales

16. SECURITY CLASSIFICATION
(This page)
Unclassified
(This report)
Unclassified

17. NUMBER OF PAGES
90

18. PRICE

☆ U.S. Government Printing Office 1985-678-049/21020

120555078877 1 1AN1R3
US NRC
ADM-DIV OF TIDC
POLICY & PUB MGT BR-PDR NUREG
W-501
WASHINGTON DC 20555